LSU Doctoral Dissertations

Graduate School

2009

Task Specific Ionic Liquids for Enantiomeric Recognition and Nanomaterials for Biomedical Imaging

David Kipkogei Bwambok
Louisiana State University and Agricultural and Mechanical College, dbwamb1@tigers.lsu.edu

Recommended Citation

TASK SPECIFIC IONIC LIQUIDS FOR ENANTIOMERIC RECOGNITION AND
NANOMATERIALS FOR BIOMEDICAL IMAGING

A Dissertation
Submitted to the graduate Faculty of the
Louisiana State University and
Agricultural and Mechanical College
In partial fulfillment of the
Requirements for the degree of
Doctor of Philosophy

In
The Department of Chemistry

By
David Kipkogei Bwambok
B. Ed. (Sc.), Moi University, 1998
M.S., State University of New York (SUNY) at Binghamton, 2005
December 2009

DEDICATION

To my late mom: Mrs. Flomena Jesang Sawe. Mom, you always loved me and encouraged me to work hard to succeed. I believe you are now smiling in heaven.
To my dad Mr. William Kibwambok Sawe, my son Cosmas Kipkirui, my daughters Eunice Jepchumba and Maurine Jeptum, my dear wife Christine Bwambok, my brothers Michael Bwambok, Dominic Bwambok, Eliud Bwambok and Philip Bwambok, my sister Georgina Cherotich and the entire KapChepketon, Kapbutagui and Kabosi and the entire extended family for all their love and support over the years.

TABLE OF CONTENTS

LIST OF TABLES

LIST OF FIGURES

LIST OF SCHEMES

Scheme   **Page**

LIST OF ABBREVIATIONS

Abbreviation	Name
$AgBF_4$	silver tetrafluoroborate
AgLac	silver lactate
$AgNO_3$	silver nitrate
$AlCl_3$	aluminium (III) choride
$AlaC_4Cl$	alanine *tert* butyl ester
$AlaC_4NO_3$	alanine *tert* butyl ester nitrate
$AlaC_4BF_4$	alanine *tert* butyl ester tetrafluoroborate
$AlaC_4Lac$	alanine *tert* butyl ester lactate
$AlaC_4NTf_2$	alanine *tert*-butyl ester bis (trifluoromethyl) sulfonylimide
AOT	sodium bis (2-ethylhexyl) sulfosuccinate
BETI	bis(pentafluoroethane) sulfonimide
BmimCl	1-butyl-3-methylimidazolium chloride
[bmim] [FeCl$_4$]	1-butyl-3-methylimidazolium iron (IV) chloride
BNA	1,1′-binaphthyl-2,2′-diamine
CD_2Cl_2	deuterated dichloromethane
CILs	chiral ionic liquids
CE	capillary electrophoresis
CD	circular dichroism
CCD	charge coupled device
CT	computed tomography
DLS	dynamic light scattering
DMEM	Dulbecco's Modified Eagle's Medium

DMSO   dimethyl sulfoxide

DSC   differential scanning calorimetry

EEMs   Excitation-Emission Matrix spectra

EtOH   ethanol

FDA   food and drug administration

HF   hydrofluoric acid

GC   gas chromatography

GUMBOS   Group of Uniform Materials Based on Organic Salts

HPLC   high performance liquid chromatography

HMT   1,1′,3,3,3′,3′-hexamethylindotricarbocyanine

ICG   indocyanine green

ILs   ionic liquids

IC   internal conversion

ISC   intersystem crossing

LC   liquid chromatography

$LiNTf_2$ bis (trifluoromethane) sulfonimide lithium salt

MEKC   micellar electrokinetic chromatography

MCPs   mean-centered plots

NIR   near infrared

NMR   nuclear magnetic resonance

OLEDs   organic light-emitting diodes

PMT   photomultiplier tube

$PheC_2Cl$ phenylalanine ethyl ester hydrochloride

$PheC_2NTf_2$ phenylalanine ethyl ester bis (trifluoromethane) sulfonimide

RTILs	room temperature ionic liquids
RET	resonance energy transfer
TGA	thermal gravimetric analysis
TFAE	2,2,2-trifluoroanthrylethanol
TMS	tetramethyl silane
TSILs	task specific ionic liquids
TEM	transmission electron microscopy
THF	tetrahydrofuran
SAED	selected area electron diffraction pattern
UV	ultraviolet
Vis	visible

ABSTRACT

Ionic liquids (ILs) are organic salts that melt at or below 100°C. Interest in ILs continues to grow due to their unique properties such as lack of measurable vapor pressure, high thermal stability, tunability and recyclability. The first part of this dissertation explores the use of chiral ionic liquids (CILs) for enantiomeric recognition of chiral analytes using fluorescence spectroscopy. Chiral analyses continue to be a subject of considerable interest primarily as a result of legislation introduced by the Food and Drug Administration. This has led to an increased need for suitable chiral selectors and methods to verify the enantiomeric forms of drugs. In this study, CILs derived from amino acid esters were used simultaneously as solvents and chiral selectors for enantiomeric recognition of various fluorescent as well as non-fluorescent chiral analytes.

The second part of this dissertation focuses on the development of a new class of fluorescent near infrared (NIR) nanoparticles from a Group of Uniform Materials Based on Organic Salts (GUMBOS) largely comprising frozen ILs. The GUMBOS were subsequently used to fabricate nanoGUMBOS using a reprecipitation method. The potential of the NIR nanoGUMBOS for non-invasive imaging was evaluated by fluorescence imaging of Vero cells incubated with nanoGUMBOS. Fluorescence imaging of diseased cells and tissues is useful for early detection and treatment of diseases. The work presented here is significant and may improve the quality of human life by employing NIR nanoGUMBOS as contrast agents for early diagnosis and treatment of some diseases. Through variations in the anion, different spectral properties were observed for nanoGUMBOS presenting the possibility of using a single dye for multiple applications.

CHAPTER 1

INTRODUCTION

1.1. Ionic Liquids (ILs)

ILs are defined as organic salts with a melting point at or below 100 ºC.[1, 2] Although ILs received increased attention recently, they have been known since 1914 when Paul Walden discovered ethylammonium nitrate with a melting point of 12 ºC, which is now regarded as the first ionic liquid.[3] An arbitrary temperature limit of 100 °C has been used to distinguish ILs from inorganic molten salts which generally have high melting points.[4] The low melting point of ILs has been attributed to asymmetry of the component cations and anions leading to frustrated crystal packing.[5, 6] The effect of cation symmetry is further illustrated by the higher melting points reported for ILs containing symmetrical 1,3-dimethylimidazolium and 1,3-diethylimidazolium salts compared to the more unsymmetrical 1-ethyl-3-methylimidazolium or 1-butyl-3- methylimidazolium cations.[7] It has also been reported by Holbrey *et al.* that crystal polymorphism in 1-butyl-3-methylimidazolium halides inhibits crystal formation resulting in ILs.[8]

One of the widely used method in the synthesis of ILs is anion metathesis between a halide salt and the metal (or ammonium) salt of the desired anion. This results in ILs with cations such as imidazolium, ammonium, pyridinium, and phosphonium cations. Examples of commonly used anions include bis (trifluoromethyl) sulfonimide, hexafluorophosphate, tetrafluoroborate and nitrate.[9] Another method that results in ILs is the acid-base neutralization reaction followed by removal of water *in vacuo*. Indeed the first ionic liquid reported, ethyl ammonium nitrate, was prepared using the acid-base neutralization reaction between ethylamine and nitric acid.[3] Various ILs containing amino acid anions and tetrabutylammonium or tetrabutylphosphonium cations have also been prepared using the acid-base neutralization

reaction.[10] Direct combination of a halide salt with a metal halide is another approach that affords ILs. This approach is illustrated by the first preparation of the magnetic ionic liquid [bmim] [FeCl$_4$] by mixing equimolar amounts of [bmim] [Cl] and FeCl$_3$.[11] A further example of direct combination is the synthesis of a series of transition metal based magnetic ILs by Del Sesto and coworkers.[12] It is interesting to note that in this combination type of reaction, there are no by-products.[11, 12]

Interest in ILs stems from their unique properties such as negligible vapor pressure, high thermal stability, high ionic conductivity, high solubility for various compounds (polar/non-polar, organic/inorganic), and recyclability.[9] In addition, ILs are easily tunable by careful choice of cation or anion. The lack of measurable vapor pressure and high thermal stability of ILs has been attributed to large cohesive energy density provided by Coulombic interactions between the constituent ions.[13] After being latent for sometime, research activity in room temperature ionic liquids (RTILs) was renewed with the discovery of alkylpyridinium and 1,3-dialkylimidazolium haloaluminate salts.[14] In 1975, the first electrochemical study on these new liquid salts such as [ethylpryidinium bromide]-[AlCl$_3$] was reported.[15] The Lewis acidity of these ILs could be tuned by varying the molar ratio of the two ionic components. However, these haloaluminate ionic liquids are extremely sensitive to hydrolysis by atmospheric moisture and require handling strictly under anhydrous conditions. This problem was alleviated with the discovery of imidazolium ILs containing tetrafluoroborate and hexafluorophosphate anions that do not impose such special handling requirements.[16, 17] However, it has been reported that hexafluorophosphate ionic liquids releases HF in the presence of moisture and may not be suitable for electrochemical applications.[18] Overall, there are approximately 10^{18} possible combinations of various cations and anions to generate ILs compared to only 600 molecular solvents currently used.[19] Examples

of some cations and anions commonly used to prepare ILs are shown (Scheme 1.1).[20, 21] Such ILs

are generally regarded as non-functionalized ILs.
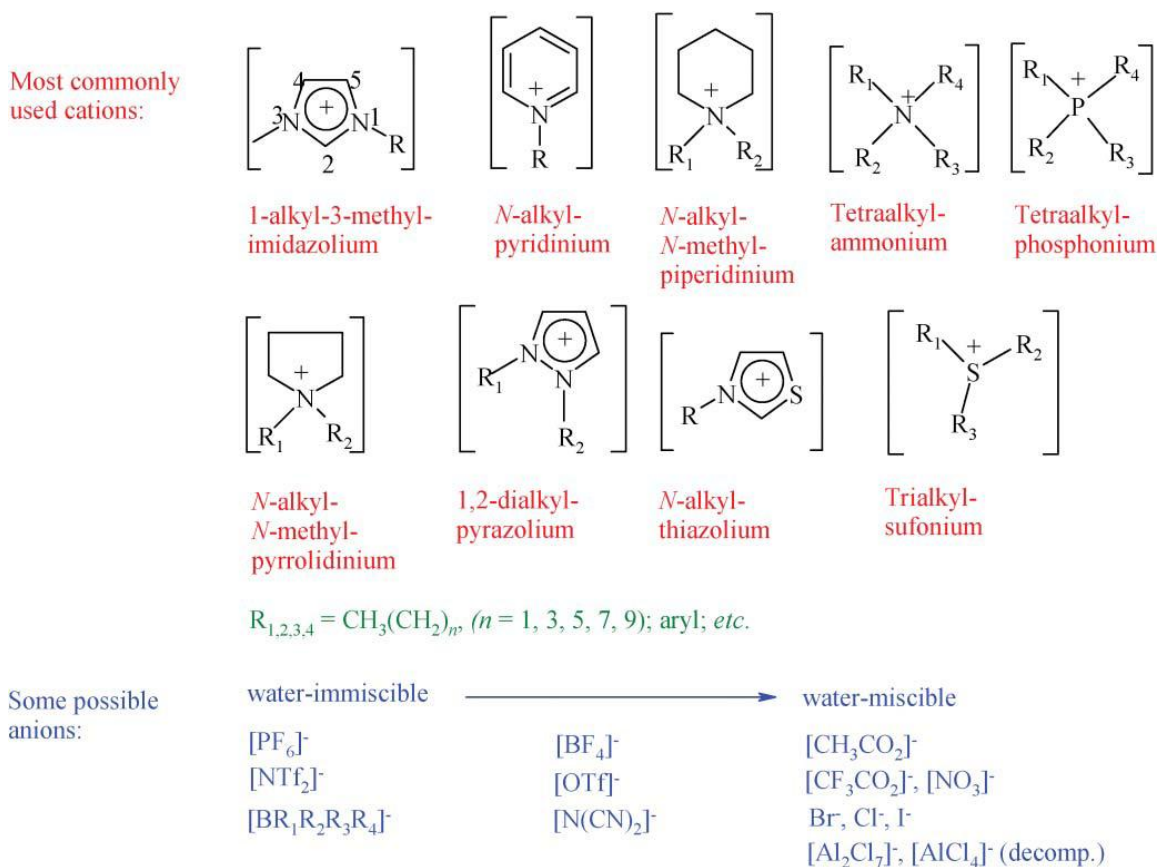
Scheme 1.1. Representative common cations and anions used in the synthesis of ILs. (Adapted from reference 18).

Over the last two decades, there has been tremendous interest in ILs research as reflected

by the steeper than exponential growth in the number of publications and patents (Figure 1.1).[18]

The ability to tailor the properties of ILs for specific applications has led to preparation of

various novel ILs generally known as task specific ionic liquids (TSILs). An example of TSILs is

chiral ionic liquids (CILs)[22] and their use in spectroscopic chiral discrimination will be described

later in this dissertation. Novel functionalized TSILs for metal extraction have also been

reported.[23, 24] Other examples of TSILs include magnetic ILs[11, 12] and protic ILs.[25] In general, ILs

A.
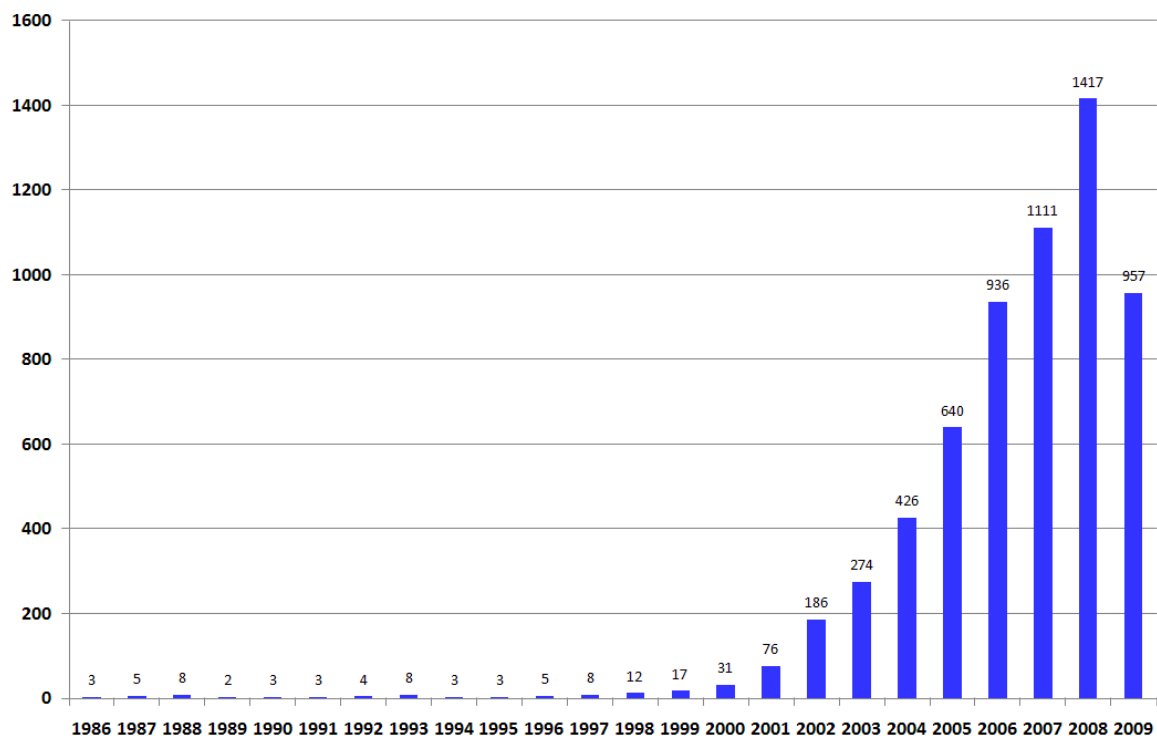
B.
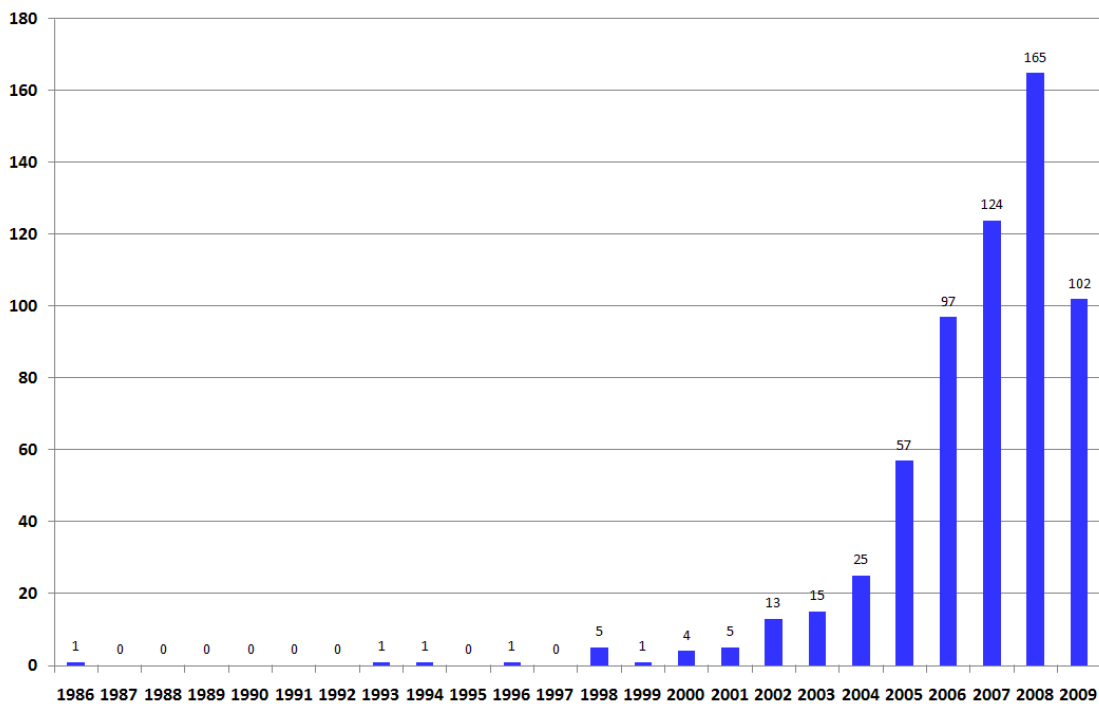
Figure 1.1. Annual growth of ionic liquid (A) publications from 1986-2009, and (B) patents from 1986-2009. Note that data for 2009 is for part of the year upto July. (Adapted from reference 18).

4

have found wide range of applications such as in catalysis[26], organic synthesis[27], separation[28], sensors[29], electrochemistry[30, 31] and energy storage.[32] ILs have also been used as alternatives to conventional organic solvents in organic synthesis[33], solvent extractions[34], thermal lensing[35] and in enzymatic reactions.[36] In addition, ILs have proven to be useful in chromatography as buffers in capillary electrophoresis (CE),[37] stationary phases in gas chromatography (GC)[38, 39] and high performance liquid chromatography (HPLC).[40] A review on analytical applications of ILs have been published.[41]

In the past, ILs was a matter of academic curiosity but are now finding their way into industry. Some industrial applications of ILs such as their uses in solar panels, batteries, fuel cells, lubricants, drug delivery, catalysis, and gas chromatography have been extensively reviewed.[18] Interesting novel uses are being made of the unique physical properties of ILs including sending them to the moon. Borra et al. have proposed the deposition of metal films on an ionic liquid for use in space telescopes.[42] According to Borra and coworkers, this is possible because the non volatile nature of ILs enables their use under the lunar vacuum conditions. In addition, handling of ILs in space is a lot easier since they are less dense compared to the currently used mercury.[42] The future of ILs looks even brighter since an extrapolation of their potential uses extends to almost every possible industrial application process (Figure 1.2).[18] This dissertation focuses on the use of CILs for enantiomeric recognition of chiral analytes using spectroscopy.

1.2. Chiral Ionic Liquids (CILs)

CILs are a subclass of ILs in which the cation or the anion (or both) may be chiral. During the synthesis of the N-heterocyclic carbene complexes based on imidazolium precursors, Herrmann and coworkers[43] prepared two chiral imidazolium chloride salts as synthesis intermediates. However, during this time, the two chiral imidazolium chloride salts were not referred to as CILs in Hermann's work.[43] Generally, CILs are a recent development as compared to achiral ILs. To
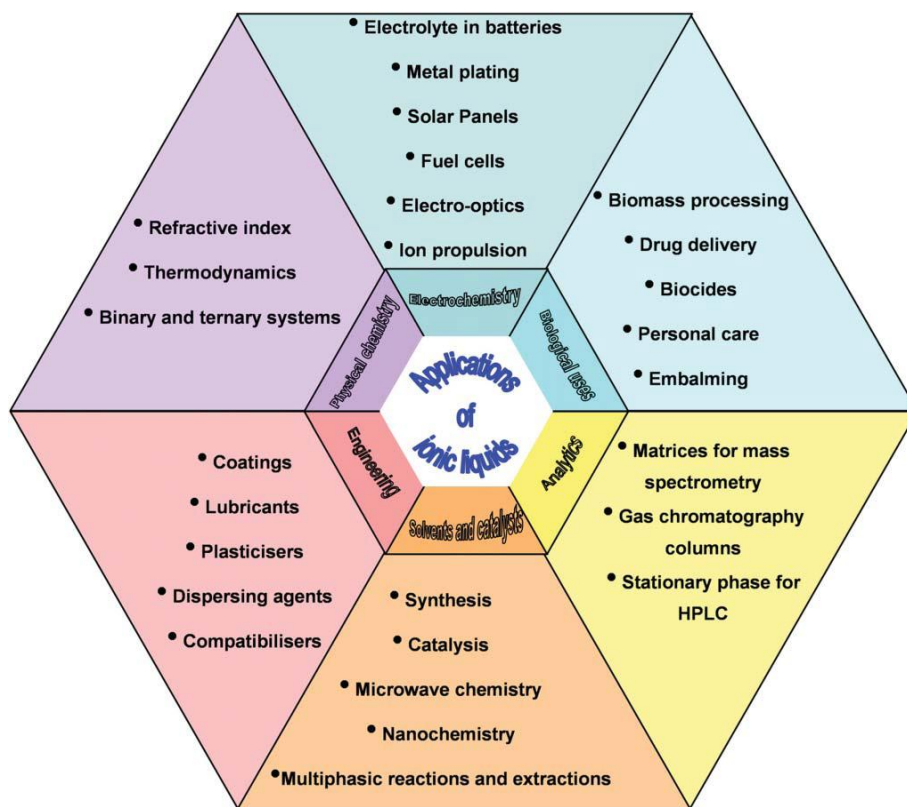
Figure 1.2. Prediction of the future commercial uses of ILs in various fields (adapted from reference 18).

our knowledge, Howarth *et al.* synthesized the first example of a CIL in 1997 with a chiral dialkylimidazolium cation, *N*,*N*-bis[(2*S*)-2-methylbutyl]imidazolium bromide, **1** (Scheme 1.2).[22] This moisture stable imidazolium bromide salt was used as the Lewis acid catalyst in the Diels-Alder reaction.[22] In 1999, Seddon and coworkers reported the first synthesis of CIL containing chiral anion, 1-butyl-3-methyl imidazolium lactate, **2** (Scheme 1.2).[44] To our knowledge, CILs in which both ions are chiral were rare until Machado and Dorta reported the first "doubly chiral" ILs containing imidazolium cations and anions derived from camphor, tartaric acid and β-pinene.[45] Another example of CIL containing both chiral cation and anion, L-alanine butyl ester lactate, **3**, has been reported by the Warner group (Scheme 1.2).[46] Most of the CILs that have been explored have point (or central) chirality. We note that CILs with axial[47] and planar[48] chirality have also been recently synthesized.

6
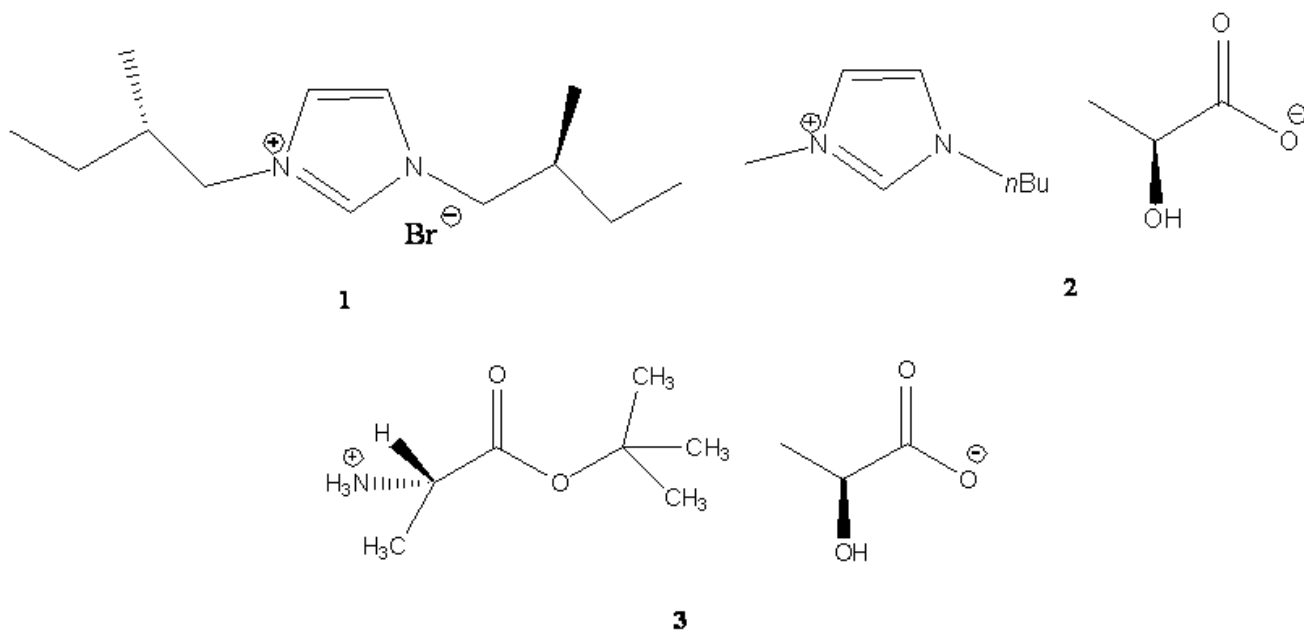
Scheme 1.2. Structural examples of CILs containing chiral: cation (1), anion (2) cation and anion (3).

Since the discovery of CILs, there have been extensive studies on their synthesis and applications. The most commonly used methods in the synthesis of CILs are anion metathesis[46] and acid-base neutralization reactions.[10] Details of the synthesis and applications of various CILs are provided in several outstanding reviews.[49-55] More interestingly, CILs can be designed and tailored to specific applications by simply changing the cation, anion or their combination. The tunability of CILs is one of the unique and highly desirable properties of ILs. The applications of CILs may be categorized into asymmetric synthesis and catalysis, enantiomeric chromatographic separation, and chiral spectroscopic discrimination.[56] Although the the focus of this dissertation is on the use of CILs for enantiomeric recognition using nuclear magnetic resonance (NMR) and fluorescence spectroscopy, the various applications of CILs will be discussed briefly in the following section.

1.2.1. Applications of Chiral Ionic Liquids

1.2.1.1. CILs in Asymmetric Catalysis and Synthesis

As noted earlier, CILs have been used for various applications. In contrast to regular organic solvents, CILs can serve as chiral solvents and catalysts. Moreover, the relatively simple synthesis of CILs from the readily available chiral starting materials such as amino acids and the possibility of recycling CILs (due to their non-volatility) make them promising new chiral solvents in asymmetric catalysis and synthesis. Thus CILs have been used as chiral solvents and catalysts for various organic reactions such as Baylis-Hillman[57], hydrogenation[58], Heck reaction[59], and Michael addition.[60] The application of CILs in asymmetric synthesis and catalysis have been extensively reviewed.[52, 53, 55]

1.2.1.2. CILs in Enantiomeric Chromatographic Separation

The three common methods for enantiomeric separation include gas chromatography (GC), capillary electrophoresis (CE) including micellar electrokinetic chromatography (MEKC), and high performance liquid chromatography (HPLC). CILs can be used for chromatographic separations due to their properties such as high thermal stability and ionic conductivity.

1.2.1.2.1. CILs in GC Separation

The low vapor pressure and high thermal stability of CILs render them suitable for enantioseparations in gas chromatography (GC). Recently, CILs have been used as chiral stationary phases in GC.[61] Armstrong and coworkers carried out enantiomeric separation of chiral alcohols and diols, chiral sulfoxides, some chiral epoxides and acetamides using a CIL based on ephedrinium salt. Another example is the use of the CIL, (R)-N,N,N-trimethyl-2-aminobutanol-bis(trifluoromethanesulfon) imidate as chiral selector for a variety of compounds in GC.[62]

1.2.1.2.2. CILs in CE and MEKC Separation

The conductivity of ILs offers the possibility of using them as electrolytes in CE. Enantiomeric separation using CILs in CE is often a desirable alternative, especially when there is a trace amount of sample available and short analysis time is required. Yuan and coworkers found that the CIL, (R)-N,N,N-trimethyl-2-aminobutanol bis(trifluoromethylsulfonyl)imide, is a good chiral selector that could be used in CE for enantioseparation of various compounds such as propranolol.[62] Recently, Tran and Mejac demonstrated the separation of various pharmaceutical products using a CIL, S-[3-(chloro-2-hydroxypropyl) trimethylammonium] [bis(trifluoromethylsulfonyl)imide,], as co-electrolyte and chiral selector in the presence of additives such as sodium cholate.[63] The chiral buffer was also capable of enantiomeric recognition of iburprofen. It is worth noting that no resolution was achieved when additives were not used. Tran and Mejac suggest that the additives provide the three point interaction required for chiral recognition.[63]

Two CILs [(ethyl and phenyl choline cations with bis (trifluoromethylsulfonyl) imide) anion] have been evaluated by Francois *et al.* as chiral selectors for enantiomeric separation of arylpropionic acids by CE.[64] No direct enantioselectivity was observed for these two CILs, except in the presence of β-cyclodextrins, suggesting that a synergistic effect of the two selectors is responsible for increased resolution and separation efficiency. Tran and Mejac demonstrated an influence of the β-cyclodextrin on the competition between the analyte and the IL cation with respect to β-cyclodextrin complexation. However, the presence of the phenyl group in the IL cation appeared to be less important in enhancing the synergistic effects. This indicates that specific ion-pairing interactions could be involved.[64] Maier and coworkers synthesized a new CIL, [S-(−)-2-hydroxymethyl-1,1-dimethylpyrrolidinium tetrafluoroborate] derived from L-

proline alcohol and found it to be an effective additive to acidic background electrolytes affording the separation of a mixture of five achiral tricyclic antidepressants using CE.[65]

The application of novel IL-type surfactants and their polymers for chiral separation of acidic analytes in MEKC was reported in 2006 by Rizvi and Shamsi.[66] These were derived from the monomers and polymers of undecenoxycarbonyl-L-leucinol bromide which is an IL at room temperature, and undecenoxy carbonyl- L-pyrolidinol bromide, that forms a greasy solid with a melting point of 30-35°C. Chiral separation was suggested to be strongly dependent on the presence of opposite charge as well as the structural compatibility between the chiral selector and the analyte.[66]

1.2.1.2.3. CILs in HPLC Separation

In liquid chromatography (LC), the low vapor pressure of CILs is not a crucial requirement. However, CILs may provide the desired selectivity and solubility for enantiomeric separations. The possibility of replacing organic solvents by ILs in LC is limited by their rather high viscosities. In addition, the use of ILs on silica stationary phases often produces interactions between IL cations and the anionic silanol stationary phase, which lead to peak tailing and longer retention times. To circumvent the aforementioned problems, CILs may be used as additives or silanol blocking agents may be used to afford enantiomeric separation.[67] The CIL, (R)-N,N,N-trimethyl-2-aminobutanol-bis (trifluoromethanesulfon) imidate, has also been used in HPLC for enantioseparation of compounds such as alcohols, amines, and amino acids.[62]

1.2.1.3. Applications of Chiral Ionic Liquids in Enantiomeric Spectroscopic Discrimination

In contrast to chromatographic methods, there is no "real" separation of enantiomers using spectroscopic techniques for chiral discrimination. Interestingly, chiral spectroscopic techniques are very useful in chiral technology for rapid and accurate determination of the enantiopurity of chiral compounds. In addition, spectroscopy may provide important information

regarding the structure-property relationship and mechanism of chiral interaction and recognition. Recently, CILs have been used as the chiral selectors in spectroscopic techniques such as nuclear magnetic resonance (NMR), fluorescence, and near infrared (NIR). In this dissertation, NMR and fluorescence spectroscopy were used for enantiomeric recognition studies.

1.2.1.3.1. Chiral Discrimination Using CILs in NMR Spectroscopy

One of the most common methods employed for analyses of chiral compounds is NMR spectroscopy.[68, 69] In NMR, nuclei can be classified as isochronous or anisochronous. Where diastereotopic protons show the same chemical shift, they are said to be equivalent or isochronous, and where they have different chemical shifts, the protons are described as anisochronous. Enantiomers cannot be discriminated in an achiral medium because the resonances of enantiotopic nuclei are isochronous. However, diastereoisomers may be distinguished as the resonances are anisochronous. As long as there is a large enough nonequivalent chemical shift to give baseline resolution of the appropriate signals, then integration gives a direct measure of enantiomeric composition.[70]

Recently, CILs have been widely used as the chiral solvating agents in NMR studies. In these applications, CILs can be dissolved in deuterated NMR solvents and used as the chiral solvating agent. They can form diastereomeric associates *in situ* with substrate enantiomers via rapidly reversible equilibriums in competition with the bulk solvent. This method is quick and simple to perform with no problems of kinetic resolution or sample racemization which may occur when chiral derivatizing agents are used. Nonpolar solvents such as deuterated chloroform, benzene, and carbon tetrachloride tend to maximize the observed anisochrony between the diastereoisomeric complexes whereas the more polar solvents such as deuterated acetonitrile, dimethyl sulfoxide may solvate the solute and decrease peak splitting.[70]

Most chiral discrimination studies of CILs in NMR have been carried out using Mosher's acid (α-methoxy-α-(trifluoromethyl)phenylacetic acid).[71] Mosher's acid was first introduced as a chiral derivatizing agent by Mosher in 1969.[71, 72] The absence of α-hydrogen in the carboxylic group of Mosher's acid alleviates the problem of racemization during the derivatization. It is now commercially available in enantiopure form, either as the acid or acid chloride. In addition, both the ^{1}H NMR and ^{19}F NMR can be employed to investigate the diastereomeric interactions since Mosher's acid contains both hydrogen and fluorine nuclei. The enantiomeric recognition of the CILs described in this dissertation was investigated using Mosher's sodium salt.

To our knowledge, the first example of ^{19}F NMR investigation of CILs was reported in 2002 by Wasserscheid and co-workers using chiral cations derived directly from the chiral pool.[73] The diastereomeric interactions between a racemic mixture of sodium Mosher's salt as substrate and the ephedrine-based CIL, as the chiral selector was investigated using ^{19}F NMR spectroscopy. The splitting of the racemic Mosher's salt signal using ^{19}F NMR clearly indicates diastereomeric interactions between Mosher's salt and the CIL (Figure 1.3).[73]
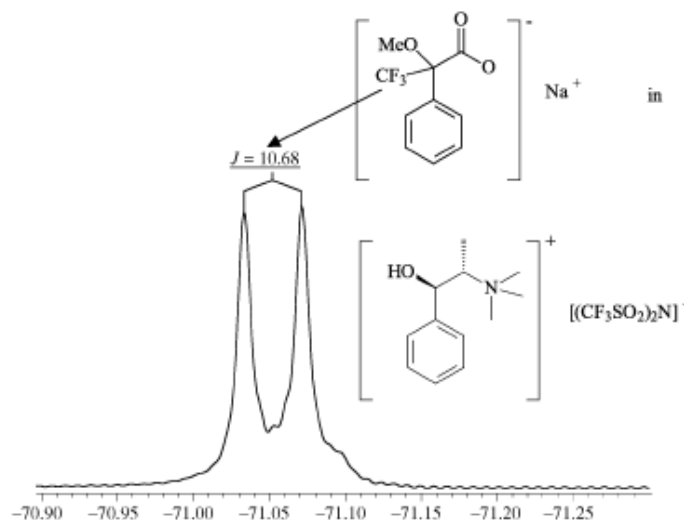
Figure 1.3. ^{19}F NMR of racemic sodium Mosher's salt in presence of ephredrinium CIL. (Adapted from reference 73).

12

The extent of peak splitting can be assigned to the strength of the diastereomeric interactions. In other words, under identical experimental conditions, the greater splitting indicates stronger chiral discrimination abilities of the CILs used as chiral selectors. It is also noteworthy that the chemical shift difference for the two diastereomeric CF_3-groups largely depends on the concentration of the CILs in the deuterated solvent. Generally, the higher the concentration of CIL, the greater the splitting of of the CF_3 signal in ^{19}F NMR. It has also been demonstrated that the addition of water to the chiral ionic liquid solution may increase the extent of signal splitting.[73]

We note that the increase in the extent of peak splitting in presence of added water is dependent on the analyte used. For instance, Guillemin and coworkers while investigating enantiomeric discrimination using valine based CILs found that addition of water to the NMR solvent diminished the chemical shift difference.[74] This is contradictory to the previous findings by Wasserscheid in which the addition of water was found to significantly increase the extent of splitting of the CF_3 signals.[73] The decreased chemical shift difference was attributed to breaking of hydrogen bonds responsible for diastereomeric interaction by the water molecules. These findings suggest that water plays different roles in chiral discrimination depending on the chiral interaction mechanism between the CILs and the chiral analytes.

After the pioneering work by Wasserscheid, a wide variety of CILs have been investigated for their chiral recognition ability using ^{19}F NMR. Examples of these CILs include chiral thiazolinium[75], carbohydrate[76], spiro imidazolium[77], planar cyclophane imidazolium[78], amino acids[79], amino acid esters[46], phenylethylamines[80], and spiral borates.[81]

1.2.1.3.2. Chiral Discrimination Using CILs in Fluorescence Spectroscopy

Fluorescence is a spectroscopic technique which has been widely used to study molecular interactions such as in biological systems.[82] It is also a useful tool for the study of chiral

interaction and discrimination. It can provide useful information about molecular interactions with high sensitivity. The application of fluorescence to specifically study enantioselective interactions and chiral recognition has been reported.[83-85] Most of these fluorescence studies involve the measurements of fluorescence emission intensities, spectral shifts and quenching effects.

Steady state fluorescence spectroscopy has been successfully employed for enantiomeric discrimination of chiral molecules of pharmaceutical products. The emission spectral properties of enantiomers of a chiral molecule are identical in a non-chiral environment. In contrast, enantiomers of chiral molecules have significantly different spectral properties in a chiral environment as a result of induced diastereomeric complex formation with chiral selectors. Differences in the spectral properties of enantiomers in a chiral environment therefore permit the use of fluorescence spectroscopy for effective chiral discrimination of enantiomers. For instance, Tran *et al.* used steady state fluorescence spectroscopy and partial least squares regression analysis to accurately predict the enantiomeric excess of independent samples of propranolol, naproxen, and warfarin.[86] We note that differences in fluorescence lifetime of enantiomers in presence of a CIL have also been used as a measure of chiral discrimination.[87] In this dissertation, steady state has been used for enantiomeric discrimination of various fluorescent and non-fluorescent chiral analytes using amino acid based CILs.

1.2.1.3.3. Chiral Discrimination Using CILs in Near Infrared (NIR) Spectroscopy

The use of NIR for chiral discrimination is particularly appealing due to fast analysis time and inexpensive instrumentation. In addition, almost all organic molecules and most inorganic molecules are known to have NIR absorption of C-H, O-H, N-H or C=O overtone and combination transition. This makes the non-destructive NIR spectroscopy a potentially universal technique for chiral discrimination of guest-host complexes. An example of the practical utility

of near infrared (NIR) spectroscopy for chiral discrimination has been demonstrated by Tran and coworkers using *S*-[(3-chloro-2-hydroxypropyl) trimethylammonium] [bis((tri-fluoromethyl)sulfonyl)amide] CIL.[88] As noted with NMR and fluorescence spectroscopy, the diastereomeric complexes formed by the interaction between the chiral selector and chiral analyte leads to different NIR spectra. Using regressional analysis, the enantiomeric composition of chiral analytes such as atenolol could be accurately and sensitively determined.[88]

1.3. Chirality and Its Significance

Chiral analyses continues to be a subject of great interest because it has been established that enantiomers of a chiral racemic drug may display different properties.[89] Enantiomers are stereoisomers that are non-superimposable mirror images of each other.[90] It is well established that enantiomers of a chiral molecule have the same physical and chemical properties in an achiral medium, but different properties in a chiral environment.[90] Based on this differential interaction with chiral drugs, one enantiomer of a chiral drug may have the desired medicinal properties while the other enantiomer may be harmful.[89, 91] Examples of the effects of different enantiomeric forms of drugs is provided (Table 1.1).[91] The effect of different enantiomeric forms of drugs was witnessed in the 1960s for thalidomide which as administered as a racemate at the time. The incident is sometimes referred to as "thalidomide tragedy" due to the teratogenic effects (birth defects) caused by the S-enantiomer despite the potency of the R-enantiomer in the treatment of morning sickness in expectant women.[92-94]

Due to different effects caused by different enantiomers, the FDA has issued a mandate that requires verification of the enantiomeric form of the drug.[95] This has led to a new trend called "racemic switch" implying that even drugs previously approved as racemates are being sold as single enantiomers.[95] As a result of the policy requirements, the pharmaceutical industry are striving to produce and market enantiomerically pure drugs.[96, 97] Thus there is a need to

develop various chiral selectors and suitable analytical methods to distinguish enantiomers. An effort towards meeting this goal is the subject of part of this dissertation.

Table 1.1. Effects of enantiomeric and racemic forms of various drugs (adapted from reference 91).

Drug	Uses	Effect of enatiomeric or racemic form of drug
Albuterol	Bronchodilator	- L- form therapeutic - Racemate cause irregular heartbeat
Citalopram	Antidepressant	-R- enantiomer ineffective
Fluoxetine	Prevents migraines	- S- enantiomer potent - Racemate has no effect
Ritalin	Treat attention deficit disorder in children	-D- enantiomer is 13 times more potent than L- enantiomer
Thalidomide	Antiemetic to treat morning sickness in expectant women	-S- enantiomer is teratogenic (causes Birth defects)

Consequently, various chiral selectors such as cyclodextrins[98], antibiotics[99], molecular micelles[100], and crown ethers[101] have been widely used because of their chiral recognition abilities. However, the use of many current chiral selectors is often limited due to low solubility, difficult organic syntheses, instability at high temperature, as well as high cost. In addition, many currently available chiral selectors require the use of another solvent and sometimes more than one solvent system if the analyte and the chiral selector are not soluble in the same solvent. Therefore, there is a need for the development of new chiral selectors that can be used simultaneously as solvent and chiral selector. CILs meet this requirement and have been explored as alternative chiral selectors as noted earlier.

In this dissertation, CILs derived from amino acid esters have been synthesized and used for enantiomeric recognition of various chiral analytes. The choice of amino acid esters is based on their inherent chirality thus no chiral induction is required in preparation of the

corresponding CILs. In addition, anion exchange from the commercially available amino acid ester chlorides affords CILs in a single step. Furthermore, amino acid esters have been shown to afford low melting point CILs compared to the amino acid counterparts due to reduced hydrogen bonding.[102] The intrinsic fluorescence of some amino acids enables the preparation of fluorescent CILs for the enantiomeric recognition of analytes with reduced fluorescence emission. This dissertation explores the use of both fluorescent and non-fluorescent CILs for enantiomeric recognition of fluorescent and non-fluorescent analytes.

Spectroscopic techniques including NMR and fluorescence spectroscopy were used for enantiomeric recognition studies of various chiral analytes in presence of CILs. UV-vis was used to determine the absorbance and absorption wavelength maxima of the samples before fluorescence analysis. CD was used to investigate the chiral integrity of the synthesized CILs. These spectroscopic techniques are discussed briefly in the following section.

1.4. Spectroscopic Techniques

1.4.1. UV-Vis Absorption Spectroscopy

UV-vis absorption is molecular characterization technique used for analysis of molecules that absorb ultraviolet and visible light. A schematic of a UV-vis absorption spectrophotometer is shown (Figure 1.4).[103] The light source produces radiant energy that passes through a monochromator which selects the desired wavelengths. The beam splitter results in two beams of light through the sample and the reference cells respectively. The two light outputs (transmittances) are amplified and their ratios (or log of ratios) are electronically amplified giving a measure of absorbance. The absorbance is proportional to concentration according to Beer's law equation; $A = \varepsilon bc$, where A is the absorbance, ε is molar absorptivity, b is sample path length and C is the concentration.
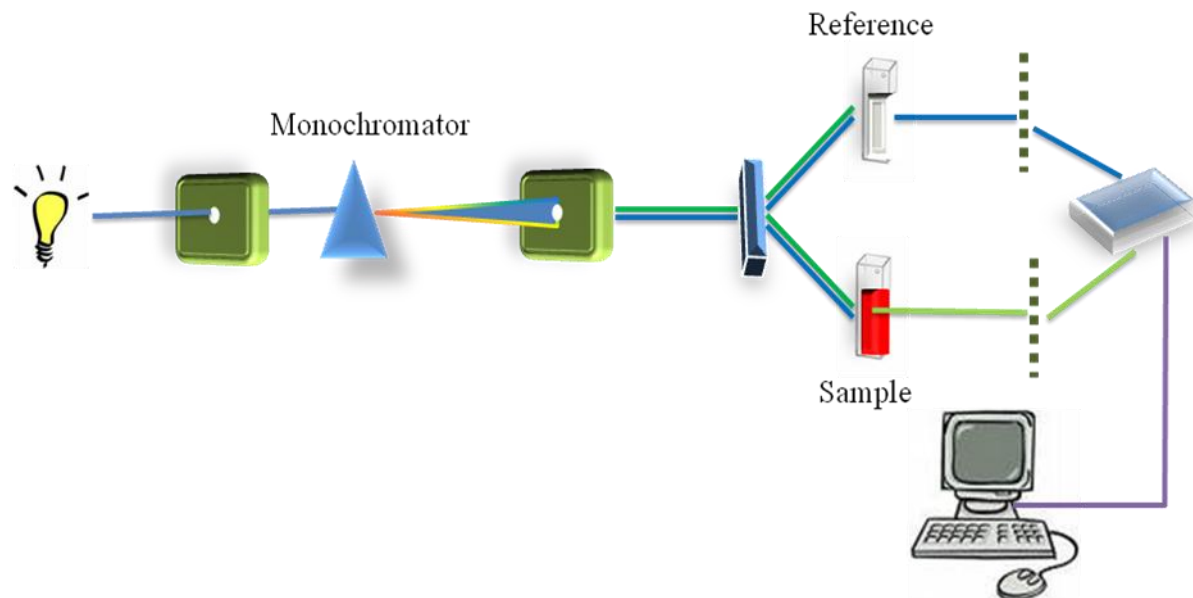
Figure 1.4. Schematic representation of a UV-vis spectrophotometer.

1.4.2. Circular Dichroism Spectroscopy

Circular dichroism (CD) is an optical technique used to determine the optical configuration of chiral molecules. Enantiomers of a chiral molecule have opposite CD bands indicating rotation of circularly polarized light in opposite directions. CD technique was used to confirm retention of chiral configuration of the synthesized CILs. A schematic of a CD instrument is shown (Figure 1.5).[104]
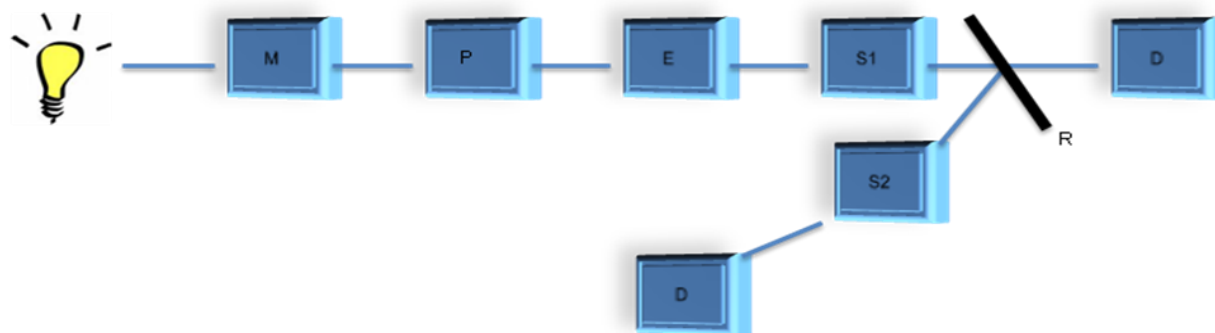
Figure 1.5. Schematic representation of a CD spectropolarimeter. (M, monochromator; P, polarizer; E, electrooptic modulator; S1, sample cell; S2, reference cell; D, photomultiplier; R, mirror.

The light from the source passes through a monochromator which selects the desired wavelengths. The circularly polarized light is absorbed on the basis of chirality of the molecules in the sample. The transmitted light is elliptically polarized hence the term ellipticity used to describe CD measurements. A second photomultiplier detector is necessary when difference CD is required. This is achieved by reflecting the light from the sample through the reference using a mirror into the second detector.

1.4.3. Fluorescence Spectroscopy

In this study, fluorescence spectroscopy was used for enantiomeric recognition studies of various chiral analytes. In addition, it was used to investigate the spectral properties of fluorescent GUMBOS and nanoGUMBOS. Fluorescence is the radiative transition between states of the same multiplicity. The processes involved in molecular fluorescence is illustrated by the Jablonski diagram (Figure 1.6).[105, 106]

Light absorption (A) from the ground state to the higher electronic states takes place on the order of femtoseconds (10^{-15}s). According to the Franck Condon principle, we can assume that no nuclear displacement occurs in such a short time and therefore all transitions are vertical. The absorbed light undergoes internal conversion (IC) to the lowest vibrational level of S_1, a fast relaxation process that occurs on the order of picoseconds (10^{-12}s). This is followed by fluorescence within about 10^{-8}s as the photon returns to the ground state. Since the energy of emission is lower than that of absorption, fluorescence occurs at a longer wavelength (Stokes shift). The emission spectrum is a mirror image of absorption spectrum (Franck Condon principle). In the excited S_1 state, molecules can undergo spin conversion to the first triplet state (T1). This process is called intersystem crossing (ISC) and occurs at a longer wavelength than fluorescence. Heavy atoms such as bromine and iodine tend to enhance phosphorescence by facilitating ISC.

Light from the source (mostly xenon lamp) passes through the monochromators to select excitation and emission wavelengths. The gratings in the monochromators decrease stray light. The emitted light from the sample monchromator is at 90° configuration to the excitation light (Figure 1.7). This is to minimize the intense excitation light from reaching the detector which would otherwise lead to poor detection of the relatively less intense fluorescence signal. The light through the sample is detected usually with a photomultiplier tube and quantified with electronic devices, presented in graphical form and stored in computers.
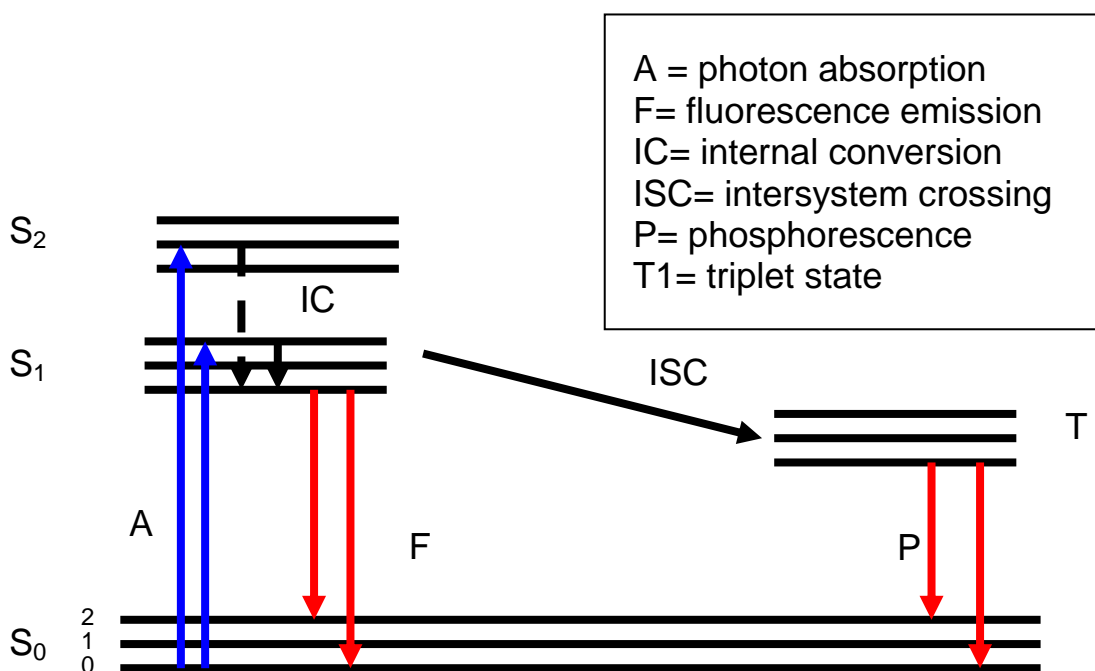
Figure 1.6. Jablonski diagram.
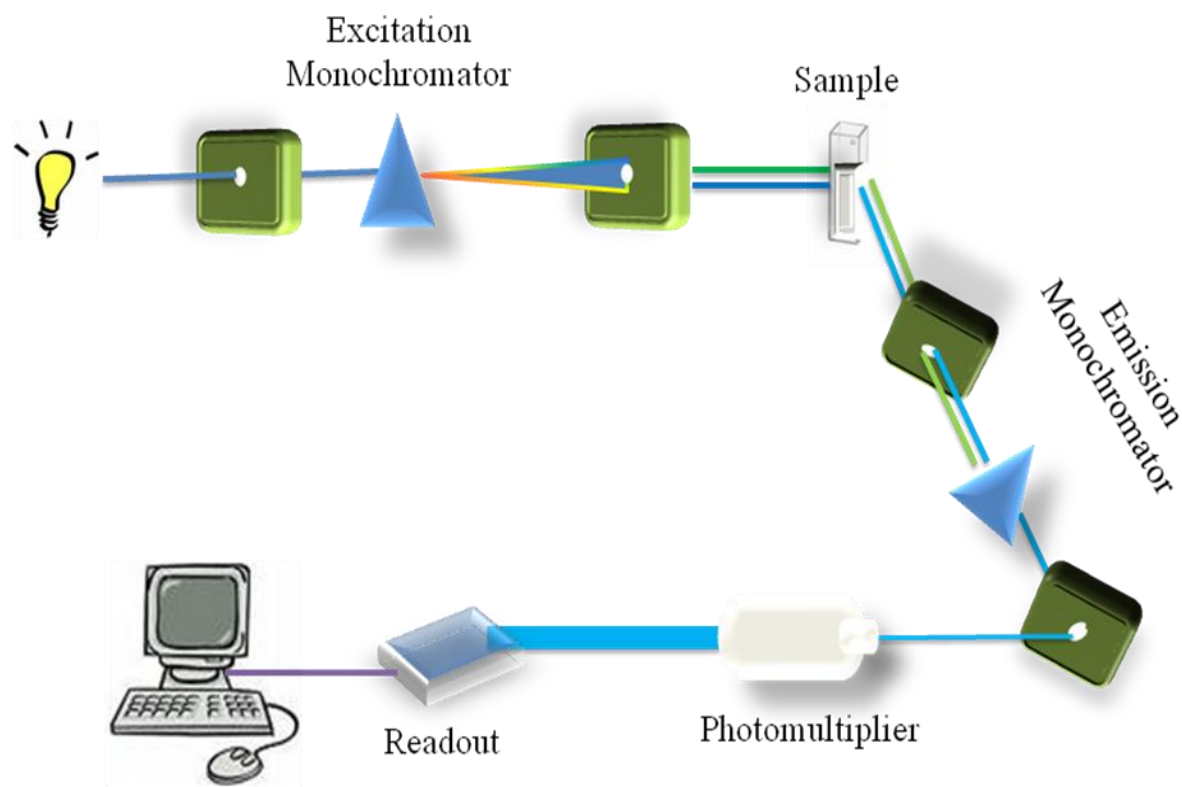
Figure 1.7. Schematic representation of a fluorometer.

1.5. Ionic Liquids and Nanotechnology

ILs have been traditionally sought for use as solvents in various reactions. Interestingly, although ILs are defined as organic salts with melting point at or below 100°C, there has been little attention paid to ILs that exist in the solid state above room temperature. This is evidenced by disappointment expressed by various researchers in the field of ILs whenever they obtain solid products in their quest for RTILs. The pursuit for RTILs has actually led to investigations such as using compressed CO_2 to depress the melting point of frozen ILs.[107] Such an example emphasizes that the focus on ILs research is mainly on the RTILs as further exemplified by the following excerpt from the article by Scurto and coworkers, "Often useful functional groups

yield solid salts. A methodology or process to increase the range of ionic compounds for use as solvents would be highly useful."[107] Another example in which obtaining solid ILs was regarded as unfortunate since RTILs was desired is in the synthesis of amino acid CILs as solvents for asymmetric synthesis by Bao and coworkers.[108] Further examples in which the desired solvent properties of RTILs sometimes proved elusive precluding the application of TSILS include their uses in metal extraction[23] and enantioselective synthesis.[73]

To our knowledge, the Warner group set the first precedence that would possibly open an opportunity for frozen ILs by preparing novel nanomaterials.[109] Such IL nanomaterials are expected to have properties of ILs. In addition, they can be tailored to produce nanomaterials with properties that meet specific tasks by careful choice of the cation and the anion. Even more interestingly, the high melting point of the salts is no longer a limitation, and therefore more applications for these nanomaterials may be realized. This idea also comes in the wake of tremendous interest in ILs over the last two decades as reflected by the steeper than exponential growth in the number of publications and patents as shown earlier (Figure 1.1).[18] Interestingly, the number of publications and patents in the field of nanotechnology also increased steadily in a fashion somewhat similar to that of ILs over the last decade.[110, 111] The steady increase in nanotechnology papers and patents is illustrated in Figure 1.8.[111] It is with the consideration of unique and interesting properties of ILs and nanomaterials that our research efforts focused on preparation of nanomaterials from ILs. Consequently these materials have been termed Group of Uniform Materials Based on Organic salts (GUMBOS). In this dissertation, we explore the synthesis of near infrared (NIR) fluorescent GUMBOS and nanoGUMBOS for potential biomedical imaging applications.

A
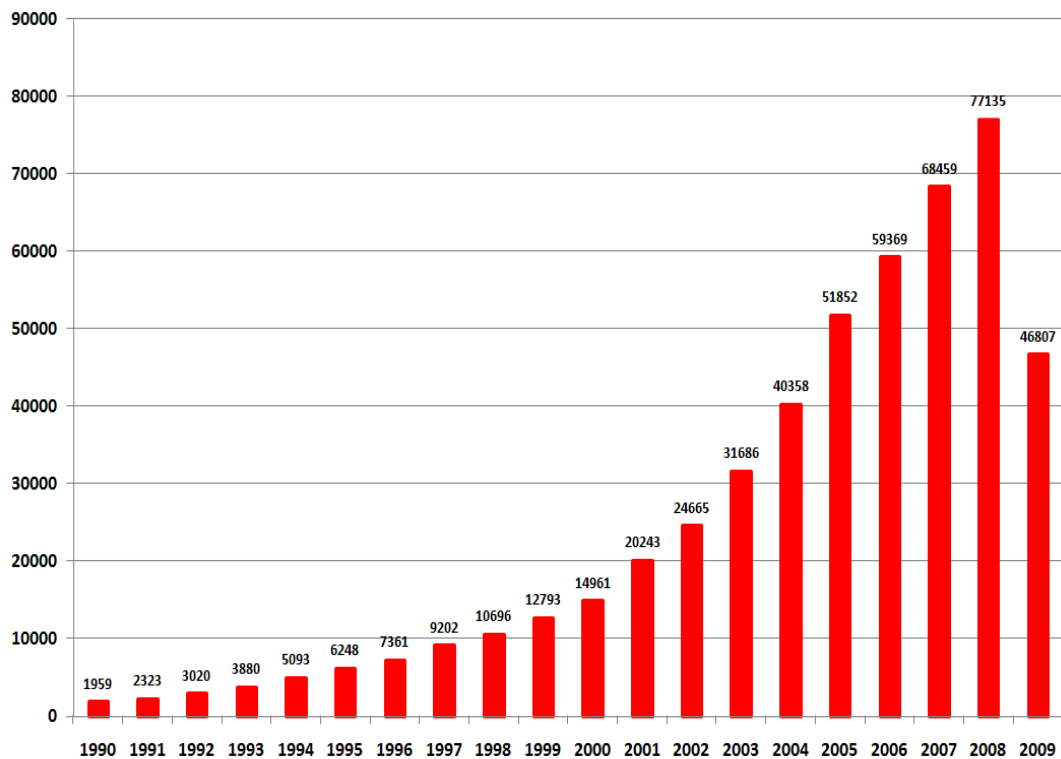
B
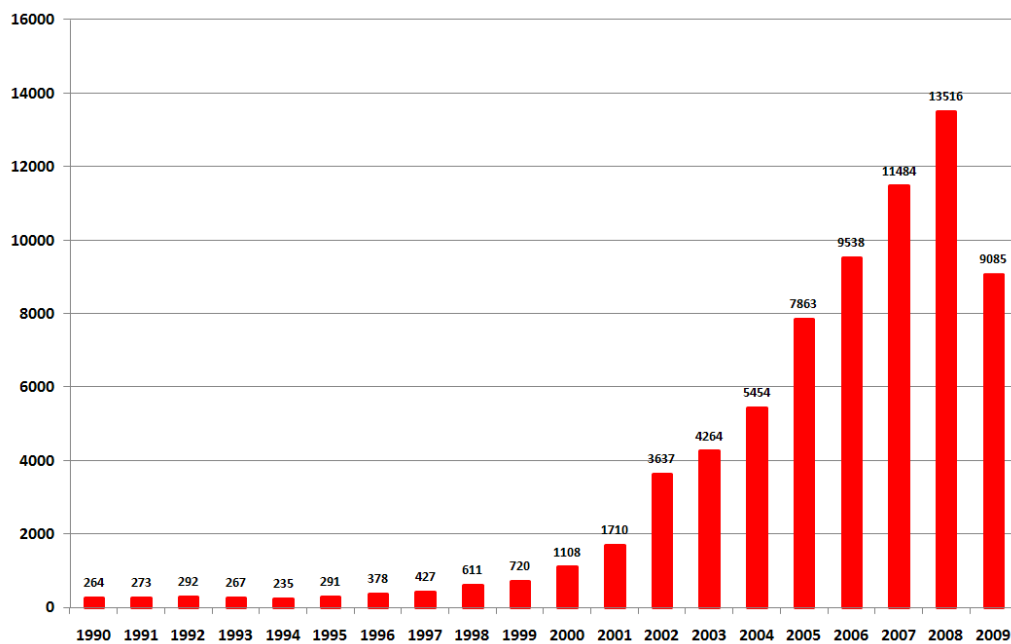
Figure 1.8. Annual growth of nanoparticle research (A) publications, and (B) patents from 1990-2009. Note that data for 2009 is for part of the year, only upto July. (Adapted from reference 111).

1.5.1. NIR Fluorescent GUMBOS and NanoGUMBOS for Biomedical Imaging

1.5.2. Significance of NIR Spectral Region as a Diagnostic Window

Dyes that emit light in the NIR region have potential applications in areas such as analytical and sensor development[112], laser dyes[113], organic light-emitting diodes (OLEDs)[114], invisible printing inks[115], probes for photodynamic therapy[116], and contrast agents for biomedical imaging.[117-119] In addition, NIR fluorescent nanoparticles are of considerable interest for *in vivo* imaging because of the low absorption coefficient of human skin tissue in the long NIR wavelength region (700-1100 nm) (Figure 1.9).[120-122] This results in a high signal to noise ratio due to minimum autofluorescence from tissues. Since light scattering is inversely proportional to the fourth power of wavelength, there is less scattering in the long NIR wavelength region.[123] Generally, NIR optical imaging is biologically safe and tissue depths of up to 12 cm have been successfully visualized.[122]
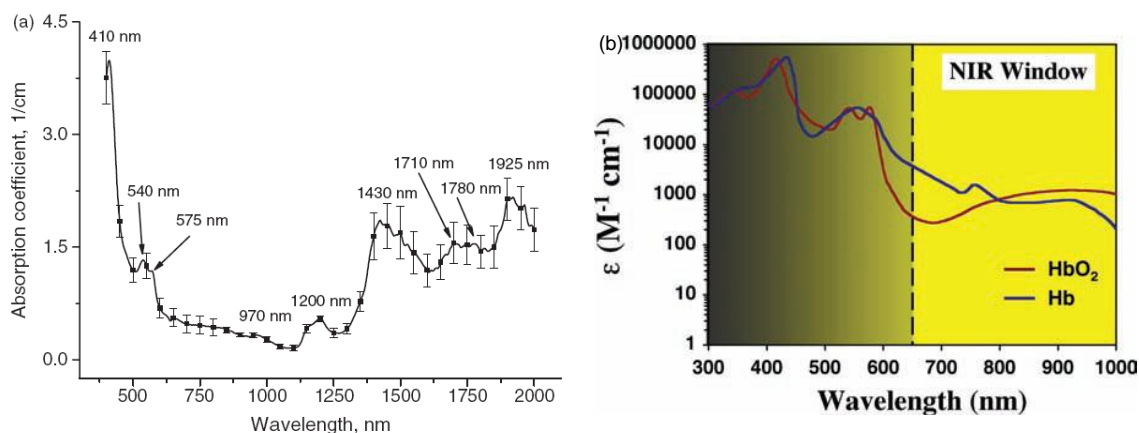
Figure 1.9. (a) Absorption coefficient of human skin tissue as a function of wavelength (Adapted from reference 120), and (b) Absorption extinction coefficient (on a log scale) as a function of wavelength for deoxyhaemoglobin (Hb) and oxyhaemoglobin (HbO$_2$). (Adapted from reference 121).

1.5.3. NIR Fluorophores for *in vivo* Imaging

Ideally, *in vivo* imaging requires NIR dyes with strong absorbance and fluorescence emission in the NIR spectral range, photostable, as well as devoid of phototoxic effects.[121, 124] In addition, the NIR dyes should be safe and easily cleared from the body.[121, 124] In reality, obtaining such NIR dye that meets all the requirements is a challenge. Several materials have been explored for their emission properties in the NIR region including quantum dots[125-127], single walled carbon nanotubes[128-130], lanthanides[131], fluorescent proteins[132], fluorophore conjugated polymers[133], gold nanoshells[134], and organic dyes.[135, 136] However, there are safety concerns on the use of most of these materials. For instance, despite their high photoluminescence efficiency, the microbial toxicity of quantum dots is well documented.[137] Single walled carbon nanotubes are also useful for photothermal cancer therapy[130]; however, the nanotubes have proven to significantly retard embryo development in zebrafish raising safety concerns.[138] Due to these safety concerns, indocyanine green (ICG) is currently the only NIR organic dye approved by the FDA for use in humans.[136, 139, 140] The low toxicity of ICG (LD_{50} of 50-80 mg/kg) has made it useful for bioimaging such as in coronary angiography[141], evaluation of hepatic function[142] and monitoring blood flow.[143] Table 1.2 provides a summary of the merits and limitations of some of the aforementioned NIR emitting materials.

Clearly, there is a limited number of NIR emitting materials for biomedical applications. In addition, ICG that is clinically proven as a contrast agent has some drawbacks such as low fluorescence quantum yield[144], poor hydrostability[145] and protein binding.[146] This suggests that there is need to explore new NIR fluorescent materials for biomedical imaging applications. This dissertation describes our research efforts towards preparation of new class of NIR fluorescent materials we refer to as GUMBOS (Group of Uniform Materials Based on Organic Salts) for

biomedical imaging. The GUMBOS were subsequently used to make nanoGUMBOS for biomedical imaging applications.

The use of contrast agents for early detection of diseased tissues such as tumors is advantageous for early disease treatment.[147] For instance, NIR contrast agents have been used for non-invasive imaging of the lymphatic system to evaluate drainage in cancerous patients.[148] This is possible because tumors generally tend to be more permeable to the contrast agents due to enhanced permeability and retention effect (EPR) attributed to poor lymphatic drainage by cancerous cells.[149, 150] The EPR phenomenon is illustrated in Figure 1.10.[150] The use of nanoparticles as contrast agents is particularly attractive because their small size (defined as 1-100 nm)[150] permits them to escape renal filtration and accumulate in the leaky tumor cells.[150, 151] In addition, various studies have shown that fluorescent nanoparticles may exhibit amplified signal as well as prolonged *in vivo* stability.[152-155]

Most contrast agents used for bioimaging are encapsulated in some form of delivery agent such as silica or polymeric nanoparticles.[153, 156] Such nanoparticle systems have suffered from dye leakage or encapsulation inefficiencies.[153, 156] In an effort to alleviate these problems, we explore the fabrication of NIR fluorescent nanoGUMBOS without doping or encapsulating the dye. In addition, the GUMBOS are expected to enjoy the properties of frozen ILs such as negligible vapor pressure and the capability of tuning the properties by judicial choice of cation and anion. The GUMBOS were prepared via anion exchange of the fluorescent NIR halide with various anions. The nanoGUMBOS were synthesized using a simple, additive free reprecipitation method and their bioimaging potential was explored by Vero cell labeling and imaging using fluorescent microscopy. The synthesis, characterization and biomedical imaging potential of these new NIR nanoGUMBOS are discussed in the following sections.

Table 1.2. Advantages and disadvantages of common NIR fluorophores

NIR fluorophore	Advantages	Disadvantages
Organic dyes	-Safety: IndoCyanine Green (ICG), an organic dye is the only NIR dye approved by FDA for use in humans -Have desired photophysical properties in the NIR spectral region	-Poor photostability -Poor hydrostability -Low quantum yield in aqueous medium
Quantum dots	-Photostable -Have high luminescence efficiency	-Low molar absorptivity and quantum yield in NIR spectral region -Absorption and emission size dependent -Laser excitation damage biological samples -Limited functionalization -Toxic
Fluorescent proteins	Useful for live cell fluorescence imaging	-Limited colors available -Prone to photobleaching
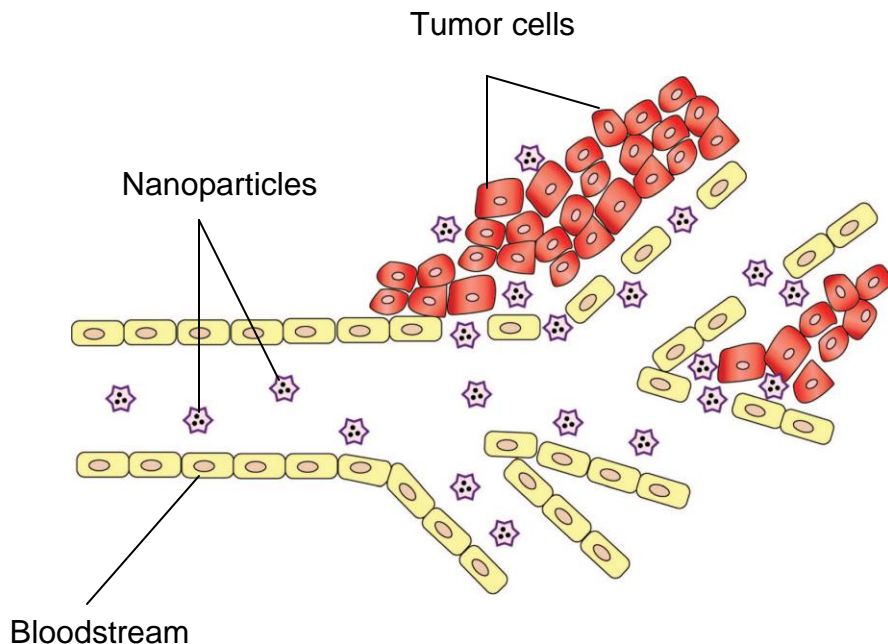
Figure 1.10. Nanoparticles exit blood vessels in the tumor owing to the enhanced permeability and retention (EPR) effect. (Adapted from reference 150).

1.5.4. Synthesis of NanoGUMBOS

In general, there are several methods used to prepare nanoparticles such as aerosol preparation, sol-gel process, microemulsions templates and reprecipitation methods. In this dissertation, the nanoGUMBOS were fabricated using simple, additive free reprecipitation method by dispersing the nanoGUMBOS in water at room temperature.

1.5.4.1. Reprecipitation Method for the Synthesis of NIR NanoGUMBOS

The reprecipitation method being simple and additive free has been employed for the preparation of various organic nanoparticles.[157-160] In the reprecipitation method used in this study, the target compound is first dissolved in an organic solvent (such as alcohols, acetonitrile or acetone) to obtain a millimolar (mM) concentration range. This is followed by rapid injection of a few microlitres of the solution into a vigorously stirred (or sonicated) poor solvent (water is commonly used) at constant temperature (usually room temperature). Reprecipitation of the

28

target compound takes place in the poor solvent affording nanoparticles dispersed in the dispersion medium. An example of the reprecipitation process for the synthesis of NIR nanoGUMBOS described in this dissertation work is depicted in scheme 1.3.

We note that hydrocarbon solvents (such as hexane, heptane, and iso-octane) may be used as poor sovents for nanoparticle fabrication of water soluble compounds. The only requirement is that the target compound should be soluble in corresponding hydrocarbon miscible solvents such as acetone. It is also interesting that the nanoparticle dispersion has the same color as the dissolved stock solution. There are factors that affect the shape, size and spectral properties of reprecipitated nanoparticles such as the concentration of the injected solution, temperature of the poor solvent, aging time and additives in the poor solvent (such as surfactants).[157-160]
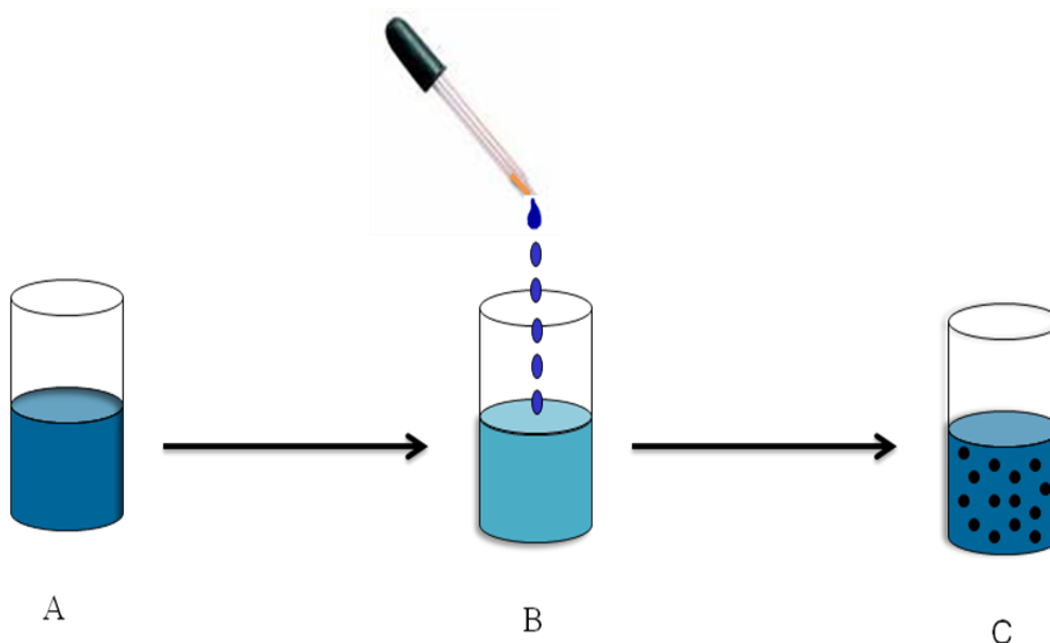
Scheme 1.3. Scheme of reprecipitation process of nanoGUMBOS fabrication showing (A) 1 mM stock solution of NIR GUMBOS solution in ethanol, (B) injection of 100 μL of the NIR GUMBOS solution into 5 mL of deionized water while stirring or sonicating the mixture at room temperature, and (C) reprecipitation of NIR GUMBOS to afford NIR nanoGUMBOS dispersed in water.

1.6. Characterization of NanoGUMBOS

The size and size distribution of the resultant nanoparticle suspension was determined using dynamic light scattering (DLS). The shape and size of the nanoGUMBOS was further confirmed using electron microscopy such as transmission electron microscopy (TEM). In addition, the aforementioned UV-vis and fluorescence spectroscopy was used to analyze the spectral properties of the nanoGUMBOS. The use of nanoGUMBOS for biomedical imaging was evaluated by cellular labeling studies using Vero cells and an epifluorescent microscope was used for cell imaging. These instrumental techniques are discussed briefly in the following section.

1.6.1. Dynamic Light Scattering (DLS)

DLS is among the techniques used for particle size determination based on the scattering of laser light. Other light scattering methods include static light scattering (SLS), photon correlation spectroscopy (PCS) and quasi-elastic light scattering (QELS). DLS was used to determine the size of particles investigated in this dissertation. In DLS, light scattered from nanoparticle surface in all directions is recorded as a function of time.[161] This is in contrast to SLS in which the scattered light is colleted as a function of direction. The Brownian motion of particles is correlated to the fluctuations in intensity of scattered light.[161] The diffusion coefficient is obtained from this relationship enabling the determination of the particle size from the Stokes-Einstein equation:

$$r = k_B T / 6\pi\eta D$$

Where r is the radius in m; k_B Boltzmann constant (1.380×10^{-23} J. K^{-1}; T is the temperature in kelvins; η is the viscosity in pascals per second (or centipoles); D is the diffusion coefficient in $m^2 s^{-1}$.

1.6.2. Transmission Electron Microscopy (TEM)

TEM is an electron probe technique in which a beam of electrons is transmitted through the specimen resulting in formation of an image due to the interaction of electrons with the sample.[161] The specimen needs to be a few nanometers (~ 100 nm) in thickness (i.e. ultrathin) in order to be transparent to the electron beam. In addition, the electron beam is operated in a vacuum (achieved using pumps) to avoid the deflection of the lighter electrons by the relatively heavier gas molecules.[161] A schematic representation of a TEM microscope is shown in Figure 1.11.
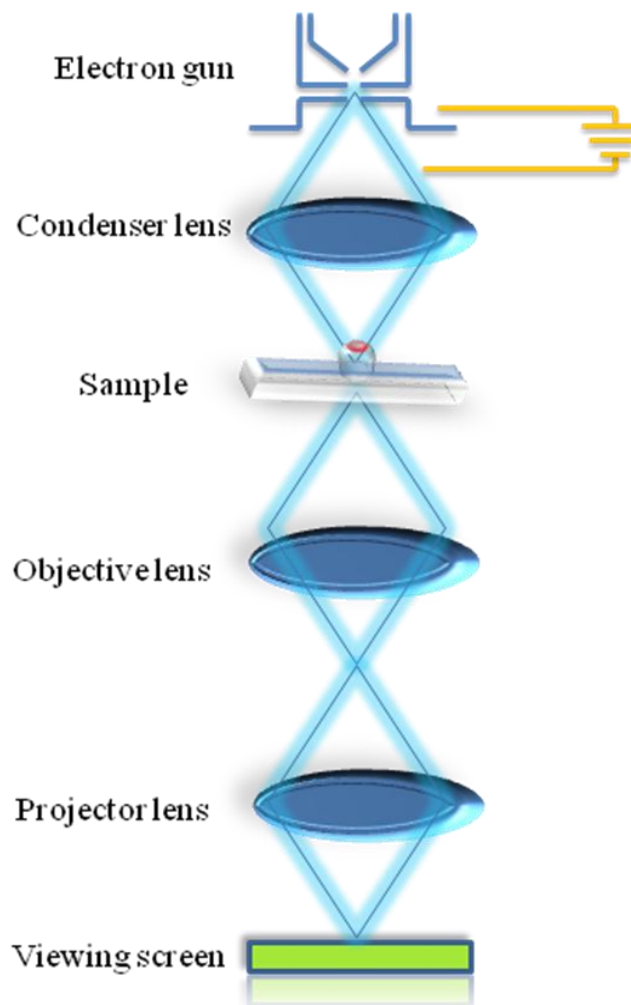
Figure 1.11. Schematic representation of TEM microscope.

The electron gun produces a stream of electrons accelerated at high voltage (100-400kV). The electrons are accelerated by an anode through an aperture via the condenser lens which focuses the electrons onto the sample. The sample is usually dropcasted onto a copper coated carbon grid (100 μm thick, 3 mm diameter). The electrons transmitted through the sample passes through another aperture onto an objective lens and are projected for viewing onto the phosphor fluorescent screen by the projector lens. The CCD camera captures the "shadow" of the image based on the density of the sample components.[161]

The advantages of using TEM imaging include high resolution (in the range of 0.05 nm) and the capability to image any type of sample including conductors, semiconductors and insulators.[161] However, TEM has some limitations such as extensive sample preparation which is time consuming, limited number of samples that can be imaged, small field of view, change in structure and morphology of the sample due to high electron energy which also leads to damage of biological samples. In addition, the requirement of vacuum conditions increases the cost of TEM operation and maintenance.

1.6.3. Fluorescence Microscopy

Fluorescence imaging is widely used in both medicine and biological sciences. To our knowledge, the use of fluorescence imaging in the field of medicine was first reported in 1924. It was observed that the endogenous porphyrins exhibited autofluorescence in tumors when irradiated with ultraviolet light.[162] Since then, fluorescence has evolved into a highly developed imaging system with the use of fluorescein[163] and NIR fluorophores[118] to image brain tumors. NIR fluorophores have since gained more popularity due to the aforementioned advantages such as better light penetration and minimum autofluorescence in the NIR wavelength range. In this dissertation, cellular uptake of the NIR nanoGUMBOS by Vero cells was monitored using an epifluorescent microscope.

In principle, fluorescence microscopy involves irradiation of the sample with the appropriate band of wavelengths, and detection of the emitted light. In an epifluorescent microscope which was used for this study, the excitation and observed fluorescence is from above (*epi-*) the sample. A diagram illustrating an epifluorescent microscope is shown below (Figure 1.12).
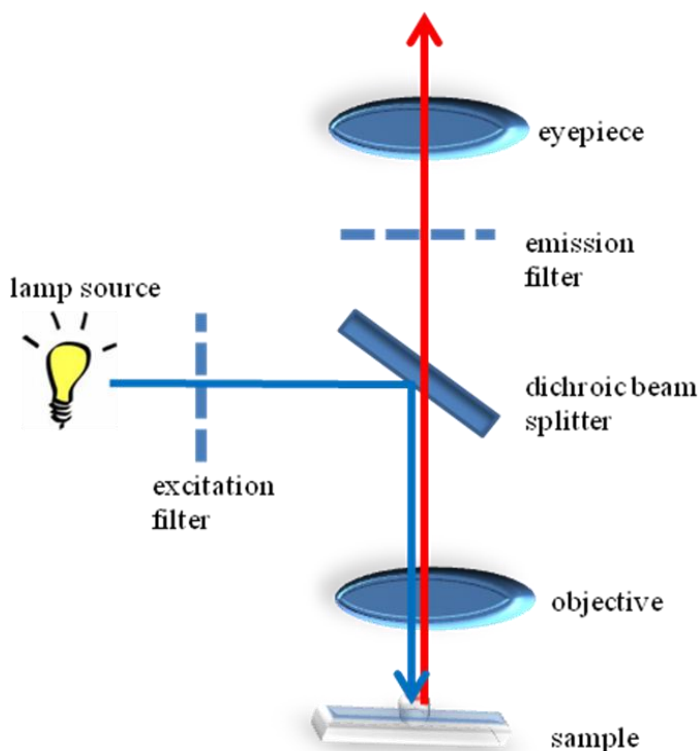
Figure 1.12. Schematic diagram of an epifluorescent microscope.

As depicted in Figure 1.12 above, the excitation light from the lamp source passes through an excitation filter where desired wavelengths are selected. The selected wavelengths reach the dichroic mirror tilted at 45-degree angle which reflect the light at a right angle through the objective onto the sample. In this study, the sample represents the Vero cells labeled with NIR fluorescent nanoGUMBOS. The fluorescence emission from the irradiated sample is

collected by the objective forming a fluorescent image. Since the emitted light is of longer wavelengths than excitation light (due to the aforementioned Stokes shift), it can pass the dichroic mirror through the emission filter onto the detector (CCD camera was used to capture the images in this study). We note that a Zeiss Axiovert epifluorescent microscope used in this study incorporates the light source, the excitation filter, dichromatic mirror, and emission filter into an optical block referred to as a cube.

1.7. Fluorescent NIR Aggregates

The NIR nanoGUMBOS described in this dissertation displayed spectral properties that were strikingly different from that of the corresponding GUMBOS dilute solution. Such spectral differences have been associated with and may be due to formation of molecular dye aggregates. This observation prompted our investigation of the type of aggregation that may be exhibited by the NIR fluorescent nanoGUMBOS. Current extensive research in molecular dye aggregation is stimulated by their uses in various fields such as light harvesting systems[164-167], photovoltaics[166], and light emitting diodes.[166]

There are two types of molecular dye aggregates namely, J and H-aggregates. The J-aggregates (also known as Scheibe aggregates) were discovered independently in 1936 by Jelly[168] and Scheibe.[169] In this pioneering work, a high concentration of a pseudoisocyanine (PIC) dye depicted in Scheme 1.4 exhibited a narrow red shifted absorption band compared to the monomer.[168, 169] In addition, the fluorescence emission had narrow band and small Stokes shift. Initially Scheibe postulated that this was due to reversible polymerization of chromophores.[169] This observation is now ascribed to strong coupling between transition dipole moments of the molecules resulting in excitonic states upon optical excitation.[170, 171]
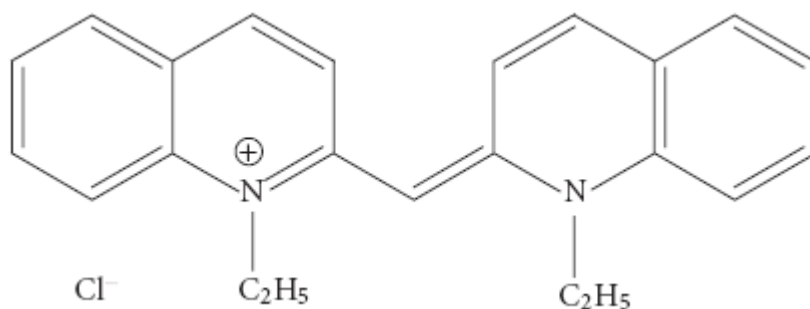
Scheme 1.4. Pseudoisocyanine chloride (PIC).

Since their inception, considerable attention has been paid to molecular dye aggregates due to the aforementioned potential applications. In addition, the possibility of both H and J aggregates exhibiting superradiance, a phenomena resulting from cooperative emission has sparked tremendous interest in studies of molecular self assemblies.[172, 173] Conceptually, the molecules are arranged in a "brickwork" manner in J-aggregates whereas in H-aggregates, the molecules exhibit "card-pack" arrangement (Figure 1.13).[174]
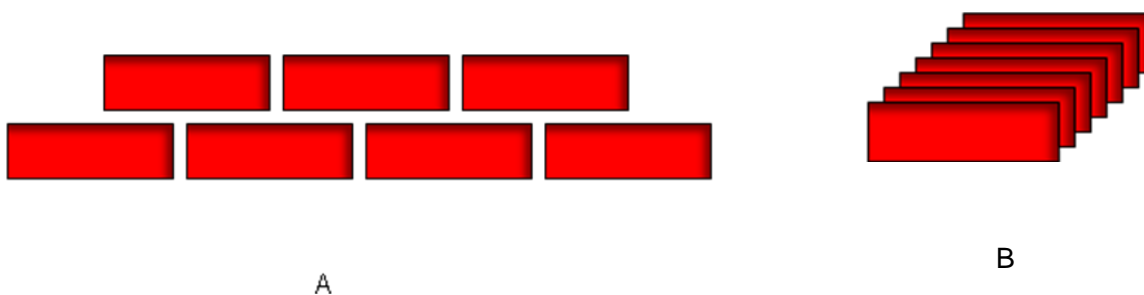
Figure 1.13. Representation of molecular arrangements in aggregates showing (A) "brickwork" arrangement in J aggregates and (B) "card-pack" arrangement in H-aggregates).

An energy level diagram has been proposed by several groups to explain the dye aggregation phenomenon.[175-177] In general, the type of aggregate formed is determined by the type of

transitions from the excitonic interactions between electronically coupled chromophores. Large hypsochromic shift in absorption typical for dye H-aggregates is attributed to transition dipole interactions between two or more chromophores (H-aggregates) arranged parallel to each other with a small dislocation (Fig. 1.14).[177] The excited state is split into two components $m+$ and $m-$, due to the interaction of two transition dipoles M1 and M2. There is a parallel arrangement of the molecules in H-aggregates and the allowed $m+$ state has a higher energy than the $m-$ state and the excited monomer (Fig. 1.14), leading to hypsochromic shift in absorbance compared to the monomer. Note that the $m+$ state undergoes fast internal conversion process to the non-emitting $m-$ state accounting for quenched emission in H-aggregates and a large Stokes shift (Figure 1.14).[177] In contrast, the allowed $m+$ state in J-aggregates has a lower energy relative to the monomer leading to bathochromic shift in absorbance. In addition, there is no internal conversion to an intermediate non-emitting state and hence J-aggregates are highly fluorescent with a small Stokes shift (Figure 1.14).

Several factors affect the type of aggregates formed including dye structure, dye concentration, solvent polarity, pH, ionic strength, and temperature.[178] It is worth noting that the properties of dye aggregates may also be influenced by interaction with biomolecules.[174] For instance, such an interaction may enhance the low fluorescence quantum yield of H-aggregates while quenching the more fluorescent J-aggregates. The fluorescence enhancement phenomenon have been utilized by Gabor and coworkers for non-covalent labeling of the biomolecules.[174] It is envisaged that an understanding and characterization of the tunable aggregates formed by the NIR nanoGUMBOS described in this dissertation will be useful in exploiting the full potential of these novel nanomaterials.
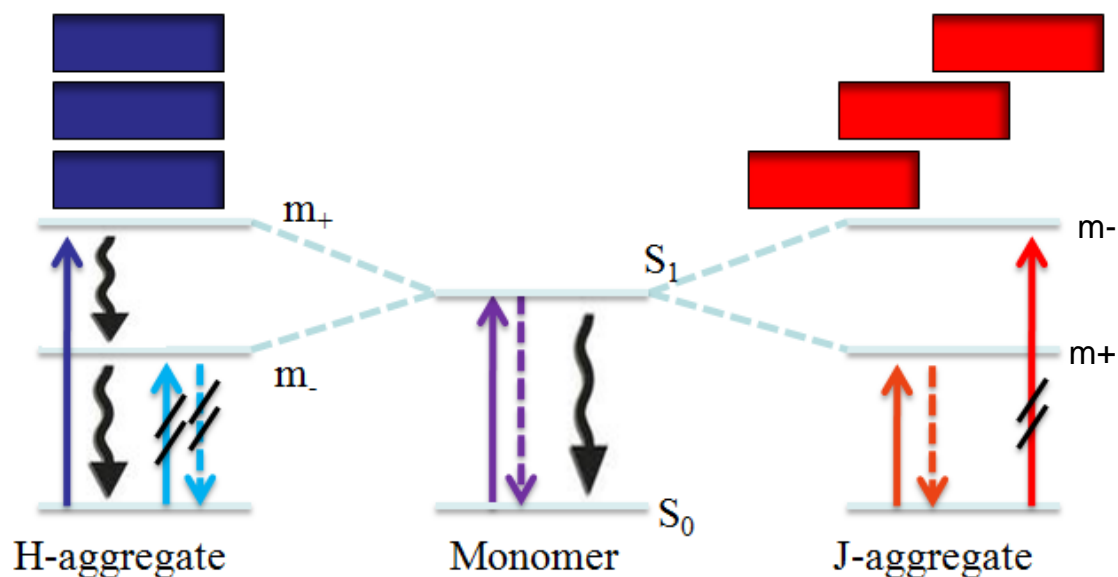
Figure 1.14. Proposed energy diagram for the formation of H- and J- dye aggregates and the resulting absorption and fluorescence properties. The blue and red blocks represent dye molecules, solid arrows mark the absorption, broken arrows the fluorescence and wavy arrows the internal conversion, crossed lines are forbidden transitions. $m+$ and $m-$ are the splitted excitonic states whereas only $m+$ is allowed for light transitions. (Adapted from reference 177).

1.7.1. Characterization of NIR NanoGUMBOS Aggregates: Fluorescence Anisotropy

In addition to UV-vis spectroscopy and steady state fluorescence spectroscopy described earlier, fluorescence anisotropy was used in this study to determine the predominant aggregation type in the NIR nanoGUMBOS as a function of varying the anion. We note that fluorescence anisotropy has been used extensively to study aggregation behavior of various fluorophores.[179-182] Most of these studies reveal that molecular stacking in H aggregates results in slower rotational diffusion and higher anisotropies. However, the enhanced intermolecular interactions often lead to quenched fluorescence. In contrast, the less rigid head-to-tail arrangement in J aggregates leads to higher rotational diffusion and lower anisotropies. Due to less intermolecular interactions, J aggregates are usually highly fluorescent. In this dissertation, fluorescence anisotropy for dilute GUMBOS solution and nanoGUMBOS was used to determine the predominant aggregation behavior in the nanoGUMBOS containing various anions.

The principle of fluorescence anisotropy is photoselective excitation of fluorophores by polarized light.[106] Figure 1.15 illustrates the measurement of fluorescence anisotropy. The sample is excited with vertically polarized light and the emission through the polarizer is measured. There is preferential absorption of photons with electric vectors aligned parallel to the transition moment of the fluorophore. This process called photoselection results in polarized emission. The intensity observed is either parallel (I_{vv}) or perpendicular (I_{vh}) to the direction of polarized excitation.[106] Anisotropy is calculated from the values of I_{vv} and I_{vh}: $r = (I_{vv}-GI_{vh})/(I_{vv}+2GI_{vh})$, where G is the grating factor that has been included to correct the wavelength response for polarization response of the emission optic and the detector. I_{vv} and I_{vh} are the fluorescence intensity measured parallel and perpendicular to the vertically polarized excitation, respectively. Anisotropy is dimensionless and does not depend on total intensity of the sample.[106] In contrast to polarization, anisotropy is normalized to total intensity (I_T): $I_T = I_{vv}-2I_{vh}$.

Depolarization processes may be intrinsic due to inherent properties of the fluorophore or extrinsic due to factors such as rotational diffusion and resonance energy transfer (RET).[106] The main source of extrinsic depolarization is rotational diffusion within the lifetime of the excited state. In aqueous non-viscous solutions, the anisotropy is near zero since the molecule can rotate extensively during the excited state lifetime. In contrast, a fluorophore bound to a macromolecule or in a rigid microenvironment has higher anisotropy due to restricted rotation. Resonance energy transfer (RET) also results in decreased anisotropy. RET occurs in concentrated solutions where the average distance between fluorophores is small enough to induce the transfer of energy between a donor and acceptor molecule. The resulting radiationless transfer of energy reduces the anisotropy considerably. Minimizing the effects of RET simply requires the dilution of the system being investigated. In general, fluorescence anisotropy has been used to provide information such as size and shape of proteins, protein interactions and

rigidity of the molecular environment.[106] In this study, fluorescence anisotropy was used to characterize the aggregates formed by NIR nanoGUMBOS when the anions are varied.
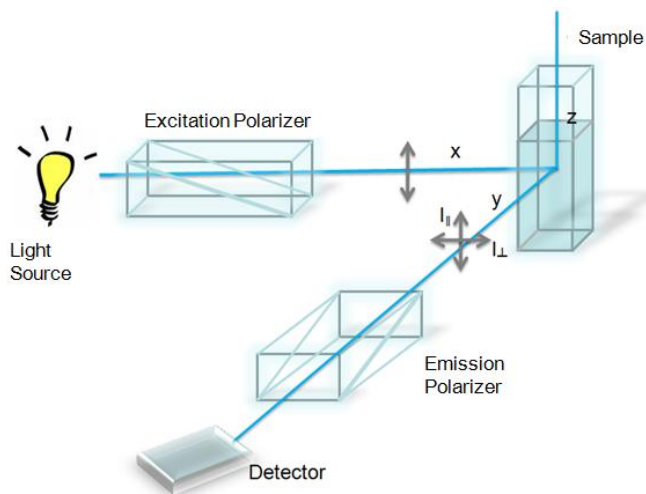
Figure 1.15. Schematic diagram depicting the measurement of fluorescence anisotropy.

1.8. Scope of the Dissertation

This dissertation has two main parts namely; the use of CILs for spectroscopic enantiomeric recognition and the synthesis of novel fluorescent NIR nanoGUMBOS for biomedical imaging. Chapter 1 outlines useful background information related to the dissertation work mainly covering ILs, CILs and fluorescent NIR GUMBOS and nanoGUMBOS. In Chapter 2, the synthesis of novel CILs and investigation of their enantiomeric recognition properties is described. In this study enantiomeric recognition was carried out using ^{19}F NMR and fluorescence spectroscopy exclusively on chiral fluorescent analytes. Chapter 3 extends the enantiomeric recognition studies to include fluorescent and non-fluorescent analytes using a fluorescent amino acid CIL as a potential universal selector. Chapter 4 entails the preparation of a new class of fluorescent NIR GUMBOS and nanoGUMBOS for biomedical imaging applications. Chapter 5 focuses on the characterization of tunable aggregates formed by

nanoGUMBOS so as to exploit their full potential based on their tunable spectral properties. Chapter 6 summarizes the overall conclusions drawn from the entire dissertation and provides suggestions on future research prospects deemed feasible based on the findings described in the dissertation.

1.9. References

(1)   Hapiot, P.; Lagrost, C. *Chem. Rev.* **2008**, *108*, 2238-2264.

(2)   Huddleston, J. G.; Rogers, R. D. *Chem. Commun.* **1998**, 1765-1766.

(3)   Walden, P. *Bull. Acad. Imp. Sci. St.-Petersbourg* **1914**, 405-422.

(4)   Sundermeyer.W *Angewandte Chemie-International Edition* **1965**, *4*, 222.

(5)   Del Popolo, M. G.; Voth, G. A. *J. Phys. Chem. B* **2004**, *108*, 1744-1752.

(6)   Gordon, J. E.; Rao, G. N. S. *J. Am. Chem. Soc.* **1978**, *100*, 7445-7454.

(7)   Seddon, K. R. *J. Chem. Technol. Biotechnol.* **1997**, *68*, 351-356.

(8)   Holbrey, J. D.; Reichert, W. M.; Nieuwenhuyzen, M.; Johnson, S.; Seddon, K. R.; Rogers, R. D. *Chem. Commun.* **2003**, 1636-1637.

(9)   Welton, T. *Chem. Rev.* **1999**, *99*, 2071-2083.

(10)   Allen, C. R.; Richard, P. L.; Ward, A. J.; van de Water, L. G. A.; Masters, A. F.; Maschmeyer, T. *Tetrahedron Lett.* **2006**, *47*, 7367-7370.

(11)   Hayashi, S.; Hamaguchi, H.-o. *Chem. Lett.* **2004**, *33*, 1590-1591.

(12)   Del Sesto, R. E.; McCleskey, T. M.; Burrell, A. K.; Baker, G. A.; Thompson, J. D.; Scott, B. L.; Wilkes, J. S.; Williams, P. *Chem. Commun.* **2008**, 447-449.

(13)   Shah, J. K.; Brennecke, J. F.; Maginn, E. J. *Green Chem.* **2002**, *4*, 112-118.

(14)   Wilkes, J. S. *Green Chem.* **2002**, *4*, 73-80.

(15)   Chum, H. L.; Koch, V. R.; Miller, L. L.; Osteryoung, R. A. *J. Am. Chem. Soc.* **1975**, *97*, 3264-3265.

(16)   Fuller, J.; Carlin, R. T.; De Long, H. C.; Haworth, D. *J. Chem. Soc., Chem. Commun.* **1994**, 299-300.

(17)   Wilkes, J. S.; Zaworotko, M. J. *J. Chem. Soc., Chem. Commun.* **1992**, 965-967.

(18)   Plechkova, N. V.; Seddon, K. R. *Chem. Soc. Rev.* **2008**, *37*, 123-150.

(19)   Rogers Robin, D.; Seddon Kenneth, R. *Science* **2003**, *302*, 792-793.

(20)   Earle, M. J.; Seddon, K. R. *Pure Appl. Chem.* **2000**, *72*, 1391-1398.

(21)   Wasserscheid, P.; Welton, T.; Editors *Ionic Liquids in Synthesis*, 2003.

(22)   Howarth, J.; Hanlon, K.; Fayne, D.; McCormac, P. *Tetrahedron Lett.* **1997**, *38*, 3097-3100.

(23)   Visser, A. E.; Swatloski, R. P.; Reichert, W. M.; Davis, J. H., Jr.; Rogers, R. D.; Mayton, R.; Sheff, S.; Wierzbicki, A. *Chem. Commun.* **2001**, 135-136.

(24)   Visser, A. E.; Swatloski, R. P.; Reichert, W. M.; Mayton, R.; Sheff, S.; Wierzbicki, A.; Davis, J. H., Jr.; Rogers, R. D. *Environ. Sci. Technol.* **2002**, *36*, 2523-2529.

(25)   Greaves, T. L.; Drummond, C. J. *Chem. Rev.* **2008**, *108*, 206-237.

(26)   Zhao, D. B.; Fei, Z. F.; Geldbach, T. J.; Scopelliti, R.; Dyson, P. J. *J. Am. Chem. Soc.* **2004**, *126*, 15876-15882.

(27)   Bonnette, F.; Mincheva, Z.; Lavastre, O. *Combinatorial Chemistry & High Throughput Screening* **2006**, *9*, 229-232.

(28)   Li, M.; Wang, T.; Pham, P. J.; Pittman, C. U.; Li, T. *Separation Science and Technology* **2008**, *43*, 828-841.

(29)   Baker, G. A.; Baker, S. N.; McCleskey, T. M. *Chem. Commun.* **2003**, 2932-2933.

(30)   Donato, R. K.; Migliorini, M. V.; Benvegnu, M. A.; Dupont, J.; Goncalves, R. S.; Schrekker, H. S. *Journal of Solid State Electrochemistry* **2007**, *11*, 1481-1487.

(31)   Compton, D. L.; Laszlo, J. A. *J. Electroanal. Chem.* **2002**, *520*, 71-78.

(32)   Mastragostino, M.; Soavi, F. *Journal of Power Sources* **2007**, *174*, 89-93.

(33)   Dupont, J.; de Souza, R. F.; Suarez, P. A. Z. *Chem. Rev.* **2002**, *102*, 3667-3691.

(34)   Dietz, M. L.; Dzielawa, J. A. *Chem. Commun.* **2001**, 2124-2125.

(35)   Tran, C. D.; Challa, S.; Franko, M. *Anal. Chem.* **2005**, *77*, 7442-7447.

(36)   Laszlo, J. A.; Compton, D. L. *Biotechnology and Bioengineering* **2001**, *75*, 181-186.

(37)   Mwongela, S. M.; Numan, A.; Gill, N. L.; Agbaria, R. A.; Warner, I. M. *Anal. Chem.* **2003**, *75*, 6089-6096.

(38)   Armstrong, D. W.; He, L. F.; Liu, Y. S. *Anal. Chem.* **1999**, *71*, 3873-3876.

(39)   Anderson, J. L.; Armstrong, D. W. *Anal. Chem.* **2003**, *75*, 4851-4858.

(40)   Wang, Q.; Baker, G. A.; Baker, S. N.; Colon, L. A. *Analyst* **2006**, *131*, 1000-1005.

(41)   Baker, G. A.; Baker, S. N.; Pandey, S.; Bright, F. V. *Analyst* **2005**, *130*, 800-808.

(42)   Borra, E. F.; Seddiki, O.; Angel, R.; Eisenstein, D.; Hickson, P.; Seddon, K. R.; Worden, S. P. *Nature* **2007**, *447*, 979-981.

(43)   Herrmann, W. A.; Goossen, L. J.; Koecher, C.; Artus, G. R. J. *Angew. Chem., Int. Ed. Engl.* **1997**, *35*, 2805-2807.

(44)   Earle, M. J.; McCormac, P. B.; Seddon, K. R. *Green Chem.* **1999**, *1*, 23-25.

(45)   Machado, M. Y.; Dorta, R. *Synthesis* **2005**, 2473-2475.

(46)   Bwambok, D. K.; Marwani, H. M.; Fernand, V. E.; Fakayode, S. O.; Lowry, M.; Negulescu, I.; Strongin, R. M.; Warner, I. M. *Chirality* **2008**, *20*, 151-158.

(47)   Baudoux, J.; Judeinstein, P.; Cahard, D.; Plaquevent, J.-C. *Tetrahedron Lett.* **2005**, *46*, 1137-1140.

(48)   Ishida, Y.; Miyauchi, H.; Saigo, K. *Chem. Commun.* **2002**, 2240-2241.

(49)   Baudequin, C.; Bregeon, D.; Levillain, J.; Guillen, F.; Plaquevent, J.-C.; Gaumont, A.-C. *Tetrahedron: Asymmetry* **2005**, *16*, 3921-3945.

(50)   Baudequin, C.; Baudoux, J.; Levillain, J.; Cahard, D.; Gaumont, A.-C.; Plaquevent, J.-C. *Tetrahedron: Asymmetry* **2003**, *14*, 3081-3093.

(51)   Patil, M. L.; Sasai, H. *Chem. Rec.* **2008**, *8*, 98-108.

(52)   Winkel, A.; Reddy, P. V. G.; Wilhelm, R. *Synthesis* **2008**, 999-1016.

(53)   Ding, J.; Armstrong, D. W. *Chirality* **2005**, *17*, 281-292.

(54)   Chen, X.; Li, X.; Hu, A.; Wang, F. *Tetrahedron: Asymmetry* **2008**, *19*, 1-14.

(55)   Headly, A. D.; Ni, B. *Aldrichimica Acta* **2007**, *40*, 107-117.

(56)   Bica, K.; Gaertner, P. *Eur. J. Org. Chem.* **2008**, 3235-3250.

(57)   Pegot, B.; Vo-Thanh, G.; Gori, D.; Loupy, A. *Tetrahedron Lett.* **2004**, *45*, 6425-6428.

(58)   Schulz, P. S.; Mueller, N.; Boesmann, A.; Wasserscheid, P. *Angew. Chem., Int. Ed.* **2007**, *46*, 1293-1295.

(59)   Kiss, L.; Kurtan, T.; Antus, S.; Brunner, H. *ARKIVOC* **2003**, 69-76.

(60)   Wang, Z.; Wang, Q.; Zhang, Y.; Bao, W. *Tetrahedron Lett.* **2005**, *46*, 4657-4660.

(61)   Ding, J.; Welton, T.; Armstrong, D. W. *Anal. Chem.* **2004**, *76*, 6819-6822.

(62)   Yuan, L. M.; Han, Y.; Zhou, Y.; Meng, X.; Li, Z. Y.; Zi, M.; Chang, Y. X. *Anal. Lett.* **2006**, *39*, 1439-1449.

(63)   Tran, C. D.; Mejac, I. *J. Chromatogr., A* **2008**, *1204*, 204-209.

(64)   Francois, Y.; Varenne, A.; Juillerat, E.; Villemin, D.; Gareil, P. *J. Chromatogr., A* **2007**, *1155*, 134-141.

(65)   Maier, V.; Horakova, J.; Petr, J.; Drahonovsky, D.; Sevcik, J. *J. Chromatogr., A* **2006**, *1103*, 337-343.

(66)   Rizvi, S. A. A.; Shamsi, S. A. *Anal. Chem.* **2006**, *78*, 7061-7069.

(67)   Berthod, A.; Ruiz-Angel, M. J.; Carda-Broch, S. *J. Chromatogr., A* **2008**, *1184*, 6-18.

(68)   Buckingham, A. D.; Fischer, P. *Chem. Phys.* **2006**, *324*, 111-116.

(69)   Moyna, G. *Discrimination of Chiral Compounds Using NMR Spectroscopy by Thomas J. Wenzel*, 2007.

(70)   Parker, D. *Chem. Rev.* **1991**, *91*, 1441-1457.

(71)   Dale, J. A.; Dull, D. L.; Mosher, H. S. *J. Org. Chem.* **1969**, *34*, 2543-2549.

(72)   Sullivan, G. R.; Dale, J. A.; Mosher, H. S. *J. Org. Chem.* **1973**, *38*, 2143-2147.

(73)   Wasserscheid, P.; Boesmann, A.; Bolm, C. *Chem. Commun.* **2002**, 200-201.

(74)   Clavier, H.; Boulanger, L.; Audic, N.; Toupet, L.; Mauduit, M.; Guillemin, J.-C. *Chem. Commun.* **2004**, 1224-1225.

(75)   Levillain, J.; Dubant, G.; Abrunhosa, I.; Gulea, M.; Gaumont, A.-C. *Chem. Commun.* **2003**, 2914-2915.

(76)   Kumar, V.; Pei, C.; Olsen, C. E.; Schaeffer, S. J. C.; Parmar, V. S.; Malhotra, S. V. *Tetrahedron: Asymmetry* **2008**, *19*, 664-671.

(77)   Patil, M. L.; Rao, C. V. L.; Yonezawa, K.; Takizawa, S.; Onitsuka, K.; Sasai, H. *Org. Lett.* **2006**, *8*, 227-230.

(78)   Ishida, Y.; Sasaki, D.; Miyauchi, H.; Saigo, K. *Tetrahedron Lett.* **2004**, *45*, 9455-9459.

(79)   Gao, H.-S.; Hu, Z.-G.; Wang, J.-J.; Qiu, Z.-F.; Fan, F.-Q. *Aust. J. Chem.* **2008**, *61*, 521-525.

(80)   Ashraf, S. A.; Pornputtkul, Y.; Kane-Maguire, L. A. P.; Wallace, G. G. *Aust. J. Chem.* **2007**, *60*, 64-67.

(81)   Yu, S.; Lindeman, S.; Tran, C. D. *J. Org. Chem.* **2008**, *73*, 2576-2591.

(82)   Rawitch, A. B.; Weber, G. *J. Biol. Chem.* **1972**, *247*, 680-685.

(83)   James, T. D.; Sandanayake, K. R. A. S.; Shinkai, S. *Nature* **1995**, *374*, 345-347.

(84)   Lin, J.; Hu, Q.-S.; Xu, M.-H.; Pu, L. *J. Am. Chem. Soc.* **2002**, *124*, 2088-2089.

(85)   McCarroll, M. E.; Billiot, F. H.; Warner, I. M. *J. Am. Chem. Soc.* **2001**, *123*, 3173-3174.

(86)   Tran, C. D.; Oliveira, D. *Anal. Biochem.* **2006**, *356*, 51-58.

(87)   Adhikary, R.; Bose, S.; Mukherjee, P.; Thite, A.; Kraus, G. A.; Wijeratne, A. B.; Sharma, P. S.; Armstrong, D. W.; Petrich, J. W. *J. Phys. Chem. B* **2008**, *112*, 7555-7559.

(88)   Tran, C. D.; Oliveira, D.; Yu, S. *Anal. Chem.* **2006**, *78*, 1349-1356.

(89)   Caldwell, J. *J. Chromatogr., A* **1996**, *719*, 3-13.

(90)   Kreuzfeld, H. J.; Hateley, M. J. *Enantiomer* **1999**, *4*, 491-496.

(91)   Maier, N. M.; Franco, P.; Lindner, W. *J. Chromatogr., A* **2001**, *906*, 3-33.

(92)   Holtzman, N. A.; Khoury, M. J. *Annu Rev Public Health* **1986**, *7*, 237-266.

(93)   Niederhoff, H.; Zahradnik, H. P. *Am J Med* **1983**, *75*, 117-120.

(94)   McKenzie, B. E. *Toxicol Pathol* **1989**, *17*, 377-384.

(95)   FDA's policy statement for the development of new stereoisomeric drugs *Chirality* **1992**, *4*, 338-340.

(96)   Nunez, M. C.; Garcia-Rubino, M. E.; Conejo-Garcia, A.; Cruz-Lopez, O.; Kimatrai, M.; Gallo, M. A.; Espinosa, A.; Campos, J. M. *Curr. Med. Chem.* **2009**, *16*, 2064-2074.

(97)   Marzo, A.; Heftmann, E. *J. Biochem. Biophys. Methods* **2002**, *54*, 57-70.

(98)   Fanali, S. *J Chromatogr A* **2000**, *875*, 89-122.

(99)   Desiderio, C.; Fanali, S. *J. Chromatogr., A* **1998**, *807*, 37-56.

(100)   Williams, A. A.; Fakayode, S. O.; Alptuerk, O.; Jones, C. M.; Lowry, M.; Strongin, R. M.; Warner, I. M. *J. Fluoresc.* **2008**, *18*, 285-296.

(101)   Ho Hyun, M.; Sung Jin, J.; Lee, W. *J. Chromatogr., A* **1998**, *822*, 155-161.

(102)   Tao, G.-h.; He, L.; Sun, N.; Kou, Y. *Chem. Commun.* **2005**, 3562-3564.

(103)   Skoog, D. A. *Principles of Instrumental Analysis. 3rd Ed*, 1985.

(104)   Wong, K.-P. *J. Chem. Educ.* **1975**, *52*, A83-A84, A86, A88.

(105)   Lakowicz, J. R. *Principles of Fluorescence Spectroscopy*, 1983.

(106)   Lakowicz, J. R. *Principles of Fluorescence Spectroscopy*, 2nd Ed ed.; Plenum Press: New York, 1999.

(107)   Scurto, A. M.; Newton, E.; Weikel, R. R.; Draucker, L.; Hallett, J.; Liotta, C. L.; Leitner, W.; Eckert, C. A. *Ind. Eng. Chem. Res.* **2008**, *47*, 493-501.

(108)   Bao, W.; Wang, Z.; Li, Y. *J. Org. Chem.* **2003**, *68*, 591-593.

(109)   Tesfai, A.; El-Zahab, B.; Bwambok, D. K.; Baker, G. A.; Fakayode, S. O.; Lowry, M.; Warner, I. M. *Nano Lett.* **2008**, *8*, 897-901.

(110)   Youtie, J.; Shapira, P.; Porter, A. L. *J. Nanopart. Res.* **2008**, *10*, 981-986.

(111)   Porter, A. L.; Youtie, J.; Shapira, P.; Schoeneck, D. J. *J. Nanopart. Res.* **2008**, *10*, 715-728.

(112)   Barone, P. W.; Parker, R. S.; Strano, M. S. *Anal. Chem.* **2005**, *77*, 7556-7562.

(113)   Shealy, D. B.; Lohrmann, R.; Ruth, J. R.; Narayanan, N.; Sutter, S. L.; Casay, G. A.; Evans, L., III; Patonay, G. *Appl. Spectrosc.* **1995**, *49*, 1815-1820.

(114)   Qian, G.; Zhong, Z.; Luo, M.; Yu, D.; Zhang, Z.; Ma, D.; Wang, Z. Y. *J. Phys. Chem. C* **2009**, *113*, 1589-1595.

(115)   Yousaf, M.; Lazzouni, M. *Dyes Pigm.* **1995**, *27*, 297-303.

(116)   Zhang, P.; Steelant, W.; Kumar, M.; Scholfield, M. *J. Am. Chem. Soc.* **2007**, *129*, 4526-4527.

(117)   Law, K. Y. *Chem. Rev.* **1993**, *93*, 449-486.

(118) Jobsis, F. F. *Science* **1977**, *198*, 1264-1267.

(119) Kim, S.; Lim, Y. T.; Soltesz, E. G.; De Grand, A. M.; Lee, J.; Nakayama, A.; Parker, J. A.; Mihaljevic, T.; Laurence, R. G.; Dor, D. M.; Cohn, L. H.; Bawendi, M. G.; Frangioni, J. V. *Nat. Biotechnol.* **2004**, *22*, 93-97.

(120) Bashkatov, A. N.; Genina, E. A.; Kochubey, V. I.; Tuchin, V. V. *J. Phys. D: Appl. Phys.* **2005**, *38*, 2543-2555.

(121) Ghoroghchian, P. P.; Therien, M. J.; Hammer, D. A. *Wiley Interdiscip. Rev.: Nanomed. Nanobiotechnol.* **2009**, *1*, 156-167.

(122) Weissleder, R.; Ntziachristos, V. *Nat. Med.* **2003**, *9*, 123-128.

(123) Weissleder, R. *Nat. Biotechnol.* **2001**, *19*, 316-317.

(124) Klohs, J.; Wunder, A.; Licha, K. *Basic Res. Cardiol.* **2008**, *103*, 144-151.

(125) Fu, A.; Gu, W.; Boussert, B.; Koski, K.; Gerion, D.; Manna, L.; Le Gros, M.; Larabell, C. A.; Alivisatos, A. P. *Nano Lett.* **2007**, *7*, 179-182.

(126) Bruchez, M., Jr.; Moronne, M.; Gin, P.; Weiss, S.; Alivisatos, A. P. *Science* **1998**, *281*, 2013-2016.

(127) Gao, X.; Cui, Y.; Levenson, R. M.; Chung, L. W. K.; Nie, S. *Nat. Biotechnol.* **2004**, *22*, 969-976.

(128) Welsher, K.; Liu, Z.; Daranciang, D.; Dai, H. *Nano Lett.* **2008**, *8*, 586-590.

(129) Aprile, C.; Martin, R.; Alvaro, M.; Scaiano, J. C.; Garcia, H. *ChemPhysChem* **2009**, *10*, 1305-1310.

(130) Zhou, F.; Xing, D.; Ou, Z.; Wu, B.; Resasco, D. E.; Chen, W. R. *J. Biomed. Opt.* **2009**, *14*, 021009/021001-021009/021007.

(131) Moore, E. G.; Szigethy, G.; Xu, J.; Palsson, L.-O.; Beeby, A.; Raymond, K. N. *Angew. Chem., Int. Ed.* **2008**, *47*, 9500-9503.

(132) Shi, X.; Royant, A.; Lin, M. Z.; Agilera, T. A.; Lev-Ram, V.; Steinbach, P. A.; Tsien, R. Y. *Science* **2009**, *324*, 804-807.

(133) Kim, K.; Lee, M.; Park, H.; Kim, J.-H.; Kim, S.; Chung, H.; Choi, K.; Kim, I.-S.; Seong, B. L.; Kwon, I. C. *J. Am. Chem. Soc.* **2006**, *128*, 3490-3491.

(134) Loo, C.; Lowery, A.; Halas, N.; West, J.; Drezek, R. *Nano Lett.* **2005**, *5*, 709-711.

(135) Yang, Y.; Lowry, M.; Xu, X.; Escobedo, J. O.; Sibrian-Vazquez, M.; Wong, L.; Schowalter, C. M.; Jensen, T. J.; Fronczek, F. R.; Warner, I. M.; Strongin, R. M. *Proc. Natl. Acad. Sci.* **2008**, *105*, 8829-8834.

(136) Bringley, J. F.; Penner, T. L.; Wang, R.; Harder, J. F.; Harrison, W. J.; Buonemani, L. *J. Colloid Interface Sci.* **2008**, *320*, 132-139.

(137) Derfus, A. M.; Chan, W. C. W.; Bhatia, S. N. *Nano Lett.* **2004**, *4*, 11-18.

(138) Cheng, J.; Flahaut, E.; Cheng, S. H. *Environ. Toxicol. Chem.* **2007**, *26*, 708-716.

(139) Malicka, J.; Gryczynski, I.; Geddes, C. D.; Lakowicz, J. R. *J. Biomed. Opt.* **2003**, *8*, 472-478.

(140) Lee, C.-H.; Cheng, S.-H.; Wang, Y.-J.; Chen, Y.-C.; Chen, N.-T.; Souris, J.; Chen, C.-T.; Mou, C.-Y.; Yang, C.-S.; Lo, L.-W. *Adv. Funct. Mater.* **2009**, *19*, 215-222.

(141) Tanaka, E.; Chen, F. Y.; Flaumenhaft, R.; Graham, G. J.; Laurence, R. G.; Frangioni, J. V. *J. Thorac. Cardiovasc. Surg.* **2009**, *138*, 133-140.

(142) Caesar, J.; Shaldon, S.; Chiandussi, L.; Guevara, L.; Sherlock, S. *Clin Sci* **1961**, *21*, 43-57.

(143) Ishihara, H.; Okawa, H.; Iwakawa, T.; Umegaki, N.; Tsubo, T.; Matsuki, A. *Anesth Analg* **2002**, *94*, 781-786, table of contents.

(144) Philip, R.; Penzkofer, A.; Baeumler, W.; Szeimies, R. M.; Abels, C. *J. Photochem. Photobiol., A* **1996**, *96*, 137-148.

(145) Landsman, M. L. J.; Kwant, G.; Mook, G. A.; Zijlstra, W. G. *J. Appl. Physiol.* **1976**, *40*, 575-583.

(146) Muckle, T. J. *Biochem. Med.* **1976**, *15*, 17-21.

(147) Bornhop, D. J.; Contag, C. H.; Licha, K.; Murphy, C. J.; Editors *Advances in Contrast Agents, Reporters, and Detection. [In: J. Biomed. Opt., 2001; 6(2)]*, 2001.

(148) Rasmussen, J. C.; Tan, I. C.; Marshall, M. V.; Fife, C. E.; Sevick-Muraca, E. M. *Curr. Opin. Biotechnol.* **2009**, *20*, 74-82.

(149) Maeda, H.; Wu, J.; Sawa, T.; Matsumura, Y.; Hori, K. *J. Controlled Release* **2000**, *65*, 271-284.

(150) Rao, J. *ACS Nano* **2008**, *2*, 1984-1986.

(151) Yang, Z.; Zheng, S.; Harrison, W. J.; Harder, J.; Wen, X.; Gelovani, J. G.; Qiao, A.; Li, C. *Biomacromolecules* **2007**, *8*, 3422-3428.

(152)   Altinoglu, E. I.; Russin, T. J.; Kaiser, J. M.; Barth, B. M.; Eklund, P. C.; Kester, M.; Adair, J. H. *ACS Nano* **2008**, *2*, 2075-2084.

(153)   Yu, J.; Yaseen, M. A.; Anvari, B.; Wong, M. S. *Chem. Mater.* **2007**, *19*, 1277-1284.

(154)   Ow, H.; Larson, D. R.; Srivastava, M.; Baird, B. A.; Webb, W. W.; Wiesner, U. *Nano Lett.* **2005**, *5*, 113-117.

(155)   Zhao, X.; Bagwe, R. P.; Tan, W. *Adv. Mater.* **2004**, *16*, 173-176.

(156)   Saxena, V.; Sadoqi, M.; Shao, J. *J. Photochem. Photobiol., B* **2004**, *74*, 29-38.

(157)   An, B.-K.; Kwon, S.-K.; Jung, S.-D.; Park, S. Y. *J. Am. Chem. Soc.* **2002**, *124*, 14410-14415.

(158)   Peng, A.-D.; Xiao, D.-B.; Ma, Y.; Yang, W.-S.; Yao, J.-N. *Adv. Mater.* **2005**, *17*, 2070-2073.

(159)   Gesquiere, A. J.; Uwada, T.; Asahi, T.; Masuhara, H.; Barbara, P. F. *Nano Lett.* **2005**, *5*, 1321-1325.

(160)   Xiao, D.; Xi, L.; Yang, W.; Fu, H.; Shuai, Z.; Fang, Y.; Yao, J. *J. Am. Chem. Soc.* **2003**, *125*, 6740-6745.

(161)   Hornyak, G. L.; Tibbals, H. F.; Dutta, J.; Moore, J. J. *Introduction to Nanoscience and Nanotechnology*; CRC press: Boca Raton, 2009.

(162)   Policard, A.; Leulier, A. *C. R. Seances Soc. Biol. Ses Fil.* **1924**, *91*, 1422-1423.

(163)   Moore, G. E.; Peyton, W. T.; et al. *J Neurosurg* **1948**, *5*, 392-398.

(164)   McDermott, G.; Prince, S. M.; Freer, A. A.; Hawthornthwaite-Lawless, A. M.; Papiz, M. Z.; Cogdell, R. J.; Isaacs, N. W. *Nature* **1995**, *374*, 517-521.

(165)   Yamamoto, Y.; Fukushima, T.; Suna, Y.; Ishii, N.; Saeki, A.; Seki, S.; Tagawa, S.; Taniguchi, M.; Kawai, T.; Aida, T. *Science* **2006**, *314*, 1761-1764.

(166)   Hoeben, F. J. M.; Jonkheijm, P.; Meijer, E. W.; Schenning, A. P. H. J. *Chem. Rev.* **2005**, *105*, 1491-1546.

(167)   Miller, R. A.; Presley, A. D.; Francis, M. B. *J. Am. Chem. Soc.* **2007**, *129*, 3104-3109.

(168)   Jelley, E. E. *Nature* **1936**, *138*, 1009-1010.

(169)   Scheibe, G. *Angew. Chem.* **1936**, *49*, 563.

(170)   Kirsten, S.; Daehne, S. *Int. J. Photoenergy* **2006**, 3/1-3/21.

(171)   Knoester, J. *Int. J. Photoenergy* **2006**, 4/1-4/10.

(172)   De Boer, S.; Wiersma, D. A. *Chem. Phys. Lett.* **1990**, *165*, 45-53.

(173)   Meinardi, F.; Cerminara, M.; Sassella, A.; Bonifacio, R.; Tubino, R. *Phys. Rev. Lett.* **2003**, *91*, 247401/247401-247401/247404.

(174)   Kim, J. S.; Kodagahally, R.; Strekowski, L.; Patonay, G. *Talanta* **2005**, *67*, 947-954.

(175)   Wang, M.; Silva, G. L.; Armitage, B. A. *J. Am. Chem. Soc.* **2000**, *122*, 9977-9986.

(176)   Chowdhury, A.; Wachsmann-Hogiu, S.; Bangal, P. R.; Raheem, I.; Peteanu, L. A. *J. Phys. Chem. B* **2001**, *105*, 12196-12201.

(177)   Peyratout, C.; Donath, E.; Daehne, L. *J. Photochem. Photobiol., A* **2001**, *142*, 51-57.

(178)   Herz, A. H. *Adv. Colloid Interface Sci.* **1977**, *8*, 237-298.

(179)   Das, S.; Chattopadhyay, A. P.; De, S. *J. Photochem. Photobiol.* **2008**, *197*, 402-414.

(180)   Lopez Arbeloa, F.; Martinez Martinez, V.; Arbeloa, T.; Lopez Arbeloa, I. *J. Photochem. Photobiol., C* **2007**, *8*, 85-108.

(181)   Maiti, N. C.; Mazumdar, S.; Periasamy, N. *J. Phys. Chem. B* **1998**, *102*, 1528-1538.

(182)   Tleugabulova, D.; Zhang, Z.; Brennan, J. D. *J. Phys. Chem. B* **2002**, *106*, 13133-13138.

CHAPTER 2

SYNTHESIS AND CHARACTERIZATION OF NOVEL CHIRAL IONIC LIQUIDS AND INVESTIGATION OF THEIR ENANTIOMERIC RECOGNITION PROPERTIES[*]

2.1. Introduction

Ionic liquids (ILs) are a class of organic salts that melt at or below 100°C. These compounds typically contain an organic cation with delocalized charge and a bulky inorganic anion. ILs that that exist in the liquid state at room temperature are termed room temperature ionic liquids (RTILs). Interest in room temperature ionic liquids continues to grow because of their potential as greener solvent alternatives to conventional environmentally damaging organic solvents.[1] In addition, ILs have unique properties such as lack of measurable vapor pressure, high thermal stability, and recyclability.[1-5] Such environmentally-friendly properties make ILs relatively benign solvents for cleaner processes to minimize toxic chemical wastes which have become a priority for chemical industries.[6] Room temperature ILs have been used in various applications such as replacing conventional organic solvents in organic synthesis[7], solvent extractions[8], electrochemical reactions[9, 10], liquid-liquid extractions[11] and in enzymatic reactions.[12] In addition, analytical applications of ILs such as their use as buffers in capillary electrophoresis[13], as stationary phases in gas chromatography[14, 15] as well as high performance liquid chromatography[16], and enhancement of sensitivity in thermal lens measurement have also been investigated.[17] A review of several analytical applications of ionic liquids has been reported

by Baker and coworkers.[18] In addition, Baker and his coworkers have developed an optical sensor based on an ionic liquid.[19]

Analyses of chiral molecules are very important since different enantiomers of a chiral racemic drug may display different properties.[20] For example, one enantiomer of a chiral drug may have the desired medicinal properties, while the other enantiomer may be harmful. Various chiral selectors, such as cyclodextrins, molecular micelles, antibody, and crown ethers have been widely used because of their chiral recognition abilities.[21-24] However, the use of many current chiral selectors is often limited due to low solubility, difficult organic syntheses, instability at high temperature, as well as high cost. In addition, many currently available chiral selectors require the use of another solvent and sometimes more than one solvent system if the analyte and the chiral selector are not soluble in the same solvent. Therefore, there is a need for the development of new chiral selectors that can be used simultaneously as solvent and chiral selector. Thus, the use of chiral ILs have gained popularity since they can be used as chiral solvents for asymmetric induction in synthesis.[25] Chiral ILs can also serve as chiral stationary phases in chromatography as demonstrated by Armstrong and coworkers in gas chromatography.[26] Tran and coworkers have also recently used chiral ILs for determining the enantiomeric composition of pharmaceutical products.[27, 28]

To our knowledge, 1-butyl-3-methyl imidazolium lactate reported in 1999 by Seddon and his coworkers is among the first chiral ionic liquids synthesized.[29] This chiral ionic liquid, with a chiral anion, was prepared via anion metathesis using 1-butyl-3-methyl imidazolium chloride and sodium (S)-2-hydroxypropionate. This ionic liquid also afforded good endo/exo selectivity in a Diels Alder reaction. Recently, ionic liquids with chiral carboxylates have been synthesized by Allen and coworkers.[30] This synthesis was achieved in water by reacting tetrabutylammonium hydroxide with the corresponding amino acids or chiral carboxylic acids. In 2002, Wasserscheid

and coworkers synthesized chiral ILs from chiral starting materials affording many different chiral ILs in good yields.[31] A novel imidazolium based chiral ionic liquid with planar chirality was synthesized by Saigo, *et al.* in 2002.[32] However, this ionic liquid could only be obtained as a racemic mixture and required further separation of the enantiomers before investigating its applications. Other chiral ILs based on imidazolium[33, 34], ephedrinium[35], and pyridinium[36] cations have been synthesized. However, chiral precursors for ILs are often used in a multi-step synthesis. A detailed review of chiral ionic liquid synthesis has been reported.[37] Kou, *et al.* have also successfully prepared chiral ionic liquids from amino acids and their corresponding methyl and ethyl esters.[38] These chiral ionic liquids from amino acid esters had low melting points compared to those derived from amino acids. Other interesting amino acid derived chiral ionic liquids have also been synthesized recently.[39-42] Armstrong and Ding have successfully synthesized chiral ILs via a simple anion exchange between a commercially available halide salt with N-lithiotrifluoromethanesulfonimide.[42] This approach provides an attractive one step synthesis with a chiral precursor, while allowing the product to be easily purified by washing with water. The same approach was employed by Tran *et al.* to prepare chiral ILs.[27] The variety and applications of these ILs suggest that other chiral ILs need to be explored in order to obtain ILs for different applications.

Natural materials are often used as precursors for preparing chiral ILs in multiple step synthesis. As an example, the use of amino acids for preparation of imidazolium cations is clear evidence of such use.[33] Chiral induction in some reactions may be required to afford chiral ILs, mostly in one enantiomeric form. In addition, the few commercially available chiral ILs are often very expensive. The high cost, combined with the difficulty in chiral ionic liquid synthesis, has limited their extensive study and applications.

The primary objective of this study was to synthesize and characterize both enantiomeric forms of new chiral ILs from commercially available amino acid ester chlorides. The presence of a chiral center in the precursor further simplifies the synthesis, alleviating the need for asymmetric induction. In addition, esterification reduces hydrogen bonding of amino acids affording low melting point ILs.[38] By varying the anions, the synthesis of ILs can be tailored, resulting in ionic liquids of different properties that may be used for various applications. In addition, this study reports an investigation of the enantiomeric recognition ability of a variety of chiral amino acid ester based ILs. The synthesis of chiral ILs was accomplished via a simple anion metathesis reaction and characterization was performed using nuclear magnetic resonance (NMR), thermal gravimetric analysis (TGA), differential scanning calorimetry (DSC), circular dichroism (CD), and elemental microanalysis. The relatively simple synthetic procedure and the presence of chiral centers in the precursors is a tremendous advantage for our approach. Finally, the chiral recognition ability of *L-* and *D-* alanine *tert*-butyl ester bis (trifluoromethane) sulfonimide ionic liquid was evaluated using ^{19}F NMR with a racemic Mosher's sodium salt substrate and fluorescence spectroscopy with some chiral fluorescent analytes.

2.2. Methods

2.2.1. Chemicals and Materials

L- and *D-*alanine *tert* butyl ester hydrochloride [*L-* and *D-*AlaC$_4$Cl)], bis(trifluoromethane) sulfonimide lithium salt (LiNTf$_2$), silver tetrafluoroborate (AgBF$_4$), silver lactate (AgLac), silver nitrate (AgNO$_3$), 2-methoxy-2-(trifluoromethyl) phenylacetic acid (Mosher's acid), and methanol (ACS certified) were purchased from Sigma Aldrich Chemicals (Milwaukee, WI). In addition, enantiomerically pure *R-* and *S-* enantiomers of warfarin, naproxen and 2,2,2-trifluoroanthrylethanol (TFAE) were purchased from Sigma Aldrich Chemicals (Milwaukee, WI). All chemicals were used as received.

2.2.2. General Instrumental Methods

The NMR spectra were recorded in d_6-DMSO on a Bruker-250 MHz instrument with tetramethyl silane (TMS) as an internal standard. Melting point (T_m) was determined by differential scanning calorimeter using a thermal analysis instrument TA SDT2960 at a scanning rate of 5 °C min^{-1}. Thermal decomposition temperature (T_{dec}) of ILs was determined with a thermal analysis instrument 2950 TGA HR V6.1A (module TGA 1000 °C). The heating rate for TGA was 5 °C min^{-1} under nitrogen from 25 °C to 300 °C. A Jasco-710 spectropolarimeter was used to obtain the CD spectra of our ILs. Steady-state fluorescence measurements were recorded at room temperature by use of a Spex Fluorolog-3 spectrofluorimeter (model FL3-22TAU3; Jobin Yvon, Edison, NJ, USA) equipped with a 450-W xenon lamp and R928P photomultiplier tube (PMT) emission detector. Fluorescence emission spectra were collected in a 4 mm quartz fluorescence cuvet with slit widths set for entrance exit bandwidths of 4 nm on both excitation and emission monochromators for warfarin, 2 nm for TFAE, and 1.5 nm for naproxen, respectively. Fluorescence for warfarin, TFAE, and naproxen were respectively monitored at excitation wavelengths of 306, 365, and 280 nm. In addition, all fluorescence spectra were blank subtracted before data analysis.

2.2.3. ^{19}F NMR Experiment

Racemic Mosher's sodium salt was prepared from Mosher's acid by reacting with an equivalent of sodium hydroxide in water and the salt was dried under vacuum before ^{19}F NMR measurement. The racemic Mosher's sodium salt (8.38 mg, 0.03 mmol) and 129.07mg (0.3 mmol) of *L-* or *D-* AlaC$_4$NTf$_2$ were dissolved in 0.75 ml of d_6 DMSO. The mixture was shaken vigorously for 10 minutes on an orbital shaker before recording ^{19}F NMR spectra.

2.2.4. Synthesis of *L*- and *D*-Alanine *tert* Butyl Ester bis (trifluoromethane) Sulfonimide, AlaC$_4$NTf$_2$

An amount of 0.5 g (2.75 mmol) of *L*- or *D*-alanine *tert* butyl ester chloride was dissolved in water. An equimolar amount (0.79 g, 2.75 mmol) of bis (trifluoromethane) sulfonimide lithium salt was dissolved separately in water. The two solutions were mixed and stirred for 2 hrs at room temperature. The mixture resulted in two layers, of which the lower layer was separated and dried under vacuum overnight. This resulted in 0.94g (79 % yield) of colorless ionic liquid. Scheme 2.1 depicts the anion exchange reaction between L-alanine *tert* butyl ester chloride and bis (trifluoromethane) sulfonamide lithium salt to afford CIL.
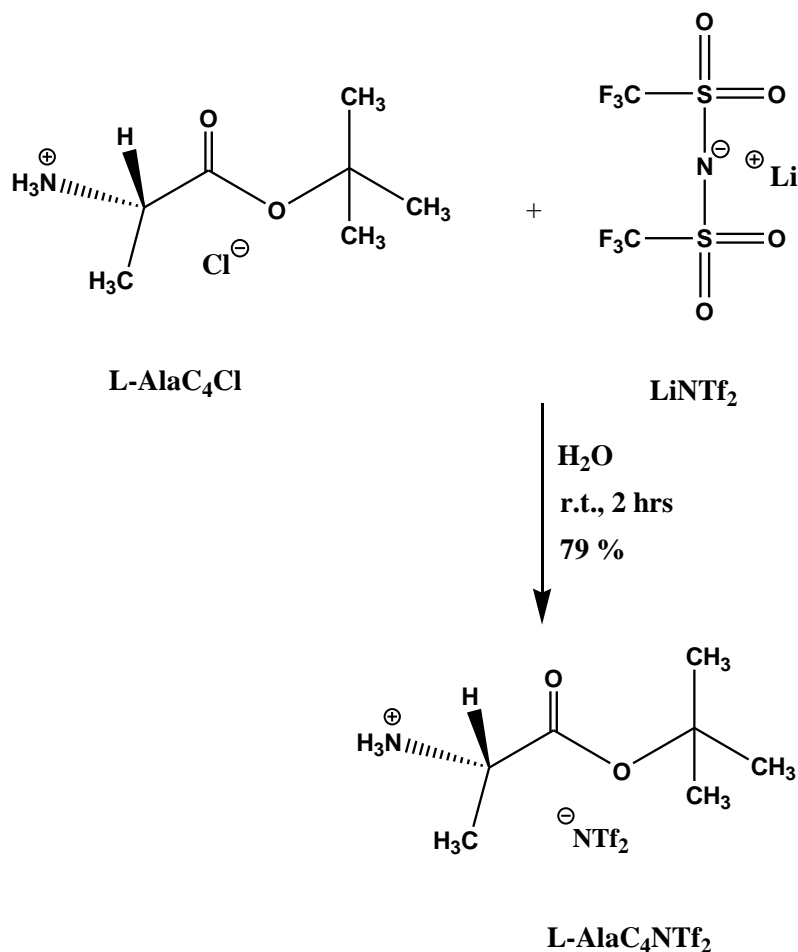
Scheme 2.1. Synthesis of *L*-AlaC$_4$NTf$_2$

The decomposition temperature (T_{dec}) of this ionic liquid was found to be 263 °C by use of TGA measurements. ^{1}H NMR (250 MHz, d_6 DMSO) δ (ppm) 8.19 (s, 3H), 3.97 (q, 1H), 1.45 (s, 9H), 1.36 (d, $J = 7.0$ Hz, 3H). ^{13}C NMR δ (ppm) 170.12, 83.66, 49.19, 28.32, 16.69. Anal. Calcd. for $C_9H_{16}N_2O_6S_2F_6$: C, 25.35; H, 3.78; N, 6.57. Found: C, 25.07; H, 3.98; N, 6.52.

2.2.5. Synthesis of [*L*- and *D*-Alanine *tert* Butyl Ester] Nitrate, Tetrafluoroborate, and Lactate

The synthesis of both enantiomeric forms of alanine *tert* butyl ester CIL containing nitrate, tetrafluoroborate and lactate anions is summarized in scheme 2.2. The synthesis of *L*- alanine *tert* butyl nitrate is described as a representative procedure to outline the experimental details of the anion exchange reaction with these anions. The procedure is similar for tetrafluoroborate and lactate anion exchange except we replace the nitrate anion with the corresponding lactate or tetrafluoroborate salt.
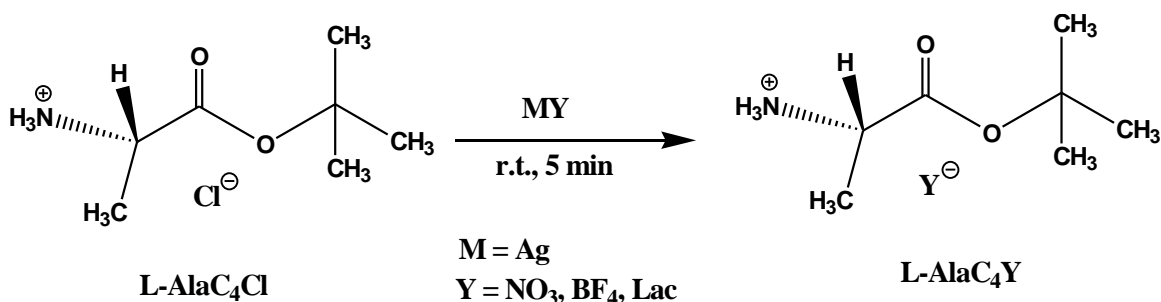
Scheme 2.2. Synthesis of $AlaC_4NO_3$, $AlaC_4BF_4$, and $AlaC_4Lac$

2.2.5.1. Representative Procedure: Synthesis of *L*-Alanine *tert* Butyl Ester Nitrate

A tenth of a gram, i.e. 0.1 g (0.55 mmol) of *L*- AlaBuCl was dissolved in methanol. An equimolar amount of silver nitrate (0.0935 g, 0.55 mmol) was suspended separately in methanol. The two solutions were mixed and stirred, and the precipitate was then filtered. The product was evaporated *in vacuo* and purified by crystallizing in methanol/ether to obtain 0.08 g (77 % yield)

of the product L-AlaC$_4$NO$_3$ as white crystals (T$_m$, 104 °C). This ionic liquid was thermally stable up to 130 °C. ^{1}H NMR (250 MHz, d$_6$ DMSO) δ (ppm) 8.36 (s, 3H), 3.92 (q, 1H), 1.44 (s, 9H), 1.35 (d, J= 7.0 Hz, 3H). ^{13}C NMR δ (ppm) 170.05, 83.51, 49.18, 28.36. Anal Calcd. for C$_7$H$_{16}$N$_2$O$_5$: C, 40.38; H, 7.75; N, 13.45. Found: C, 44.97; H, 8.53; N, 9.03.

2.2.5.2. *L*-alanine *tert* Butyl Ester Tetrafluoroborate

Yield: 80%. T$_m$, 93 °C ; T$_{dec}$, 125 °C. ^{1}H NMR (250 MHz, d$_6$ DMSO) δ (ppm) 8.18 (s, 3H), 3.94 (q,1H) 1.45 (s,9H), 1.36 (d, J = 7Hz, 3H). ^{13}C NMR δ (ppm) 170.13, 83.68, 49.19, 28.38, 16.74. Anal. Calcd. for C$_7$H$_{16}$NO$_2$BF$_4$: C, 36.08; H, 6.92; N, 6.01. Found: C, 35.71; H, 7.31; N, 6.13.

2.2.5.3. *L*-Alanine *tert* Butyl Ester Lactate

Yield: 86%. T$_m$, 114 °C; T$_{dec}$, 132 °C. ^{1}H NMR (250 MHz, d$_6$ DMSO) δ (ppm) 5.53 (s, 3H), 3.79 (q, 1H), 3.62 (q, 1H), 1.40 (s, 9H), 1.25 (d, J=7 Hz, 3H) 1.15 (d, J=6.75, 3H). ^{13}C NMR δ (ppm) 209.50, 178.31, 173.10, 110.00, 81.97, 67.28, 49.91, 28.46, 21.87, 18.98. Anal Calcd. for C$_{10}$H$_{21}$NO$_5$: C, 51.05; H, 8.99; N, 5.95. Found: C, 50.85; H, 8.96; N, 5.96.

2.3. Results and Discussion

2.3.1. Synthesis and Characterization of a New Amino Acid Ester Chiral Ionic Liquid (*L*- or *D*-AlaC$_4$NTf$_2$)

The synthesis of both enantiomeric forms of alanine *tert*-butyl ester bis (trifluoromethane) sulfonimide was accomplished via anion metathesis reaction of the corresponding amino acid ester chloride and bis (trifluoromethyl) sulfonylimide lithium salt (Scheme 2.1). The reaction proceeded well in water with good yield (79%) of *L* - or *D*-alanine *tert*-butyl ester bis (trifluoromethyl) sulfonylimide (*L*- or *D*-AlaC$_4$NTf$_2$). The ^{1}H NMR (Fig. 2.1) and ^{13}C NMR (Fig. 2.2) of the ionic liquid was consistent with the chemical structure of AlaC$_4$NTf$_2$.
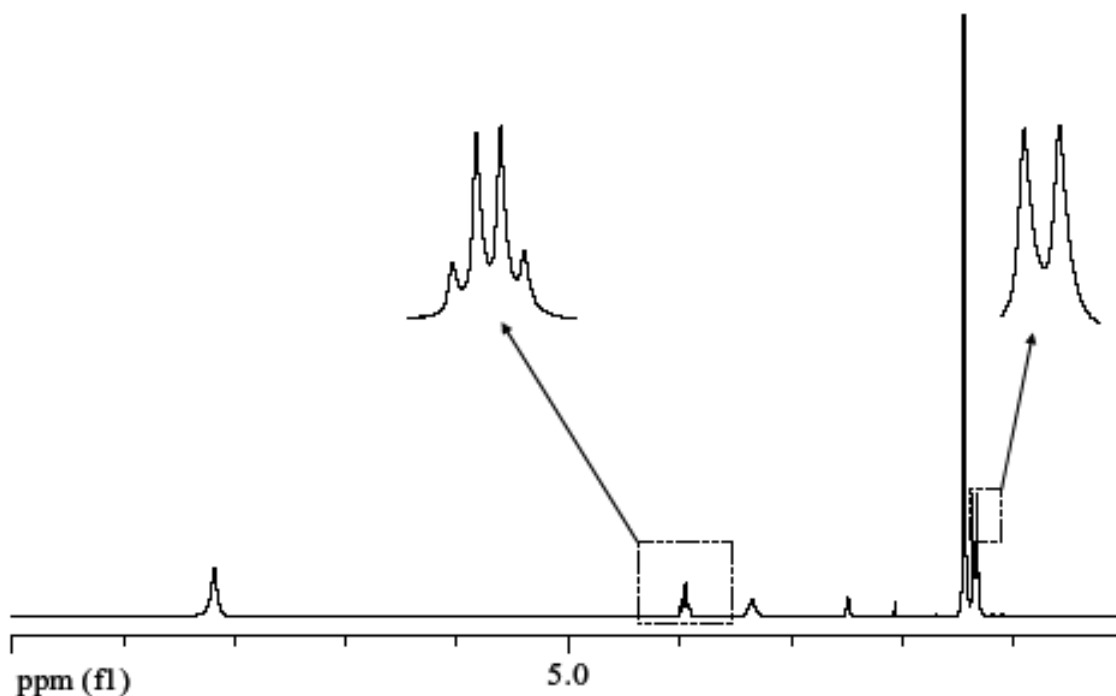
Figure 2.1. Proton (^{1}H) NMR spectrum of L-AlaC$_4$NTf$_2$ in d$_6$ DMSO with tetramethyl silane (TMS) as an internal standard at room temperature.

The NMR spectra obtained for other ILs were very similar to that of AlaC$_4$NTf$_2$. The similarity in NMR spectra was expected since only the anions were varied. The alanine tert-butyl ester bis (trifluoromethyl) sulfonylimide ionic liquid was found to be a desirable liquid at room temperature and stable up to 263 ℃, as indicated by thermal gravimetric analysis (TGA) measurement (Fig. 2.3A).

The ionic liquid L-AlaC$_4$NTf$_2$ was also heated at 225 ℃ for 2 hours to verify and confirm whether decomposition occurs at a lower temperature. From Fig. 2.3B, it seems that at this isothermal plateau (225 °C), there is a constant rate loss of 0.42%/min for the span of 120 min. The constancy of the weight loss rate might be an indication that a physical phenomenon (e.g. evaporation), rather than a chemical decomposition process, is occurring. The rather low decomposition temperature for the BF$_4$ salt (125 ℃), is still uncertain and may not be solely due

to the cation instability upon moderate heating. This is because as much as the cation might not be very stable at moderate heating, the same cation had relatively higher stability (263 ºC) with the NTf$_2$ anion.
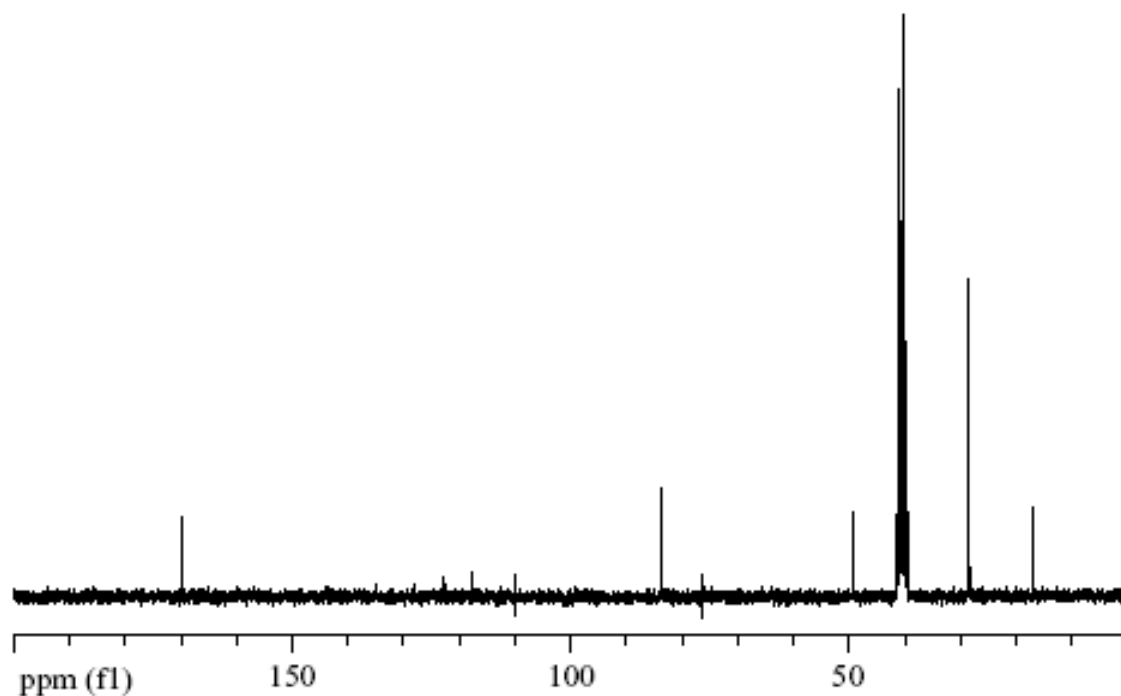
Figure 2.2. Carbon-13 NMR spectrum of *L*-AlaC$_4$NTf$_2$ in d$_6$ DMSO with tetramethyl silane (TMS) as an internal standard at room temperature.

The high thermal stability of alanine *tert*-butyl ester bis (trifluoromethyl) sulfonylimide makes it a preferred chiral selector and chiral solvent for reactions at high temperature or as a coating in gas chromatography. It is indeed extremely important that the chiral center in the precursor be retained in the final ionic liquid product. According to Jodry and Mikami, some imidazolium CILs will sometimes undergo racemization after synthesis.[34] The possibility of racemization in the synthesized ILs was investigated by use of circular dichroism (CD)

measurements of the ionic liquid products and their precursors. Examples of the CD bands obtained for both enantiomeric forms of the ionic liquids are as shown in Fig. 2.4.

(A)

(B)
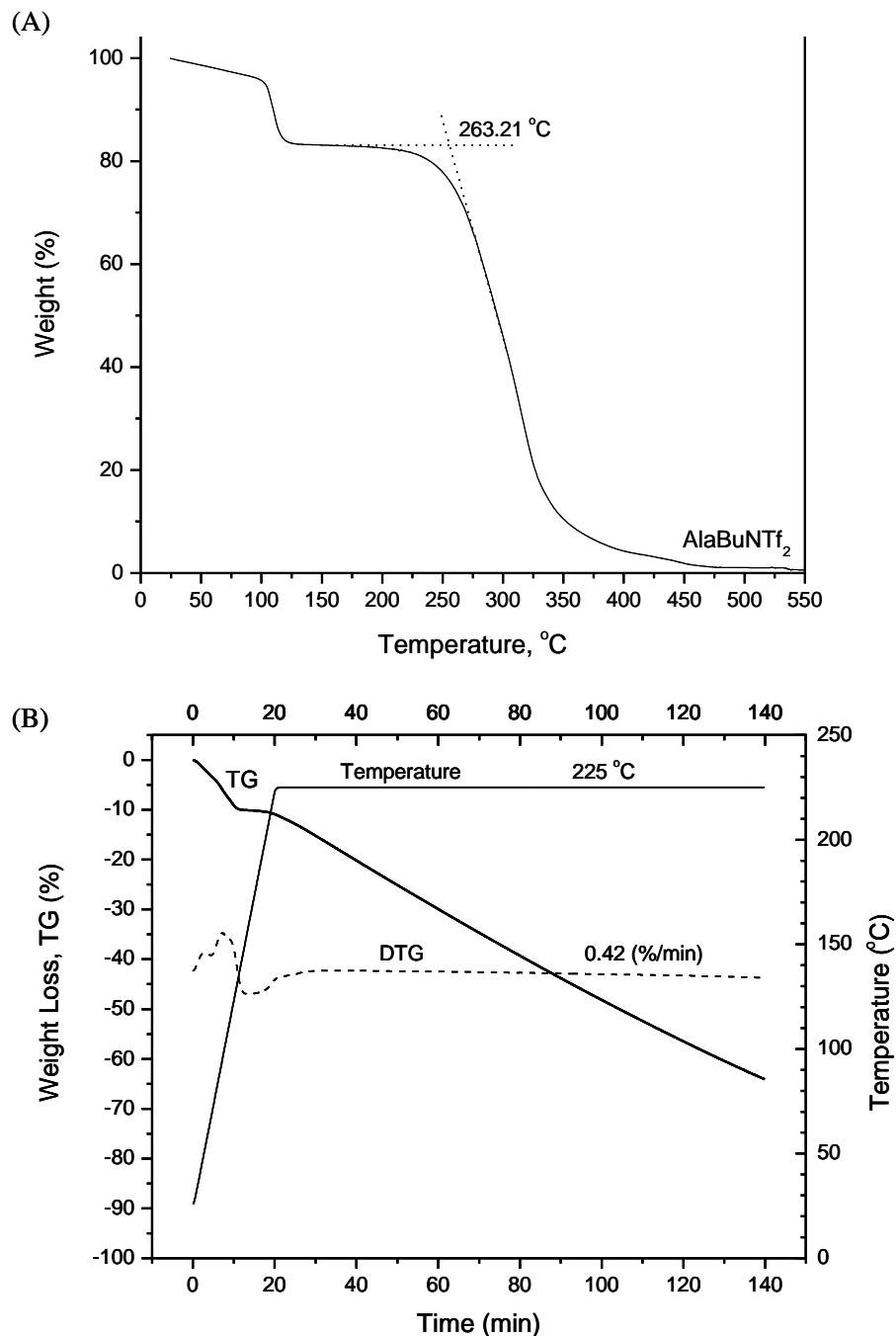
Figure 2.3. Thermal gravimetric analysis of L-AlaC$_4$NTf$_2$ with a heating rate of 5 °C min^{-1} under nitrogen (A) from 25 to 300 °C and (B) from 25 to 225 °C, then isothermally at 225 °C for 2 hrs.

As expected, the CD bands of the precursors were in the same direction as those of the ionic liquid products, confirming retention of configuration. In addition, the opposite CD bands confirmed that the *L*- and *D*- configurations of the ILs had been retained (Fig. 2.4).
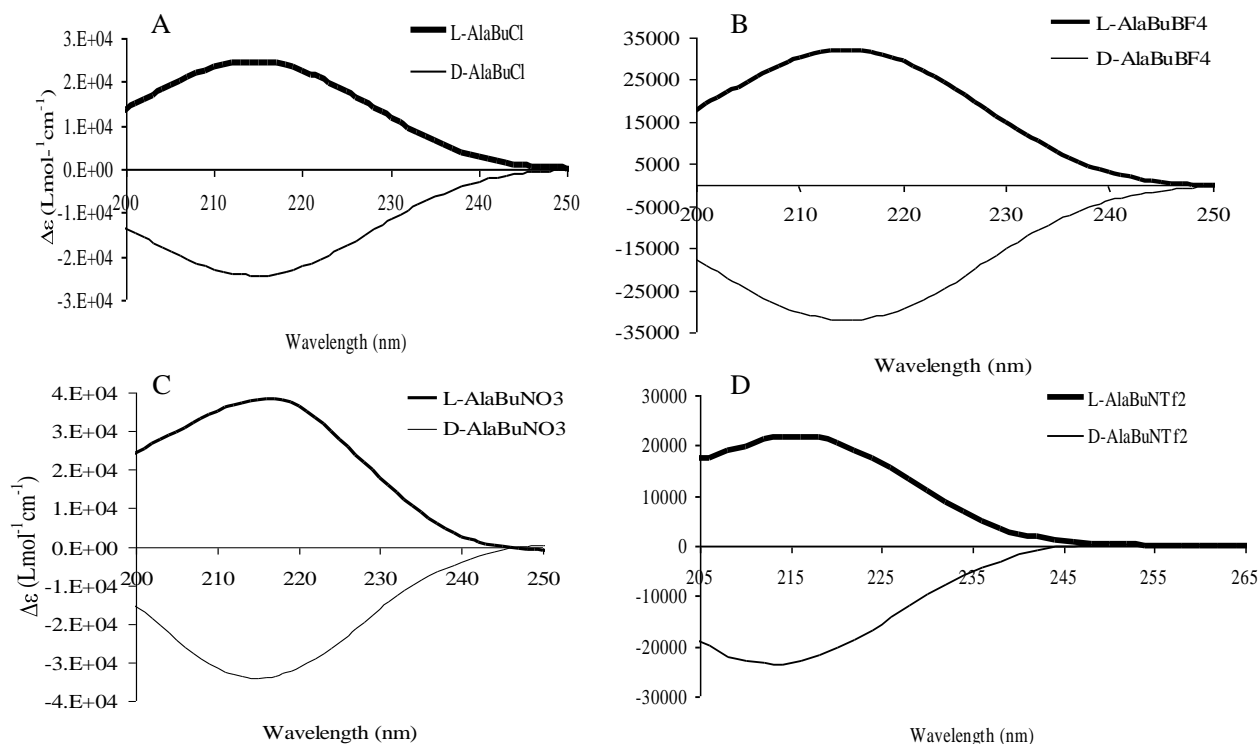
Figure 2.4. Circular dichroism spectra of *L*- and *D*- (A) AlaBuCl, (B) AlaBuBF$_4$, (C) AlaBuNO$_3$, and (D) AlaBuNTf$_2$ at room temperature.

2.3.2. Chiral Recognition Study of ILs Using ^{19}F NMR

As previously noted, *L*- and *D*- alanine *tert*-butyl ester bis (trifluoromethane) sulfonimide are liquids at room temperature. It was therefore interesting to investigate their ability to act both as solvent and chiral selector. The chiral recognition ability of *L*- and *D*-alanine *tert*-butyl ester bis (trifluoromethane) sulfonimide was investigated by use of ^{19}F NMR and racemic Mosher's sodium salt. In this experiment, various solvents such as methylene chloride, deuterium oxide, dimethyl sulfoxide (DMSO) as well as chloroform were examined. However, d$_6$-DMSO

demonstrated good solubility as compared to other solvents investigated. The results of the ^{19}F NMR study for enantiomeric recognition ability of *L*- and *D*- alanine tert-butyl ester bis (trifluoromethane) sulfonimide are shown in Fig. 2.5. The change in chemical environment lead
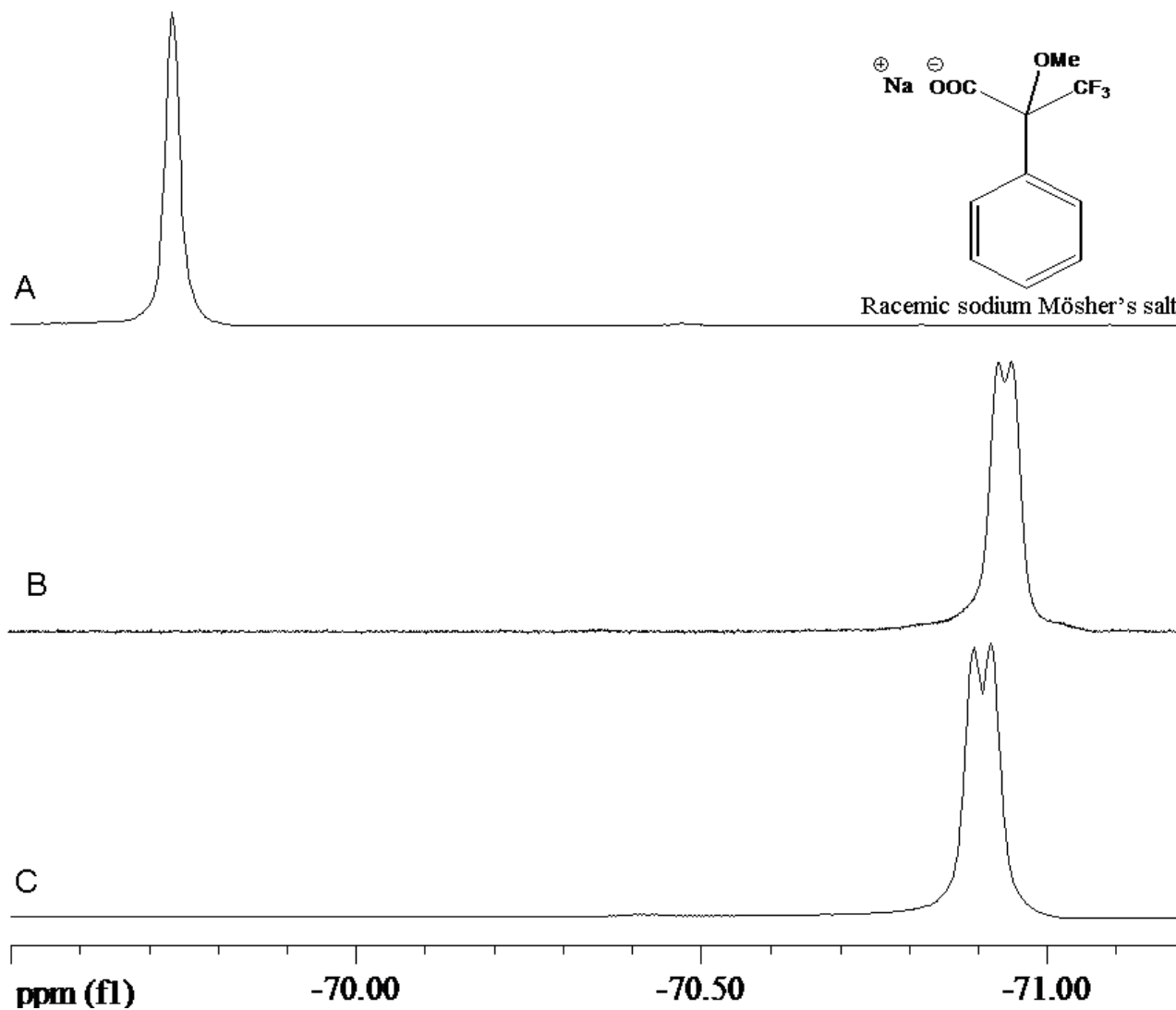
Fig 2.5. ^{19}F NMR spectra of (A) racemic sodium Mosher's salt; and a mixture of the racemic sodium Mosher's salt with (B) *D*-AlaC$_4$NTf$_2$, and (C) *L*-AlaC$_4$NTf$_2$ at room temperature.

to a shift in the ^{19}F NMR signal of the racemic Mosher's sodium salt. In addition, the split in the ^{19}F NMR signal of the racemic substrate by both enantiomeric forms of the ionic liquid demonstrates their enantiomeric recognition (Fig. 2.5). This confirms that this ionic liquid can be a suitable chiral selector for various applications such as determination of enantiomeric composition of chiral molecules of pharmaceutical, biomedical, and environmental interest.

2.3.3. Chiral Recognition of ILs Using Fluorescence Spectroscopy

Steady-state fluorescence spectroscopy was further used to evaluate the chiral recognition ability and enantio-selectivity of the chiral ILs on 2,2,2-trifluoroanthrylethanol (TFAE), warfarin, and naproxen chiral analytes. The choice of these chiral analytes in this study was due to their fluorescence properties; furthermore, they are of environmental and pharmaceutical interest. For instance, warfarin is an anticoagulant drug used for the treatment of thromboembolic diseases and is also generally used as a pesticide, while naproxen is used as an anti-infammatory drug.

The emission spectra of the 10 μM R- and S-enantiomers of TFAE, warfarin, and naproxen analytes in the presence of L-AlaC$_4$NTf$_2$ chiral ILs are respectively shown in Fig. 2.6 (A1, B1 and C1). The intensity of emission of the R-enantiomers obtained in the presence of ionic liquid solvent and chiral selector is noted to be higher than that of the S-enantiomers for all three analytes investigated. A difference in emission intensity of R- and S-enantiomers in the presence of chiral selectors is due to different diastereomeric interactions between the enantiomers and the IL chiral selectors. Such spectral differences have been widely reported and associated with enantioselectivity of chiral selectors as a result of diastereomeric complexes.[43-45]

Finally, a mean-centered plot of emission spectra, obtained by subtracting each emission spectrum from the mean spectrum on a wavelength to wavelength basis, was used to gain better insight into the enantiomeric selectivity and chiral recognition ability of the chiral ILs. The mean

centered plot of the emission spectra depicted in Fig. 2.6 (A1, B1, and C1) are shown in Fig. 2.6

(A2, B2 and C2), respectively. The spectra were obtained by subtracting the spectrum of *R*- and

S-enantiomer in the presence of chiral selectors from the *R*- and *S*-mean spectra. It is of great

importance to note that *R*- and *S*- enantiomers have opposite mean spectra, further demonstrating

the chiral recognition ability and enantio-selectivity of the ionic liquid chiral selector.

2.3.4. Synthesis and Characterization of Novel Amino Acid Ester CILs (*L*-or *D*-AlaC$_4$NO$_3$, AlaC$_4$BF$_4$, AlaC$_4$Lac)

A similar anion metathesis reaction used for the synthesis of AlaC$_4$NTf$_2$ was employed for the

synthesis of AlaC$_4$NO$_3$, AlaC$_4$BF$_4$, and AlaC$_4$Lac. However, the reaction was performed in

methanol at a shorter time of five minutes (Scheme 2.2). The silver chloride precipitate was

filtered off in each case affording good yields of the respective chiral ILs after removing

methanol *in vacuo*. Alanine *tert*- butyl ester nitrate (AlaC$_4$NO$_3$) crystallized to form a white solid

at room temperature. AlaC$_4$BF$_4$ was obtained as a colorless greasy solid, whereas AlaC$_4$Lac

forms clear needle-like crystals at room temperature. The fact that solid ILs were obtained upon

changing the anion demonstrates the tunability of the ILs synthesized in this study. By varying

the anion or cation, different ILs with different properties are obtained for various applications.

These results illustrate that bis (trifluoromethane) sulfonimide is probably a poorly coordinating

anion with an alanine *tert* butyl ester cation. The poor crystal packing between the anion and

cation results in ionic liquid. Del Po' polo describes this as frustrated packing between a bulky

inorganic anion and cation leading to lower melting point ILs.[46] Their findings are in agreement

with our results that bis (trifluoromethane) sulfonimide being the largest of the anions yielded an

ionic liquid product that was liquid at room temperature. The other smaller anions such as nitrate

afforded ILs that were solid at room temperature.
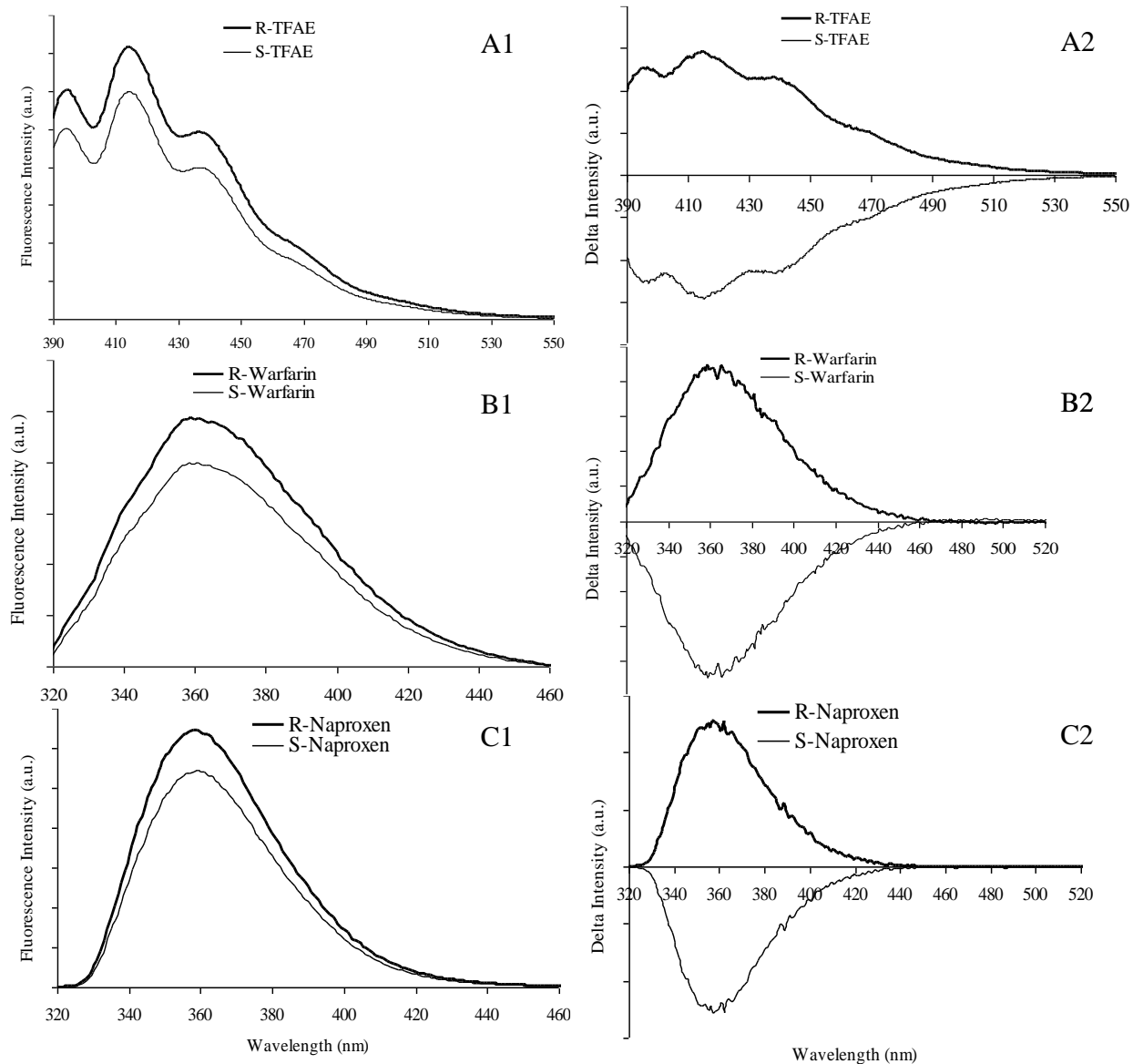
Figure 2.6. Fluorescence emission and mean centered spectral plots of 10 μM *R*- and *S*- (A) TFAE, (B) warfarin, and (C) naproxen enantiomers in the presence of *L*-AlaC$_4$NTf$_2$ chiral ionic liquid. The emission spectra of TFAE, warfarin, and naproxen were monitored at excitation wavelength of 365, 306, and 280 nm, respectively, at room temperature.

2.4. Conclusions

In summary, we have successfully synthesized a series of new chiral ILs in both enantiomeric forms using a simple metathesis reaction between the chiral chloride ester salt and the corresponding anion sources. Alanine *tert*-butyl ester bis (trifluoromethane) sulfonylimide is desirably liquid at room temperature and is thermally stable up to 263 ℃. It can therefore be

used in high temperature reactions or as a chiral selector in gas chromatography. Furthermore, the ILs presented here have the same chiral configuration as the chloride salt precursors indicating that enantiomeric salts were obtained upon anion metathesis. Both enantiomeric forms of alanine *tert*-butyl ester bis (trifluoromethane) sulfonylimide ionic liquid demonstrated enantiomeric recognition of racemic Mosher's sodium salt. This is an advantage since the ionic liquid can serve both as solvent and chiral selector, alleviating the need for use of environmentally damaging solvents to dissolve the analyte. As an example, this compound could probably be used to provide chiral selectivity in the determination of enantiomeric composition of pharmaceutical products and in chiral separations. While the solid ILs could not be used for this purpose, we believe that their synthesis and characterization is a step towards exploring their potential applications.

2.5. References

(1)   Welton, T. *Chem. Rev.* **1999**, *99*, 2071-2083.

(2)   Levillain, J.; Dubant, G.; Abrunhosa, I.; Gulea, M.; Gaumont, A.-C. *Chem. Commun.* **2003**, 2914-2915.

(3)   Tran, C. D.; De Paoli Lacerda, S. H. *Anal. Chem.* **2002**, *74*, 5337-5341.

(4)   Tran, C. D.; De Paoli Lacerda, S. H.; Oliveira, D. *Appl. Spectrosc.* **2003**, *57*, 152-157.

(5)   Mele, A.; Tran, C. D.; De Paoli Lacerda, S. H. *Angew. Chem., Int. Ed.* **2003**, *42*, 4364-4366.

(6)   Huddleston, J. G.; Rogers, R. D. *Chem. Commun.* **1998**, 1765-1766.

(7)   Dupont, J.; de Souza, R. F.; Suarez, P. A. Z. *Chem. Rev.* **2002**, *102*, 3667-3691.

(8)   Dietz, M. L.; Dzielawa, J. A. *Chem. Commun.* **2001**, 2124-2125.

(9)   Compton, D. L.; Laszlo, J. A. *J. Electroanal. Chem.* **2002**, *520*, 71-78.

(10)   Quinn, B. M.; Ding, Z.; Moulton, R.; Bard, A. J. *Langmuir* **2002**, *18*, 1734-1742.

(11)   Kazarian, S. G.; Briscoe, B. J.; Welton, T. *Chem. Commun.* **2000**, 2047-2048.

(12)   Laszlo, J. A.; Compton, D. L. *Biotechnol. Bioeng.* **2001**, *75*, 181-186.

(13)   Mwongela, S. M.; Numan, A.; Gill, N. L.; Agbaria, R. A.; Warner, I. M. *Anal. Chem.* **2003**, *75*, 6089-6096.

(14)   Armstrong, D. W.; He, L.; Liu, Y.-S. *Anal. Chem.* **1999**, *71*, 3873-3876.

(15)   Anderson, J. L.; Armstrong, D. W. *Anal. Chem.* **2003**, *75*, 4851-4858.

(16)   Wang, Q.; Baker, G. A.; Baker, S. N.; Colon, L. A. *Analyst* **2006**, *131*, 1000-1005.

(17)   Tran, C. D.; Challa, S.; Franko, M. *Anal. Chem.* **2005**, *77*, 7442-7447.

(18)   Baker, G. A.; Baker, S. N.; Pandey, S.; Bright, F. V. *Analyst* **2005**, *130*, 800-808.

(19)   Baker, G. A.; Baker, S. N.; McCleskey, T. M. *Chem. Commun.* **2003**, 2932-2933.

(20)   Caldwell, J. *J. Chromatogr., A* **1996**, *719*, 3-13.

(21)   Fanali, S. *J. Chromatogr., A* **2000**, *875*, 89-122.

(22)   Desiderio, C.; Fanali, S. *J. Chromatogr., A* **1998**, *807*, 37-56.

(23)   Ho Hyun, M.; Sung Jin, J.; Lee, W. *J. Chromatogr., A* **1998**, *822*, 155-161.

(24)   Fakayode, S. O.; Williams, A. A.; Busch, M. A.; Busch, K. W.; Warner, I. M. *J. Fluoresc.* **2006**, *16*, 659-670.

(25)   Baudequin, C.; Baudoux, J.; Levillain, J.; Cahard, D.; Gaumont, A.-C.; Plaquevent, J.-C. *Tetrahedron: Asymmetry* **2003**, *14*, 3081-3093.

(26)   Ding, J.; Welton, T.; Armstrong, D. W. *Anal. Chem.* **2004**, *76*, 6819-6822.

(27)   Tran, C. D.; Oliveira, D.; Yu, S. *Anal. Chem.* **2006**, *78*, 1349-1356.

(28)   Tran, C. D.; Oliveira, D. *Anal. Biochem.* **2006**, *356*, 51-58.

(29)   Earle, M. J.; McCormac, P. B.; Seddon, K. R. *Green Chem.* **1999**, *1*, 23-25.

(30)   Allen, C. R.; Richard, P. L.; Ward, A. J.; van de Water, L. G. A.; Masters, A. F.; Maschmeyer, T. *Tetrahedron Lett.* **2006**, *47*, 7367-7370.

(31)   Wasserscheid, P.; Boesmann, A.; Bolm, C. *Chem. Commun.* **2002**, 200-201.

(32)   Ishida, Y.; Miyauchi, H.; Saigo, K. *Chem. Commun.* **2002**, 2240-2241.

(33)   Bao, W.; Wang, Z.; Li, Y. *J. Org. Chem.* **2003**, *68*, 591-593.

(34)   Jodry, J. J.; Mikami, K. *Tetrahedron Lett.* **2004**, *45*, 4429-4431.

(35)   Thanh, G. V.; Pegot, B.; Loupy, A. *Eur. J. Org. Chem.* **2004**, 1112-1116.

(36)   Patrascu, C.; Sugisaki, C.; Mingotaud, C.; Marty, J.-D.; Genisson, Y.; Lauth-de Viguerie, N. *Heterocycles* **2004**, *63*, 2033-2041.

(37)   Ding, J.; Armstrong, D. W. *Chirality* **2005**, *17*, 281-292.

(38)   Tao, G.-h.; He, L.; Sun, N.; Kou, Y. *Chem. Commun.* **2005**, 3562-3564.

(39)   Ni, B.; Garre, S.; Headley, A. D. *Tetrahedron Lett.* **2007**, *48*, 1999-2002.

(40)   Ni, B.; Headley, A. D. *Tetrahedron Lett.* **2006**, *47*, 7331-7334.

(41)   Luo, S.-P.; Xu, D.-Q.; Yue, H.-D.; Wang, L.-P.; Yang, W.-L.; Xu, Z.-Y. *Tetrahedron: Asymmetry* **2006**, *17*, 2028-2033.

(42)   Ding, J.; Desikan, V.; Han, X.; Xiao, T. L.; Ding, R.; Jenks, W. S.; Armstrong, D. W. *Org. Lett.* **2005**, *7*, 335-337.

(43)   Smith, V. K.; Ndou, T. T.; Warner, I. M. *J. Phys. Chem.* **1994**, *98*, 8627-8631.

(44)   Dotsikas, Y.; Kontopanou, E.; Allagiannis, C.; Loukas, Y. L. *J Pharm Biomed Anal* **2000**, *23*, 997-1003.

(45)   MacDonald, S. A.; Hieftje, G. M. *Appl. Spectrosc.* **1996**, *50*, 1161-1164.

(46)   Del Popolo, M. G.; Voth, G. A. *J. Phys. Chem. B* **2004**, *108*, 1744-1752.

CHAPTER 3

A FLUORESCENT AMINO ACID-BASED CHIRAL IONIC LIQUID FOR POTENTIAL UNIVERSAL ENANTIOMERIC DISCRIMINATION

3.1. Introduction

Enantiomers of chiral drugs often differ in their pharmacological activities and pharmacokinetic profiles as a result of their interactions with optically active molecules in the human body and other biological systems. For example, one enantiomer may have the desired medicinal activity, while the other may be inactive or show a qualitatively different effect or quantitatively different potency, and/or lead to extreme toxicity.[1] Over the past decade, the marketing of single enantiomers of chiral drugs has become more common, with single enantiomers now being the leading component of drugs approved today.[2, 3] This is partly due to the Food and Drug Administration's 1992 policy statement regarding the development and regulation of new stereoisomeric drugs[4], combined with the pharmaceutical industry's use of "chiral switching" strategies to manage drug life-cycles and remarket established racemates as single enantiomers.[2, 5] Thus, there is a need for the development of methods to quantitatively determine enantiomeric purity.

Various chiral selectors have been developed for enantiomeric discrimination. These include cyclodextrins[6-11], antibodies[12-14], antibiotics[15, 16], molecular micelles[17-20], polysaccharides[21-25], and crown ethers[26, 27]. However, the use of many of these chiral selectors is often hindered with problems such as low solubility of either the analyte or selector in the solvent of choice, difficult multi-step syntheses, and instability at high temperatures. Thus, complex solvent mixtures may sometimes be required to dissolve the analyte and the chiral selector when they are not both soluble in the same solvent. We believe that multiple solvation interactions, as provided by ionic liquids (ILs), may provide a solution to this problem.[28] For example, a given IL may dissolve a variety of polar and non-polar analytes, while a chiral ionic

liquid (CIL) may simultaneously induce the required chiral selectivity.[29] Moreover, unlike many other chiral selectors, CILs do not require inclusion of the analyte into a selector's cavity to provide discrimination, thus adding to their universality. In addition, ILs are often quite simple to prepare. Many one-step synthesis of ILs, including CILs, from commercially available reagents have been reported. ILs are also known to be stable at high temperatures as evidenced through their many uses as separation reagents in gas chromatography.[30, 31] Therefore, the many useful properties of CILs may minimize some of the problems often encountered with other forms of chiral selectors.

Chiral ionic liquids belong to the more general class of compounds referred to as ionic liquids or sometimes as room temperature ionic liquids. ILs are classified as organic salts whose "frustrated packing" yields liquid salts that melt below 100 ºC. The potential utility of ILs in analytical chemistry[32, 33], spectroscopy[29], separations[34-36], synthesis or catalysis[37], and beyond has been widely reviewed.[38] Chiral ionic liquids are ILs in which either the cation, or the anion, or both may be chiral. One example of a series of CILs possessing either a chiral cation, chiral anion, or both, has been recently reported.[39] The cations of these molecules consisted of an imidazolium group, while the anions were based upon a borate ion with spiral structure and chiral substituents. A growing interest in CILs is demonstrated by an increasing number of new classes of CILs reported in the literature, including the amino acid-based CILs used in this work. The synthesis, characterization, and applications of various CILs have been thoroughly described in several recent reviews.[40-44]

Chiral ionic liquids have recently gained popularity in part based on their many potential applications, e.g. their utility as chiral stationary phases in gas chromatography[30, 31], and as additives for enantiomeric separations in micellar electrokinetic electrochromatography[45] or high performance liquid chromatography.[31] The development of ILs based on amino acids which are

chiral, biocompatible, biodegradable, and also display reduced toxicity have also increased the popularity of CILs. Ohno and co-workers reported amino acid-based ILs composed of imidazolium cations and amino acid anions and speculated as to their potential utility.[46] Subsequently, several other reports of amino acid-based ILs have appeared. Amino acid-based ILs were recently reviewed[47, 48] with a prediction that this area of research is poised for rapid development and expansion.[48]

Despite the numerous syntheses of CILs which have been reported, surprisingly only a limited number of studies have used spectrophotometric measurements to investigate their enantiomeric discrimination properties.[29] One example can be cited which uses near infrared absorption to determine the enantiomeric compositions of pharmaceutical products using a novel CIL as both the solvent and selector.[49] By taking advantage of the high sensitivity of fluorescence detection, the same group extended the technique to enantiomeric determination of intrinsically fluorescent chiral analytes, including propranolol, naproxen, and warfarin.[50] In related work, our group has recently reported the enantiomeric discrimination of amino acid-based CILs towards intrinsically fluorescent analytes.[51] Yet, there continues to be a need for a simple, universal approach to measure enantiomeric compositions at low concentrations. High sensitivity fluorescence detection provides a possible approach. However, since many analytes of interest display minimal intrinsic fluorescence emission, it would be advantageous to include a fluorescent reporter as part of the IL for such an approach.

While it has been reported that many ILs, or their impurities, display fluorescence when excited at 280-430nm, the origin of this fluorescence has not yet been explained.[33] Additionally, a series of highly photoluminescent benzobis(imidazolim) salts was recently described by Bielawski and co-workers and an application of this new class of versatile fluorescent materials was demonstrated by conjugating a maleimide-functionalized derivative to bovine serum

albumin.[52, 53] However, universal fluorescence detection in the measurement of enantiomeric compositions using a CIL as the solvent, selector, and reporter, would require a fluorescent CIL. Such a fluorescent CIL should be capable of acting simultaneously as solvent, selector, and fluorescent reporter; thus, high sensitivity detection would also be possible for non-fluorescent analytes. The intrinsic fluorescence of aromatic amino acids suggests possibilities for such a fluorescent CIL.

Herein, we report the synthesis and characterization of a fluorescent amino acid-based chiral ionic liquid, L-PheC$_2$NTf$_2$, and the investigation of its enantiomeric discrimination capabilities. To the best of our knowledge, this is the first report on the use of a fluorescent CIL as a solvent and chiral selector for enantiomeric discrimination of non-fluorescent as well as fluorescent analytes.

3.2. Materials and Methods

3.2.1. Chemicals and Materials

L-phenylalanine ethyl ester hydrochloride [L-PheC$_2$Cl], bis (trifluoromethane) sulfonimide lithium salt (LiNTf$_2$), 2-methoxy-2-(trifluoromethyl) phenylacetic acid (Mosher's acid), methanol (ACS certified), Ludox® AS-40 colloidal silica (40 Wt% suspension in water), tetramethyl silane (TMS), deuterated solvents, pure enantiomeric forms of fluorescent analytes: 2,2,2-trifluoroanthrylethanol (TFAE), 1,1′-binaphthyl-2,2′-diamine (BNA), and propranolol, and non-fluorescent analytes: camphanic acid, serine, glucose, and mannose were purchased from Sigma Aldrich Chemicals (Milwaukee, WI). All chemicals were used as received without further purification. Ultrapure water (18.2 MΩ·cm) was used for all purposes and obtained from an Elga model PURELAB Ultra water filtration system.

3.2.2. General Instrumental Methods

A Jasco-710 spectropolarimeter was used for measuring Circular Dichroism (CD) spectra of room temperature methanolic solutions (1 mM L-PheC$_2$NTf$_2$) in 1 cm quartz cells. The thermal decomposition temperature (T$_{dec}$) was determined using a thermal analysis instrument, 2950 TGA HR V6.1A (module TGA 1000 °C), at a heating rate under nitrogen of 5 °C min^{-1} from 25 °C to 300 °C. The NMR spectra were recorded using a Bruker-250 MHz instrument and using tetramethyl silane (TMS) as an internal standard. For ^{1}H and ^{13}C NMR, d$_6$-DMSO was used as the solvent, whereas CD$_2$Cl$_2$ with 30% d$_6$-DMSO was used for ^{19}F NMR measurements.

Absorption measurements were acquired at room temperature using a Shimadzu, model UV-3101PC UV-vis-NIR spectrophotometer with samples either in 4 mm square quartz cells, or between two quartz plates in the case of the neat L-PheC$_2$NTf$_2$ film. Steady-state and frequency-domain lifetime fluorescence measurements were recorded using a Spex Fluorolog-3 spectrofluorimeter (model FL3-22TAU3; HORIBA Jobin Yvon, Edison, NJ). Excitation was provided by a 450 W xenon arc lamp. Dual monochromators were used to select the excitation and emission wavelengths with bandpasses of 3nm each. The integration time was set to 0.1 sec per point, and 950 V were applied to a Hamamatsu R928 PMT. All fluorescence spectra were ratio corrected through division by the signal from a reference detector which monitored the lamp output.

Excitation-Emission Matrix spectra (EEMs) were collected in 4 mm square quartz cells with excitations from 250-400nm and emission from 250-500nm using 2.5nm and 5nm step sizes for emission and excitation, respectively. An adjacent averaging routine was performed on all EEMs in order to improve signal quality. The fluorescence quantum yield was measured in a 1 cm path-length quartz cell with right-angle collection geometry following the comparative

method reported by Williams et al.[54] A quantum yield of 0.27 for anthracene in ethanol was used as the reference.

Fluorescence decay times were measured using a variable frequency phase-modulation technique. Full-sized 1 cm quartz cells were used with 330nm excitation. The emission was collected through a 370nm long pass filter. Thirty-one logarithmically spaced frequencies were collected over a frequency range of 10–136.9 MHz using five averages and a 10 sec integration time at each frequency. Frequency-domain measurements were collected versus Ludox, a scatter reference solution, which showed a lifetime of 0 nsec. Phase and modulation decay profiles were analyzed using the Globals software package developed at the Laboratory for Fluorescence Dynamics (University of Illinois at Urbana-Champaign). Constant phase and modulation errors of 0.5° and 0.005 were used in analyses for consistency and ease of day-to-day data interpretation.

3.2.3. Synthesis of L-Phenylalanine Ethyl Ester bis (Trifluoromethane) Sulfonimide (L-PheC$_2$NTf$_2$)

The procedure was similar to that used in the preparation of alanine-based CILs previously reported.[51] Specifically, 10 g (43.53 mmol) of L-phenylalanine ethyl ester chloride (L-PheC$_2$Cl) was dissolved in water and mixed with an aqueous solution of 12.49 g (43.53 mmol) of bis (trifluoromethane) sulfonimide lithium salt (LiNTf$_2$). The mixture was stirred for more than 2 hrs at room temperature. The ionic liquid was quite hydrophobic and did not dissolve in water. The ionic liquid was higher in density than water and thus formed the lower layer of a bilayer system when mixed and stirred with water. The lower layer containing L-PheC$_2$NTf$_2$ was separated and washed five times with water. It was observed that as the number of washes increased, a slight yellow color in the ionic liquid completely disappeared. Subsequently, the ionic liquid was dried using a lyophilizer, yielding 17.49 g (83% yield) of clear, colorless, slightly viscous, but free flowing ionic liquid. The decomposition temperature (T$_{dec}$) was determined using TGA and

74

found to be 270 ºC. Characterization by ^{1}H NMR and ^{13}C NMR showed the peaks consistent with the chemical structure of the ionic liquid. ^{1}H NMR (250 MHz, d_6 DMSO) δ (ppm) 8.3 (s, 3H), 7.34-7.21 (m, 5H), 4.28 (t, J = 7.5 Hz, 1H), 4.12 (q, 2H), 3.02-3.16 (ddd, J = 6.4, 7.5, 13.2 Hz, 2H), 1.10 (t, J = 7.2 Hz, 3H). ^{13}C NMR δ (ppm) 169.91, 135.35, 130.28, 129.44, 128.16, 62.57, 59.50, 54.02, 14.53. These results were confirmed using elemental analysis. Calculated for $C_{13}H_{16}N_2O_6S_2F_6$: C, 32.91; H, 3.40; N, 5.90. Found: C, 32.00; H, 3.79; N, 5.31.

3.2.4. Circular Dichroism (CD) Measurements of CIL Liquid and Precursor

A concentration of 1.00 mM (10^{-3} M) stock solution was prepared by dissolving the precursor, L-PheC2Cl (2.29 mg) and the CIL, L-PheC2NTf2 (4.74 mg) in 10 mL of methanol. The CD spectra were then recorded using a Jasco 710 spectropolarimeter. Methanol was used as the blank and was substracted from the CD data of the CIL and the precursor. The retention of chiral configuration after prolonged heating was investigated by comparison of CD spectra of 1 mM methanolic solutions prepared from neat L-PheC$_2$NTf$_2$ at room temperature to that of a corresponding CIL solution in which the neat L-PheC$_2$NTf$_2$ had been heated in the oven for more than 18 hrs at 115 ºC.

3.2.5. Sample Preparation for Fluorescence Spectroscopy

A concentration of 1.00 mM (10^{-3} M) stock solution of R or S (or L or D)- enantiomer was prepared by dissolving appropriate weight in 25 mL of ethanol (or water in case of glucose analyte) using a calibrated 25 mL volumetric flask. Equal concentrations of 10 μM (10^{-5} M) of R or S (or D or L)- enantiomer were prepared by pipetting 5 μL of each stock solution (10^{-3} M) into a vial, allow the solvent (water for glucose and ethanol for the rest of the analytes) to evaporate under a gentle stream of ultrapure nitrogen and finally adding 500 μL (0.5 mL) of neat L-PheC$_2$NTf$_2$. This was followed by sonication for 20 mins, vortexing and finally fluorescence measurements were made using a 4 mm cuvet after equilibrating the sample for 10 mins.

3.3. Results and Discussion

3.3.1. Confirmation of Chirality and Stability Upon Extended Heating

One of the goals of the current study is to demonstrate the chiral discrimination of L-PheC$_2$NTf$_2$ when used simultaneously as the solvent and selector. Therefore, the chiral integrity of the CIL product was important as some CILs have previously been reported to undergo racemization during synthesis, although its precursor was enantiomerically pure.[55] Circular dichroism measurements of L-PheC$_2$NTf$_2$ product ionic liquid (1 mM in methanol) and its chiral starting material, PheC$_2$Cl (1 mM in methanol), were conducted to confirm the retention of the chiral configuration upon the ion-exchange. The CD spectral band of the L-PheC$_2$Cl precursor is positive (data not shown), the same shape and direction as that of the L-PheC$_2$NTf$_2$ product, thus suggesting the retention of chiral configuration. It is also important to confirm the retention of chiral configuration upon heating the CIL for an extended period of time. This was investigated
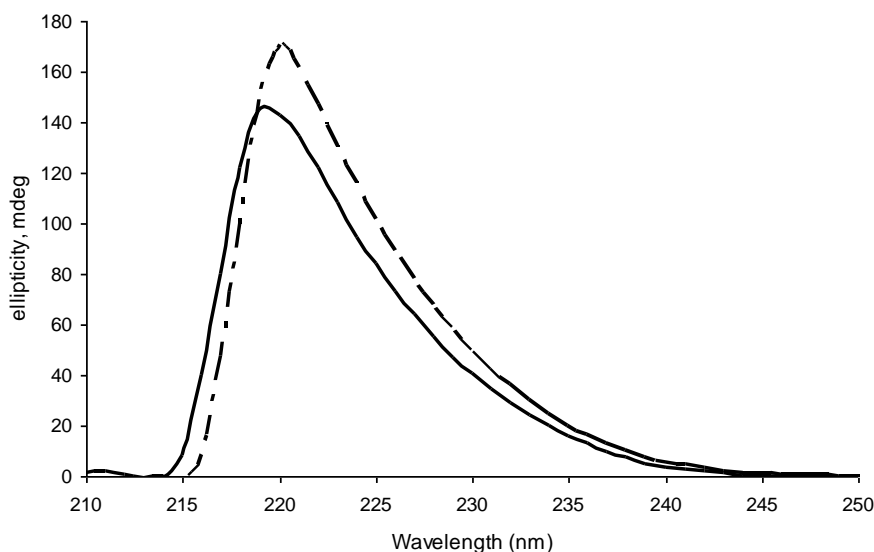
Figure 3.1. Circular dichroism spectra of 10^{-3} M L-PheC$_2$NTf$_2$ in methanol at room temperature (broken line), and corresponding 10^{-3} M L-PheC$_2$NTf$_2$ in methanol prepared from neat L-PheC$_2$NTf$_2$ previously heated at 115 ℃ for 18 hrs (continuous line).

through comparison of CD spectra of 1 mM methanolic solutions prepared from neat L-PheC$_2$NTf$_2$ at room temperature to that of a corresponding CIL solution in which the neat L-PheC$_2$NTf$_2$ had been heated in the oven for more than 18 hrs at 115 ºC. As shown in Figure 3.1, this CIL does not racemize after prolonged heating.

Thermal analysis by TGA revealed that L-PheC$_2$NTf$_2$ is stable to thermal decomposition up to 270 ºC (Figure 3.2 A). It has been observed that upon prolonged heating, some ILs decompose at temperatures lower than their measured decomposition temperatures.[56, 57] This observation prompted us to heat L-PheC$_2$NTf$_2$ for 30 minutes at a constant temperature of 225 ºC. A minimal loss of mass was observed (Figure 3.2 B). Results obtained from these studies suggest that this CIL is relatively stable when heated for a long period of time and may be potentially suitable as a solvent medium for high temperature reactions and as a chiral stationary phase in gas chromatography.
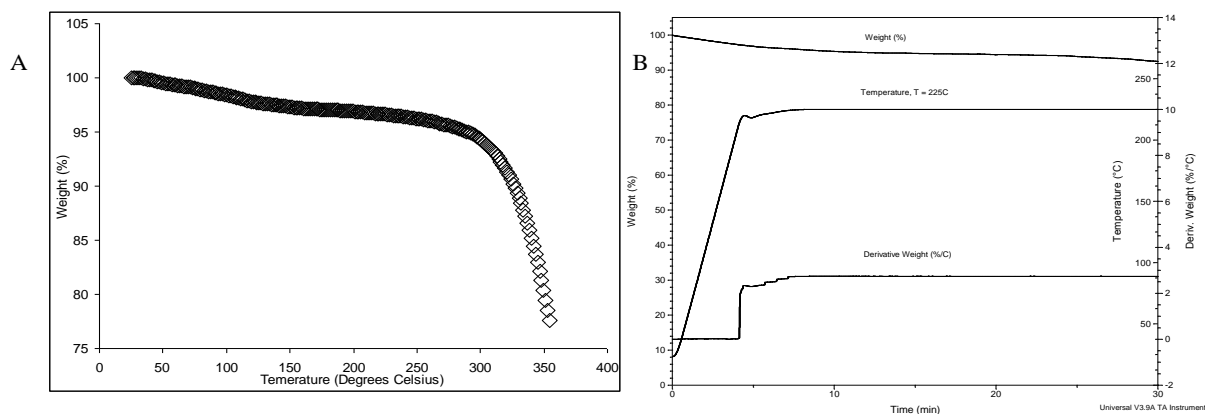
Figure 3.2. Thermal gravimetric analysis of neat L-PheC$_2$NTf$_2$ under nitrogen, with a heating rate of 5 °C min^{-1} from (A) 25 to 350 °C (B) 25 to 225°C, then isothermally at 225 °C for 30 minutes.

3.3.2. Screening of Enantiomeric Discrimination Using ^{19}F NMR

The enantiomeric discrimination properties of L-PheC$_2$NTf$_2$ were investigated using the diastereomeric interaction towards classical racemic Mosher's sodium salt. A binary solvent system consisting of CD$_2$Cl$_2$ with 30% d$_6$ DMSO was used to dissolve the mixture of racemic

Mosher's sodium salt and L-PheC$_2$NTf$_2$. The ^{19}F NMR spectrum of Mosher's salt in the absence of L-PheC$_2$NTf$_2$ displayed only a single band at 69.803 ppm (Figure 3.3 A). Addition of L-PheC$_2$NTf$_2$, 142.30 mg (0.3 mmol), to the racemic Mosher's sodium salt, 8.38 mg (0.03 mmol), resulted in peak splitting, as well as a shift to 70.832 and 70.876 ppm (Figure 3.3 B). The difference in the chemical shifts ($\Delta\delta$) was calculated as 11 Hz. This is an indication of strong diastereomeric interactions between the racemic Mosher's sodium salt and the CIL, suggesting that L-PheC$_2$NTf$_2$ has good chiral discrimination ability.
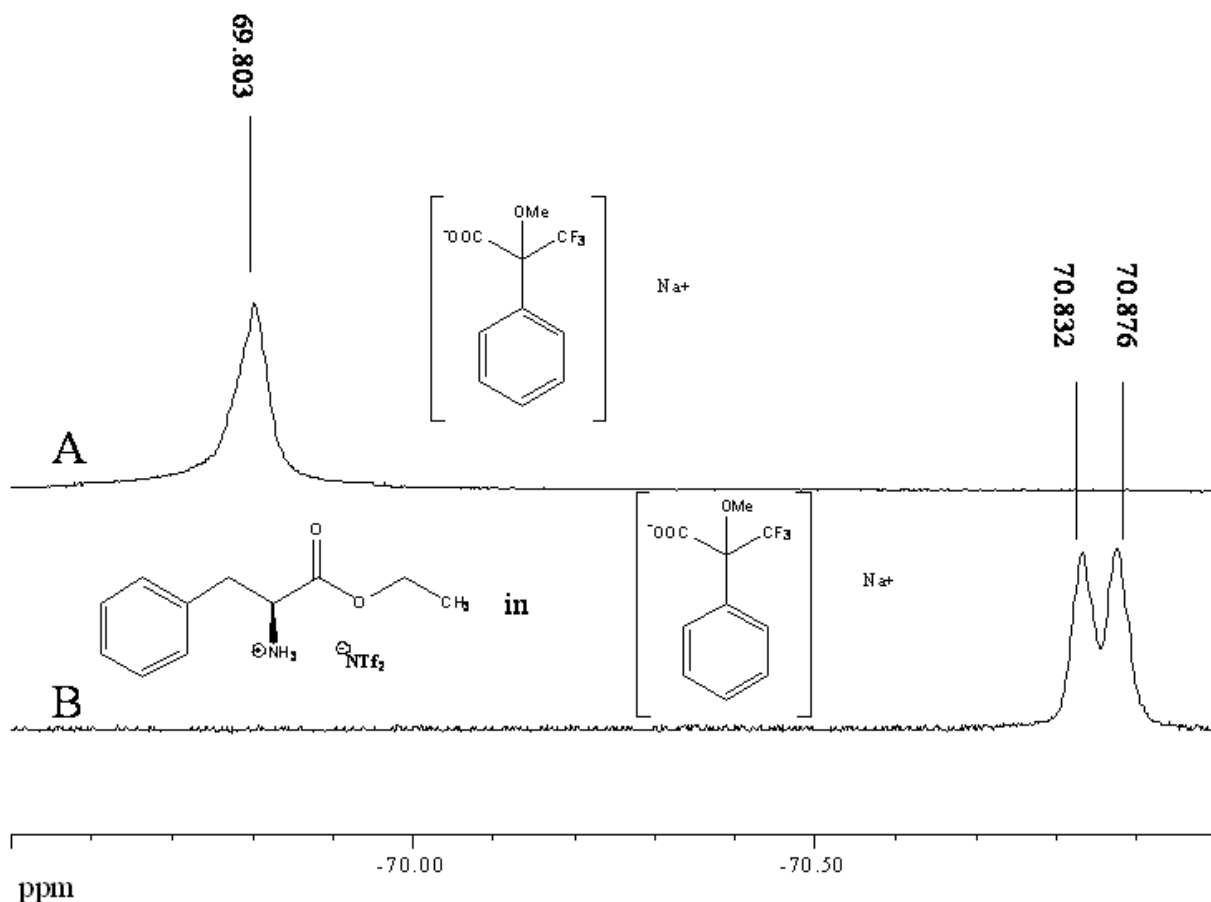
Figure 3.3. Enantiomeric recognition of Mosher's salt by L-PheC$_2$NTf$_2$. ^{19}F NMR spectra of (A) racemic sodium Mosher's salt; and (B) a mixture of the racemic sodium Mosher's salt with L-PheC$_2$NTf$_2$ at room temperature.

3.3.3. Spectroscopic Properties of L-PheC$_2$NTf$_2$

The absorption and fluorescence properties of L-PheC$_2$NTf$_2$ were studied as neat CIL (Table 3.1) and using ethanol as a solvent as needed (Figure 3.4). These data are presented in Table 3.1. Neat L-PheC$_2$NTf$_2$ was observed to be colorless. A thin film of neat L-PheC$_2$NTf$_2$ displayed a maximum absorption at 257nm and a spectral shape similar to the characteristic phenylalanine amino acid absorbance. However, unlike phenylalanine and L-phenylalanine ethyl ester hydrochloride (a CIL precursor), L-PheC$_2$NTf$_2$ displayed a weakly absorbing tail in its absorption spectrum extending to wavelengths beyond 400nm as compared to the characteristic absorption of phenylalanine. The absorption spectra of neat L-PheC$_2$NTf$_2$ in a 4 mm path-length

Table 3.1. Photophysical characteristics of L-PheC$_2$NTf$_2$.

CIL	Absorption Properties [a]		Fluorescence Properties				
			Emission Properties [b]		Lifetime (nsec) [c]		
	λ_{max} (nm)	ε (L mol^{-1} cm^{-1})	λ_{exc} (nm)	Peak(s):λ_{em} (nm)	τ_1	τ_2	τ_3
L-PheC$_2$NTf$_2$[d]	257	~95	260	~280, 320	0.68 (0.25)	3.57 (0.61)	12.72 (0.14)
			280	320, ~400			
			300	~340, ~400			
			320	~450			

[a] Properties of neat ionic liquid. A thin film (~29 μm) of neat L-PheC$_2$NTf$_2$ between two quartz plates displayed a spectral shape similar to phenylalanine. Neat ionic liquid in a 4 mm path-length cell displayed an absorption greater than 3 at wavelengths below ~270nm, ~0.1 near 350nm, and ~0.05 at 400nm.

[b] Properties of neat ionic liquid. Front face collection geometry was used in an effort to minimize inner filter effects.

[c] Properties of neat ionic liquid. Frequency-domain measurements were collected versus Ludox, a scatter reference solution, which showed a lifetime of 0 nsec. Full-sized 1 cm quartz cells were used with 330nm excitation. The emission was collected through a 370nm long pass filter. Fractional contributions of each lifetime are shown in parentheses.

[d] The high absorbance of the neat L-PheC$_2$NTf$_2$ necessitated using dilute ethanolic solutions in the determination of its quantum yield. A quantum yield of 0.06 was calculated upon excitation at 257nm in a 1 cm path-length quartz cell with right-angle collection geometry.

cell (Figure 3.2) displayed an absorbance of ~0.1 near 350nm decreasing to ~0.05 at 400nm. Absorption was greater than 3 at wavelengths below ~270nm. It is also interesting to note that subtle differences appeared in the spectral region between 280-320nm as L-PheC$_2$NTf$_2$ was diluted in ethanol (Figure 3.4).

The high absorbance of the neat L-PheC$_2$NTf$_2$ necessitated using dilute ethanolic solutions in determination of its quantum yield. A quantum yield of 0.06 was calculated for L-PheC$_2$NTf$_2$ dissolved in ethanol upon excitation at 257nm. For comparison, this value is slightly greater than the value of 0.022 reported for phenylalanine amino acid in water.[58] It should be noted that a low quantum yield does not preclude the use of this CIL for enantiomeric discrimination studies. Its use as a solvent (without dilution) resulted in sufficiently high concentration (molarity = 3.14 moles L^{-1}, calculated based on its measured density) to obtain more than adequate absorption and fluorescence signal.

The absorption spectrum of a thin film (~29 μm) of L-PheC$_2$NTf$_2$ between two quartz plates was qualitatively similar to that of a 1 mM solution of L-PheC$_2$Cl (a CIL precursor) in ethanol (Figure 2). The molar absorptivity of the L-PheC$_2$NTf$_2$ thin film was estimated to be 95 L mol^{-1} cm^{-1} at 257nm, which is lower than that reported for phenylalanine amino acid dissolved in H$_2$O (195 L mol^{-1}cm^{-1} at 257.5nm).[59] Decreased absorption was also observed for 0.01 M L-PheC$_2$Cl (a precursor of the CIL) in H$_2$O as compared to 0.01 M phenylalanine in H$_2$O (ratio of 1.77 at the absorption maxima) which accounts for most of the observed decrease in absorption for the phenylalanine-based CIL as compared to phenylalanine. The seemingly low molar absorptivity of L-PheC$_2$NTf$_2$ does not pose a problem for applications outlined for this study. In fact, high absorption values and the resulting inner filter effects presented greater difficulties. Therefore, front face collection geometry was used for fluorescence measurements in an effort to minimize inner filter effects. These data indicate that it was not generally practical to use

excitation wavelengths below ~280nm where absorption of the incident excitation light was observed to reduce the observed emission intensity.
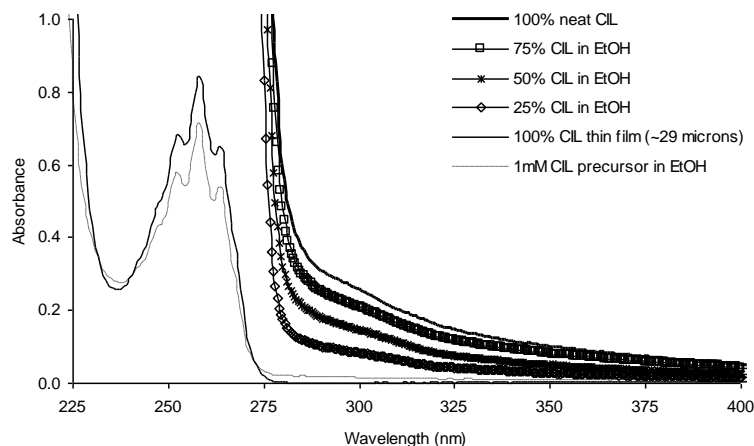
Figure 3.4. Absorption spectra of neat L-PheC$_2$NTf$_2$, various dilutions in ethanol (EtOH), and 1 mM L-PheC$_2$Cl ionic liquid precursor in EtOH measured in 4 mm thick cell. Figure also includes 29 μM thick layer of neat L-PheC$_2$NTf$_2$.

The fluorescence Excitation-Emission Matrix (EEM) of L-PheC$_2$NTf$_2$ revealed complex fluorescence behavior with multiple excitation and emission bands for the neat CIL. The full EEM contour plot can be found in Figure 3.5A with a subset of emission spectra collected using various excitation wavelengths as shown in Figure 3.5B. Although the emission intensity was impacted by absorption of the incident light, excitation at 260nm (near the 257nm absorption maximum of L-PheC$_2$NTf$_2$) revealed broad overlapping emissions with peak maxima near the characteristic 280nm emission of phenylalanine, as well as near 320nm. The latter peak has been previously identified as phenylalanine excimer by Leroy et al.[60] Longworth had also observed similar excimer emission for L-poly-phenylalanine in THF.[61] Increasing the excitation wavelength to 280nm reduced the impact of inner filter effects as the absorption decreased. A prominent excimer peak at 320nm resulting from 280nm excitation provided the largest emission intensity for excitation at any wavelength. A lower intensity emission peak near 400nm was also

81

apparent upon excitation at 280nm, which became more readily observable as the excitation wavelength increased to 300nm. At excitation of 320nm, the peak at near 400nm was the only emission peak. Excitations greater than 320nm resulted in a red shift of this long-wavelength emission. Concentration-based studies conducted by Leroy et al.[60] clearly demonstrated excimer emission at 320nm for a phenylalanine concentration of 0.1 M in water. However, no longer wavelength emitting species were reported at this concentration. It is not surprising that the extremely high phenyalanine concentration (3.14 moles L^{-1}) occurring in neat L-PheC$_2$NTf$_2$ results in much more complex spectral behavior than low concentration solutions. Explaining these complexities is beyond the scope of this present study. However, it should be noted that imidazolium ILs have also been reported to display unconventional fluorescence behavior. In such solutions, fluorescence emission shifted towards the red with increasing excitation wavelength. This observation was attributed to the presence of energetically different associated forms of the constituent ions and to a slow rate of excited state relaxation processes in the viscous IL.[62]

The complexity observed in the steady-state EEMs was also displayed in time-resolved measurements. Instrumental limitations and the high absorption of neat L-PheC$_2$NTf$_2$ complicated the measurements and required excitation at a longer wavelength than the 257nm maximum absorption of L-PheC$_2$NTf$_2$. In an effort to minimize inner filter effects, measurements were performed upon 330nm excitation with emission collected through a 370nm long pass filter. Leroy, et al. reported the lifetime of phenylalanine amino acid (8×10^{-4} M in H$_2$O at 20° C) to be 6.8±0.2 nsec and observed a slight increase in decay time at increasing concentrations.[60] In this work, three lifetime components including both significantly longer (~12 nsec) and shorter (<1 nsec) lifetimes were required to adequately model the decay of room temperature L-

PheC$_2$NTf$_2$ (Table 3.1). The more complex decay observed for the phenylalanine-based CIL is expected considering the complexity of the spectral behavior described above.
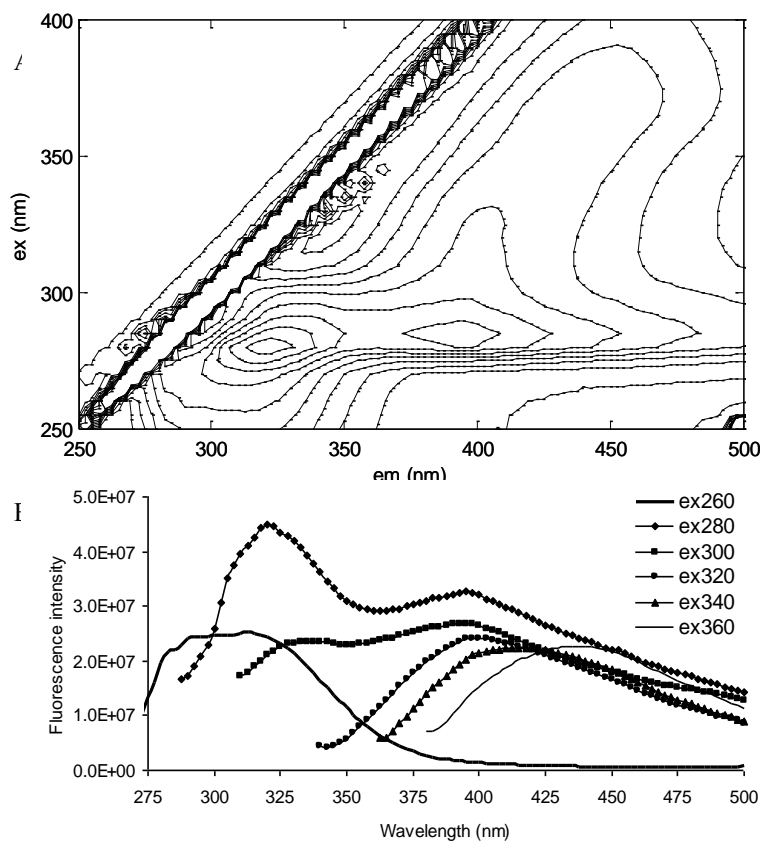
Figure 3.5. Fluorescence of neat L-PheC$_2$NTf$_2$ (A). Excitation-Emission Matrix (EEM), (B) subset of emission spectra collected with various excitation wavelengths extracted from the EEM at various excitation wavelengths (260-360nm in 20nm intervals).

It is also interesting to note that complex spectral behavior was observed in a phenylalanine-based fluorescent chiral molecular micelle, previously reported by our group.[19, 20] Long-wavelength emission and a triple exponential decay similar to that obtained for L-PheC$_2$NTf$_2$ were observed.

3.3.4. Enantiomeric Discrimination Using Steady-State Fluorescence Spectroscopy

In these studies L-PheC$_2$NTf$_2$ served simultaneously as solvent and chiral selector, as well as a fluorescent reporter in the case of non-fluorescent chiral analytes. In the case of chiral analytes possessing intrinsic fluorescence, comparisons of the spectral alterations induced upon the analyte's emission as compared to those induced upon the CIL's emission were made.

Equal concentrations (10 µM) of either pure R- or S- (D- or L-) enantiomer of each chiral analyte were dissolved into neat L-PheC$_2$NTf$_2$. All mixtures were prepared from ethanolic stock solutions of analytes (except glucose which was prepared in water). Required amounts of analyte stock solution were delivered into a vial; the ethanol was gently evaporated with a stream of nitrogen, and a known volume of L-PheC$_2$NTf$_2$ was added to the vials. Mixtures were shaken vigorously to ensure complete dissolution of the analytes.

Structures of L-PheC$_2$NTf$_2$, and all fluorescent and non-fluorescent chiral analytes used in this study are shown in Figure 3.6. A variety of fluorescent and non-fluorescent analytes were chosen with a wide range of chemical structures. It is interesting to note that L-PheC$_2$NTf$_2$ could dissolve all of these structurally diverse analytes and at the same time induce spectral differences between enantiomerically pure forms of each pair of analytes. Chiral ionic liquids show discrimination by solvating, and thus requires being in the presence of the analyte.[29, 49-51] For this reason, solubility is an important factor in the formation of diastereomeric complexes. In previous work using a phenylalanine-based molecular micelle as the chiral selector, we observed that the addition of methanol to aqueous solutions of analyte and selector improved the discrimination towards non-polar analytes.[20] The ability of ILs to solvate a wide range of both relatively polar and non-polar analytes may eliminate the need for this step, thus simplifying the measurement and increasing the universality of the method.
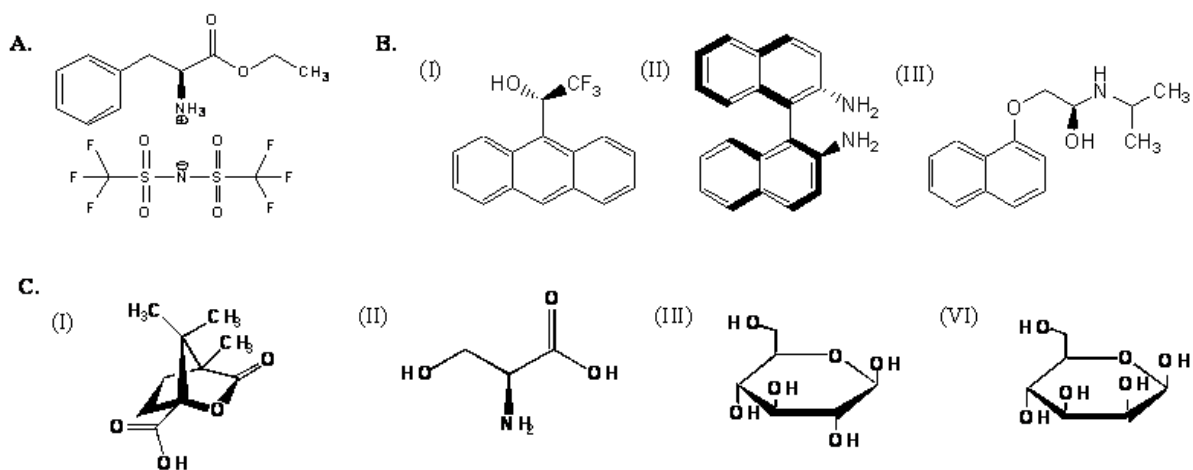
Figure 3.6. Chemical structures of chiral ionic liquid and chiral analytes investigated: A. selector L-phenylalanine ethyl ester bis (trifluoromethane) sulfonimide (L-PheC$_2$NTf$_2$), B. fluorescent analytes (I) TFAE (II) BNA (III) Propranolol. C. non-fluorescent analytes (I) Camphanic acid (II) Serine (III) Glucose (IV) Mannose.

The spectral properties of neat L-PheC$_2$NTf$_2$ are complex, with multiple emissions upon using different excitation wavelengths. In order to 1) measure the response of these various emissions to the presence of a chiral analyte and to 2) measure the response from intrinsically fluorescent analytes when present, it was essential to measure the EEM over a broad range of excitation and emission wavelengths. The use of multiple excitation wavelengths was imperative because many dipolar fluorescent molecules exhibit relatively strong excitation-wavelength-dependent fluorescence behavior in ILs.[62] The excitation-wavelength-dependent shift of the fluorescence maximum has been reported to be between 10-35nm.[62] The dynamic stokes shift and excitation wavelength-dependent fluorescence of dipolar molecules in room temperature ILs has been discussed at length.[63]

A comparison of the emission spectrum for neat fluorescent CIL with the spectrum of each enantiomer dissolved in L-PheC$_2$NTf$_2$ for a given wavelength is informative; however, mean-centered spectral plots have also proven to be a valuable tool in the presentation of spectral

differences induced by a chiral selector; thus providing insight into the enantiomeric composition of mixtures.[18, 19, 51] In this work, mean-centered plots (MCPs) were obtained by averaging spectra measured when pure R- and S- (or D- and L) enantiomers were dissolved in $L-PheC_2NTf_2$ and then these average values were subtracted from the corresponding spectra of each individual sample on a wavelength-by-wavelength basis. MCPs are generally useful to demonstrate the extent of chiral recognition displayed by a chiral selector towards a particular analyte, and for rapid screening of unknown samples to identify whether they are racemic or rich in one enantiomeric form. The best chiral selectors induce the largest spectral differences and also display the largest magnitudes in their MCPs. MCPs of racemic mixtures will lie on the origin, while MCPs of mixtures rich in one enantiomer will lie between the origin and the limiting value defined by the MCP of the corresponding pure enantiomer. The magnitude of the MCPs is an indication of the enantioselectivity displayed by a chiral selector towards a particular analyte.

In previous studies[18, 19, 51] a single excitation wavelength was generally chosen near the absorption maxima of the fluorescent analyte or fluorescent chiral selector. This greatly simplified the presentation of data as compared to the multidimensional fluorescence excitation-emission matrixes (EEMs) collected in this study. Emission spectra were collected for all excitations between 250-400nm. For simplicity, representative excitation wavelengths were chosen for presentation. Emission spectra of the neat fluorescent CIL and each enantiomer dissolved in $L-PheC_2NTf_2$ was collected at excitation wavelengths of 280nm and 360nm. These wavelengths were chosen because emission from $L-PheC_2NTf_2$ was efficiently generated. Intrinsically fluorescent propranolol was also efficiently excited at 280nm. Long-wavelength emission from $L-PheC_2NTf_2$ as well as emissions of intrinsically fluorescent TFAE and BNA were generated by excitation at 360nm. We note that other wavelengths are also of interest.

3.3.4.1. Enantiomeric Discrimination of Fluorescent Analytes

The fluorescent analytes investigated include propranolol, TFAE and BNA. TFAE and propranolol have asymmetric carbon and hydroxyl groups, whereas BNA has axial chirality and amine groups. Propranolol is a beta blocker commonly used for treatment of hypertension. BNA and TFAE are often used as starting materials for asymmetric synthesis.

The presence of BNA and TFAE resulted in ~25nm red shift and slight enhancement of the 320nm L-PheC$_2$NTf$_2$ emission upon 280nm excitation; however, there was minimal enantioselectivity apparent in the resultant emission. The emission of propranolol in S-CHTA NTf$_2$ upon 280nm excitation has been reported near 340nm with a shoulder near 350nm.[50] Its emission in L-PheC$_2$NTf$_2$ is dim, although it appears to be similar to the emission reported above. It overlaps with the 320nm phenylalanine excimer peak of L-PheC$_2$NTf$_2$ and possibly the shifted emission described above if it also exists in the presence of propranolol. The long-wavelength emission of CIL upon 360nm excitation in the presence of propranolol is quenched; however, there does not appear to be appreciable enantioselectivity in this spectral region. The emission of BNA and TFAE overlaps that of the long-wavelength L-PheC$_2$NTf$_2$ emission; however, it appears that this long-wavelength CIL emission is also quenched in a similar way as observed in the presence of propranolol and adds little to the chiral selectivity apparent in the emissions of the fluorescent analytes in this spectral region.

A subset of mean-centered plots (excitations from 260-360nm in 20nm intervals) for these fluorescent analytes in the presence of L-PheC$_2$NTf$_2$ are shown in Figure 3.7. L-PheC$_2$NTf$_2$ shows selectivity towards each of these diverse analytes. Of the data shown in Figure 3.7, the greatest difference was displayed for TFAE excited at 360nm. For propranolol, the greatest differences in emission between the enantiomers was at ~290nm. These plots demonstrate the

wavelength-dependent selectivity. Thus, the choice of excitation wavelengths has a major impact on the degree of selectivity.

3.3.4.2. Enantiomeric Discrimination of Non-fluorescent Analytes

Since many analytes of interest have limited or virtually no intrinsic fluorescence emission, it would be advantageous to measure alterations in the fluorescence emission of a fluorescent CIL, L-PheC$_2$NTf$_2$, caused by diasteromeric interactions with chiral analytes. The various non-fluorescent chiral analytes used for this study include camphanic acid, serine, glucose, and mannose. Camphanic acid is a chiral auxiliary in the synthesis of aza sugars and is also used in the resolution of chiral alcohols. Serine is a naturally occurring amino acid useful in metabolism such as biosynthesis of purines and pyrimidines. It also plays important catalytic functions in enzymes such as trpysin and chymotrypsin. Glucose and mannose are carbohydrates, useful sources of energy, and are useful in protein synthesis.

The presence of the non-fluorescent analytes, clearly induced spectral alterations to L-PheC$_2$NTf$_2$. For example, a similar ~25nm red shift and slight enhancement of the 320nm L-PheC$_2$NTf$_2$ emission upon 280nm excitation that was described in the presence of fluorescent analytes (BNA and TFAE) was also observed in the presence of camphanic acid. Interestingly, while this emission displayed minimal enantioselectivity in the presence of BNA and TFAE, it showed considerable enantioselectivity in the presence of the non-fluorescent camphanic acid.

A subset of mean-centered plots (excitations from 260-360nm in 20nm intervals) for the non-fluorescent analytes in the presence of L-PheC$_2$NTf$_2$ are shown in Figure 3.8. L-PheC$_2$NTf$_2$ shows selectivity towards each of these analytes. Comparisons of Figures 3.7 and 3.8 reveal that although the magnitude of differences were generally greater for 10 μM of fluorescent analytes, the presence of 10 μM non-fluorescent analytes induced more than adequate alterations to the emission of the fluorescent CIL solvent.
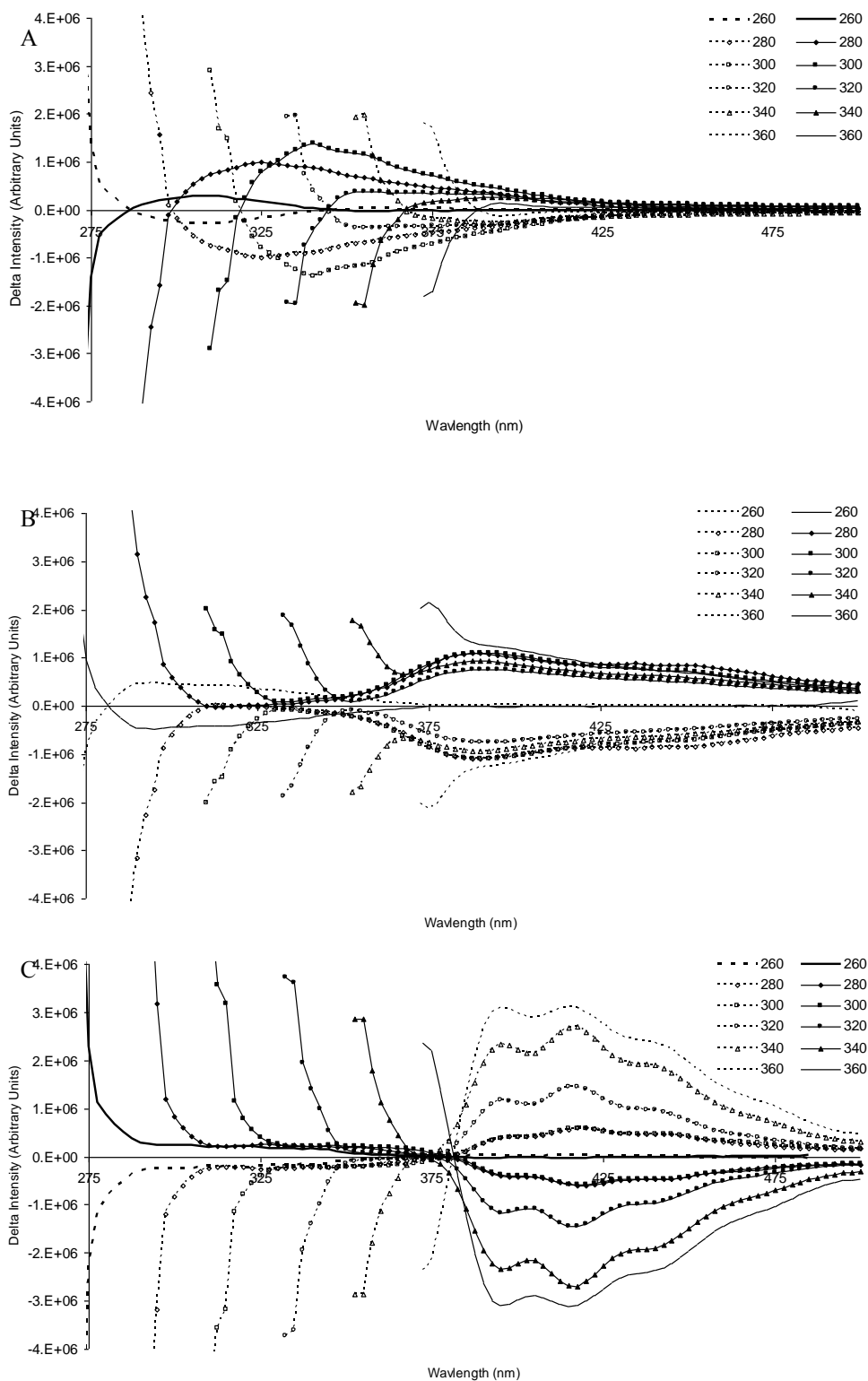
Figure 3.7. Fluorescence mean-centered plots (MCPs) for 10 μM individual fluorescent enantiomers in L-PheC$_2$NTf$_2$ presented at various excitation wavelengths (260-360nm in 20nm intervals). A. Propranolol, B. BNA, and C. TFAE. Solid lines represent the R- (or D-) enantiomer. Broken lines represent the S- (or L-) enantiomer.
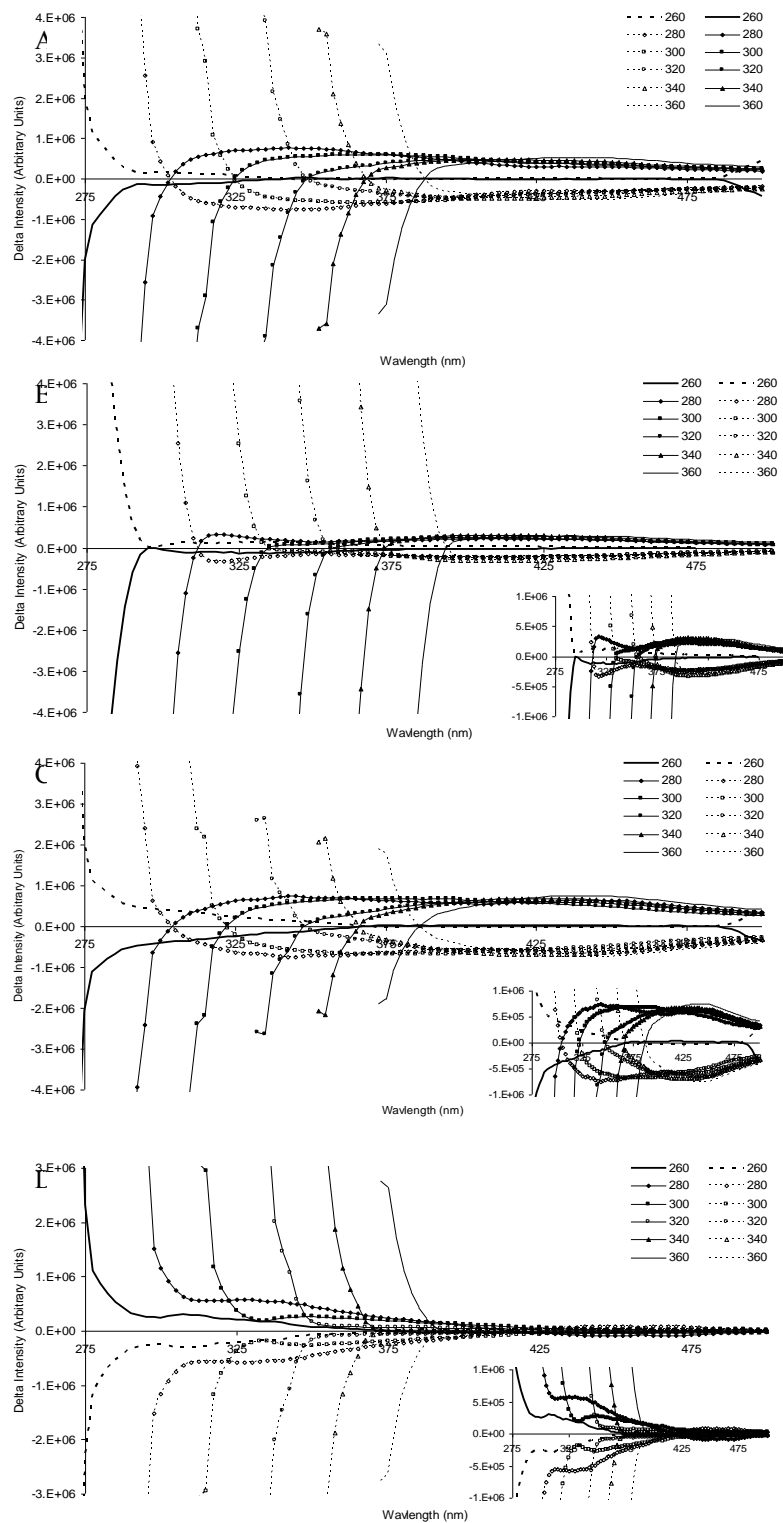
Figure 3.8. Fluorescence mean-centered plots (MCPs) for 10 μM individual non-fluorescent enantiomers in L-PheC$_2$NTf$_2$ presented at various excitation wavelengths (260-360nm in 20nm intervals). A. Camphanic acid, B. Serine, C. Glucose, and D. Mannose. Solid lines represent the R- (or D-) enantiomer. Broken lines represent the S- (or L-) enantiomer. Insets zoom in the y-axis.

3.3.5. Potential for Chemoselective and Enantioselective Fluorescent Discrimination of Monosaccharides

Saccharide sensing is an extremely active area of research. There are a total of 16 possible aldohexose stereoisomers with D-glucose, D-galactose, and D-mannose being the three most common hexoses present in nature. The three isomers differ only in the axial/equatorial configuration of their hydroxyl groups. Among these, sensing of D-glucose is of particular interest. There has been a large focus in recent years on boronic acid-based molecular receptors since their "rediscovery" in the mid 1990s.[64] While boronic acid-sugar chemistry has been known for well over a century, the first rationally designed fluorescent photoinduced electron transfer sensor for saccharides utilizing the boronic acid-tertiary amine interaction was reported by the Shinkai group in 1994.[65, 66] Boronic acid-based sensors have also been recently reviewed.[67] While there has been significant progress, the development of boronic acid-based molecular receptors has been hampered by synthetic difficulties. Another potential difficulty is the cleavage of boronic acids under relatively mild conditions.

We note that there is a large difference between the emissions of L-PheC$_2$NTf$_2$ in the presence of D-glucose as compared to D-mannose. Figure 3.9 clearly demonstrates the difference is excitation wavelength-dependent. The difference in emission between two individual sugar solutions (D-glucose minus D-mannose) of L-PheC$_2$NTf$_2$ is depicted as a contour map (Figure 3.9A). A subset of slices, with various excitation wavelengths extracted from the contour map, are also shown for clarity (Figure 3.9B). The largest difference in emission occurs near 350nm upon excitation at 280nm. Excitations beyond ~350nm also lead to relatively large difference in the long-wavelength CIL emission in the presence of these two compounds. Thus, L-PheC$_2$NTf$_2$ may show potential in the chemoselective discrimination of saccharides.
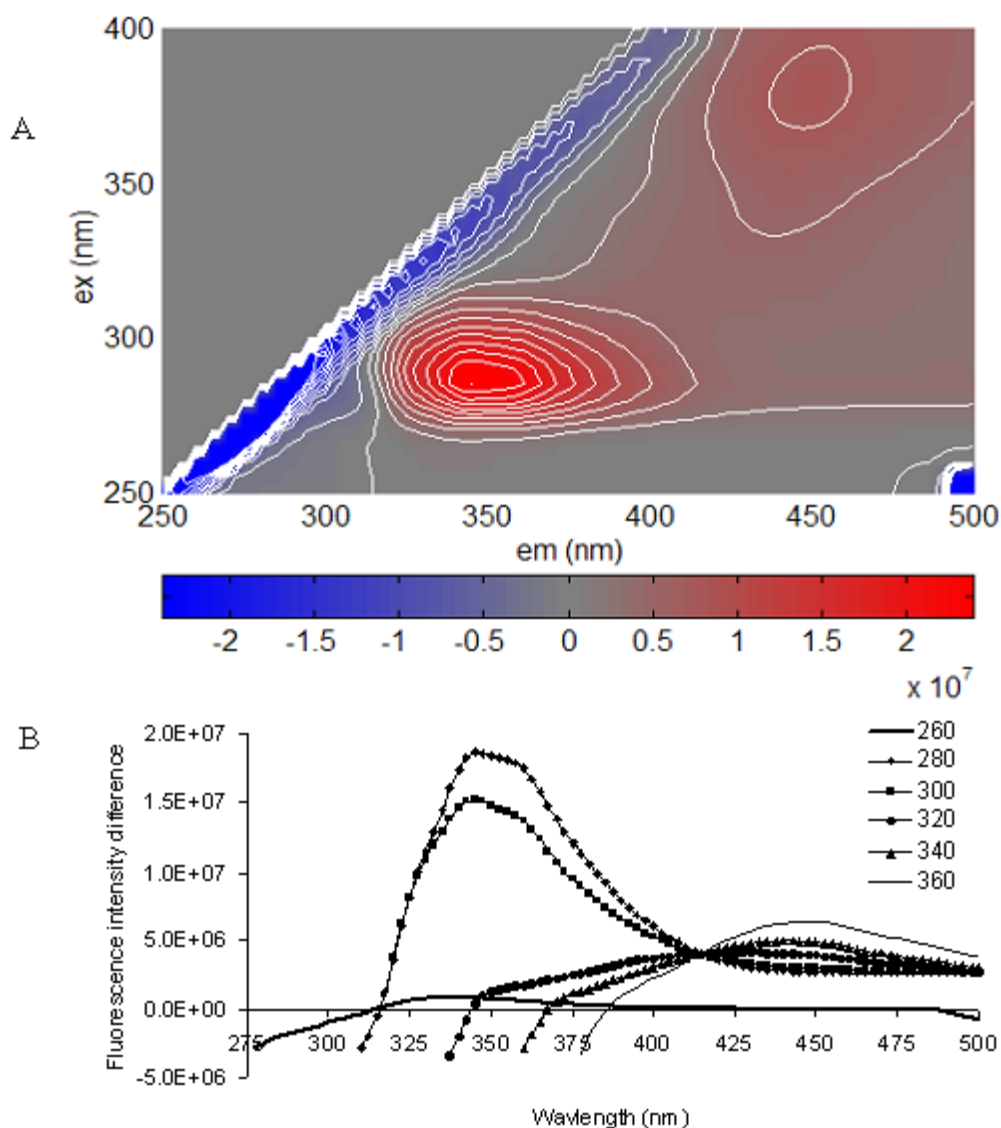
Figure 3.9. Fluorescence intensity differences (D-glucose minus D-mannose) between 10 μM D-glucose and D-mannose enantiomers in L-PheC$_2$NTf$_2$. A. Contour plot, B. Subset of difference spectra collected with various excitation wavelengths extracted from the contour plot at various excitation wavelengths (260-360nm in 20nm intervals).

The importance of chiral discrimination of monosaccharides has also been recognized. For example, James et al. reported the chiral discrimination of D- and L-monosaccharides using a chiral diboronic acid which incorporated a fluorescent naphthyl moiety.[68] Binding of each enantiomer of various monosaccharides altered the fluorescence intensity of the sensor to

differing degrees, thus allowing them to be distinguished. Other studies in this area have been reported, for example consider the recent study of enantioselective and chemoselective fluorescent chemosensors for sugar alcohols, such as D-sorbitol and D-mannitol.[69]

Not only does the CIL, L-PheC$_2$NTf$_2$, described herein, display selectivity between D-glucose and D-mannose. It also shows selectivity toward the individual enantiomeric forms of each. It is informative to compare the emission spectra for glucose and mannose enantiomers in the presence of L-PheC$_2$NTf$_2$ with each other, and with the corresponding emission of neat CIL. It is apparent that when excited at 260nm, the sugars have minimal effect on the emission of L-PheC$_2$NTf$_2$. However, at excitations greater than ~275nm, both sugars induced dramatic spectral alterations. For example, the presence of glucose resulted in a ~25nm red shift and slight enhancement of the 320nm L-PheC$_2$NTf$_2$ emission upon excitation at 280nm, with significant enantioselectivity toward glucose enantiomers apparent in this emission. Mannose did not induce a similar shift; rather it enantioselectively quenched the 320nm L-PheC$_2$NTf$_2$ emission. Enantioselectivity toward glucose was also displayed in the long-wavelength CIL emission and at longer excitation wavelengths; however, the quenching of this long-wavelength emission by mannose showed no enantioselectivity. The presence of each enantiomer of the two monosaccharides altered the fluorescence emission of L-PheC$_2$NTf$_2$ to differing degrees and in differing spectral regions, thus demonstrating the potential for chemoselective and enantioselective fluorescent discrimination of monosaccharides. For this reason, this phenomenon will be examined further in more detail.

3.4. Conclusions

In summary, we have synthesized and investigated the enantiomeric recognition properties of a fluorescent amino acid-based chiral ionic liquid, L-phenylalanine ethyl ester bis (trifluoromethane) sulfonimide (L-PheC$_2$NTf$_2$). Such a CIL is advantageous over previously

reported non-fluorescent CILs, whose applications were limited to the use of less sensitive modes of detection such as absorption, or to the use of fluorescence in discrimination of a small subset of intrinsically fluorescent analytes. To the best of our knowledge, this is the first report on the use of a fluorescent CIL as a solvent and chiral selector for enantiomeric recognition of non-fluorescent as well as fluorescent analytes. Preparation of L-PheC$_2$NTf$_2$ was simple, using commercially available starting materials, and the CIL was liquid at room temperature with thermal stability up to 270 ºC. In addition, the chiral configuration was retained upon prolonged exposure to high temperatures at 115 ºC, which is indicative of the high stability of L-PheC$_2$NTf$_2$ to thermal racemization, suggesting its potential as a stationary phase for chiral gas chromatography. Chiral discrimination studies were performed using ^{19}F NMR and steady-state fluorescence spectroscopy. The results suggest that L-PheC$_2$NTf$_2$ is a potential solvent, chiral selector, and fluorescent reporter for enantiomeric recognition of several chiral compounds with a wide range of structures. L-PheC$_2$NTf$_2$ may also prove useful in the chemoselective and enantioselective fluorescent discrimination of monosaccharides.

3.5. References

(1)   Islam, M. R.; Mahdi, J. G.; Bowen, I. D. *Drug Saf.* **1997**, *17*, 149-165.

(2)   Agranat, I.; Caner, H.; Caldwell, A. *Nat. Rev. Drug Discov.* **2002**, *1*, 753-768.

(3)   Caner, H.; Groner, E.; Levy, L.; Agranat, I. *Drug Discov. Today* **2004**, *9*, 105-110.

(4)   *FDA's Policy Statement for the Development of New Stereoisomeric Drugs. FED REGISTER* **1992**, http://www.fda.gov/cder/guidance/stereo.htm.

(5)   Agrawal, Y. K.; Bhatt, H. G.; Raval, H. G.; Oza, P. M.; Gogoi, P. J. *Mini-Rev. Med. Chem.* **2007**, *7*, 451-460.

(6)   Kano, K. *J. Phys. Org. Chem.* **1997**, *10*, 286-291.

(7)   Fanali, S. *J. Chromatogr. A* **2000**, *875*, 89-122.

(8)   Fillet, M.; Hubert, P.; Crommen, J. *J. Chromatogr. A* **2000**, *875*, 123-134.

(9)   Chankvetadze, B. *Chem. Soc. Rev.* **2004**, *33*, 337-347.

(10)   Dodziuk, H.; Kozminski, W.; Ejchart, A. *Chirality* **2004**, *16*, 90-105.

(11)   Juvancz, Z.; Kendrovics, R. B.; Ivanyi, R.; Szente, L. *Electrophoresis* **2008**, *29*, 1701-1712.

(12)   Got, P. A.; Scherrmann, J. M. *Pharm. Res.* **1997**, *14*, 1516-1523.

(13)   Hofstetter, H.; Cary, J. R.; Eleniste, P. P.; Hertweck, J. K.; Lindstrom, H. J.; Ranieri, D. I.; Smith, G. B.; Undesser, L. P.; Zeleke, J. M.; Zeleke, T. K.; Hofstetter, O. *Chirality* **2005**, *17*, S9-S18.

(14)   Hofstetter, H.; Hofstetter, O. *Trac-Trends Anal. Chem.* **2005**, *24*, 869-879.

(15)   Ward, T. J.; Farris, A. B. *J. Chromatogr. A* **2001**, *906*, 73-89.

(16)   Ilisz, I.; Berkecz, R.; Peter, A. *J. Sep. Sci.* **2006**, *29*, 1305-1321.

(17)   Shamsi, S. A.; Palmer, C. P.; Warner, I. M. *Anal. Chem.* **2001**, *73*, 140A-149A.

(18)   Fakayode, S. O.; Williams, A. A.; Busch, M. A.; Busch, K. W.; Warner, I. M. *J. Fluoresc.* **2006**, *16*, 659-670.

(19)   Williams, A. A.; Fakayode, S. O.; Alpturk, O.; Jones, C. M.; Lowry, M.; Strongin, R. M.; Warner, I. M. *J. Fluoresc.* **2008**, *18*, 285-296.

(20)   Williams, A. A.; Fakayode, S. O.; Lowry, M.; Warner, I. M. *Chirality* **2009**, *XX*, XXXX-XXXX Early View 05/29/08 (DOI: 10.1002/chir.20580).

(21)   Okamoto, Y.; Yashima, E. *Angew. Chem.-Int. Edit.* **1998**, *37*, 1020-1043.

(22)   Tachibana, K.; Ohnishi, A. *J. Chromatogr. A* **2001**, *906*, 127-154.

(23)   Yashima, E. *J. Chromatogr. A* **2001**, *906*, 105-125.

(24)   Stringham, R. W. In *Advances in Chromatography, Vol 44*; CRC PRESS-Taylor & Francis Group: Boca Raton, 2006; Vol. 44, pp 257-290.

(25)   Ali, I.; Aboul-Enein, H. Y. *Curr. Pharm. Anal.* **2007**, *3*, 71-82.

(26)   Kuhn, R. *Electrophoresis* **1999**, *20*, 2605-2613. (27)Hyun, M. H. *Bull. Korean Chem. Soc.* **2005**, *26*, 1153-1163.

(28)   Anderson, J. L.; Ding, J.; Welton, T.; Armstrong, D. W. *J. Am. Chem. Soc.* **2002**, *124*, 14247-14254.

(29)   Tran, C. D. *Anal. Lett.* **2007**, *40*, 2447-2464.

(30)   Ding, J.; Welton, T.; Armstrong, D. W. *Anal. Chem.* **2004**, *76*, 6819-6822.

(31)   Yuan, L. M.; Han, Y.; Zhou, Y.; Meng, X.; Li, Z. Y.; Zi, M.; Chang, Y. X. *Anal. Lett.* **2006**, *39*, 1439-1449.

(32)   Baker, G. A.; Baker, S. N.; Pandey, S.; Bright, F. V. *Analyst* **2005**, *130*, 800-808.

(33)   Anderson, J. L.; Armstrong, D. W.; Wei, G. T. *Anal. Chem.* **2006**, *78*, 2892-2902.

(34)   Stalcup, A. M.; Cabovska, B. *J. Liq. Chromatogr. Relat. Technol.* **2004**, *27*, 1443-1459.

(35)   Shamsi, S. A.; Danielson, N. D. *J. Sep. Sci.* **2007**, *30*, 1729-1750.

(36)   Polyakova, Y.; Koo, Y. M.; Row, K. H. *Rev. Anal. Chem.* **2007**, *26*, 77-98.

(37)   Welton, T. *Chem. Rev.* **1999**, *99*, 2071-2083.

(38)   Smiglak, M.; Metlen, A.; Rogers, R. D. *Accounts Chem. Res.* **2007**, *40*, 1182-1192.

(39)   Yu, S. F.; Lindeman, S.; Tran, C. D. *J. Org. Chem.* **2008**, *73*, 2576-2591.

(40)   Bica, K.; Gaertner, P. *Eur. J. Org. Chem.* **2008**, 3235-3250.

(41)   Patil, M. L.; Sasai, H. *Chem. Rec.* **2008**, *8*, 98-108.

(42)   Winkel, A.; Reddy, P. V. G.; Wilhelm, R. *Synthesis* **2008**, 999-1016.

(43)   Ding, J.; Armstrong, D. W. *Chirality* **2005**, *17*, 281-292.

(44)   Baudequin, C.; Bregeon, D.; Levillain, J.; Guillen, F.; Plaquevent, J. C.; Gaumont, A. C. *Tetrahedron: Asymmetry* **2005**, *16*, 3921-3945.

(45)   Rizvi, S. A. A.; Shamsi, S. A. *Anal. Chem.* **2006**, *78*, 7061-7069.

(46)   Fukumoto, K.; Yoshizawa, M.; Ohno, H. *J. Am. Chem. Soc.* **2005**, *127*, 2398-2399.

(47)   Ohno, H.; Fukumoto, K. *Accounts Chem. Res.* **2007**, *40*, 1122-1129.

(48)   Chen, X. W.; Li, X. H.; Hu, A. X.; Wang, F. R. *Tetrahedron: Asymmetry* **2008**, *19*, 1-14.

(49)   Tran, C. D.; Oliveira, D.; Yu, S. F. *Anal. Chem.* **2006**, *78*, 1349-1356.

(50)   Tran, C. D.; Oliveira, D. *Anal. Biochem.* **2006**, *356*, 51-58.

(51)   Bwambok, D. K.; Marwani, H. M.; Fernand, V. E.; Fakayode, S. O.; Lowry, M.; Negulescu, I.; Strongin, R. M.; Warner, I. M. *Chirality* **2008**, *20*, 151-158.

(52) Boydston, A. J.; Pecinovsky, C. S.; Chao, S. T.; Bielawski, C. W. *J. Am. Chem. Soc.* **2007**, *129*, 14550-14551.

(53) Boydston, A. J.; Vu, P. D.; Dykhno, O. L.; Chang, V.; Wyatt, A. R.; Stockett, A. S.; Ritschdbrff, E. T.; Shear, J. B.; Bielawski, C. W. *J. Am. Chem. Soc.* **2008**, *130*, 3143-3156.

(54) Williams, A. T. R.; Winfield, S. A.; Miller, J. N. *Analyst* **1983**, *108*, 1067-1071.

(55) Jodry, J. J.; Mikami, K. *Tetrahedron Lett.* **2004**, *45*, 4429-4431.

(56) Baranyai, K. J.; Deacon, G. B.; MacFarlane, D. R.; Pringle, J. M.; Scott, J. L. *Aust. J. Chem.* **2004**, *57*, 145-147.

(57) Kosmulski, M.; Gustafsson, J.; Rosenholm, J. B. *Thermochim. Acta* **2004**, *412*, 47-53.

(58) Chen, R. F. *Journal of Research of the National Bureau of Standards Section C-Engineering and Instrumentation* **1972**, *A 76*, 593-606.

(59) Fasman, G. D. *Handbook of Biochemistry and Molecular Biology, Proteins, I, 3 ed.*; CRC Press, Boca Raton, 1976.

(60) Leroy, E.; Lami, H.; Laustria.G *Photochem. Photobiol.* **1971**, *13*, 411-421

(61) Longwort, J. W. *Biopolymers* **1966**, *4*, 1131-1148.

(62) Mandal, P. K.; Sarkar, M.; Samanta, A. *J. Phys. Chem. A* **2004**, *108*, 9048-9053.

(63) Samanta, A. *J. Phys. Chem. B* **2006**, *110*, 13704-13716.

(64) James, T. D.; Sandanayake, K.; Shinkai, S. *Angew. Chem.-Int. Edit. Engl.* **1996**, *35*, 1910-1922.

(65) James, T. D.; Sandanayake, K.; Shinkai, S. *J. Chem. Soc.-Chem. Commun.* **1994**, 477-478.

(66) James, T. D.; Sandanayake, K.; Iguchi, R.; Shinkai, S. *J. Am. Chem. Soc.* **1995**, *117*, 8982-8987.

(67) Wang, W.; Gao, X. M.; Wang, B. H. *Curr. Org. Chem.* **2002**, *6*, 1285-1317.

(68) James, T. D.; Sandanayake, K.; Shinkai, S. *Nature* **1995**, *374*, 345-347.

(69) Liang, X. F.; James, T. D.; Zhao, J. Z. *Tetrahedron* **2008**, *64*, 1309-1315.

CHAPTER 4

NEAR INFRARED FLUORESCENT NANOGUMBOS FOR BIOMEDICAL IMAGING

4.1. Introduction

Near infrared (NIR) fluorescent materials have been successfully applied in areas such as analyses and sensor development,[1] laser dyes,[2] organic light-emitting diodes (OLEDs),[3] invisible printing inks,[4] photodynamic therapy,[5] and as biomedical imaging contrast agents.[6-10] For *in vivo* imaging applications, the low absorption coefficient of human skin tissues in the 700–1100 nm NIR wavelength region[11] minimizes scattering and background interference, allowing for deep tissue imaging.[12] A number of NIR-emissive materials have been exploited based on their desirable luminescence in this spectrally quiet region, especially those that fall in the nano-regime. These nanomaterials include quantum dots,[13] single walled carbon nanotubes,[14] lanthanides,[15] fluorescent proteins,[16] gold nanoshells,[12] fluorophore-tagged polymers,[17] and organic dyes.[18, 19] However, many of these nanomaterials have had concerns raised regarding both their environmental safety and their cytotoxicity. For instance, quantum dots have been reported to cause microbial toxicity[20] and pose serious environmental safety concerns which are difficult to either control or predict. In this regard, the development of alternative nanomaterials that are biocompatible, non-toxic, and tunable, while exhibiting well-defined delivery behavior, is highly sought.

When employed for biological applications such as imaging, fluorophores are typically encapsulated or doped into a polymeric[21] or silica[22] carrier particle, primarily for purposes of biocompatibility. However, dye encapsulation using these materials often leads to additional challenges such as dye leakage[21] and permeability problems.[23] There are also concerns that the use of surfactant stabilizers in the preparation of these particles may induce systemic toxicity.[24]

Again, an urgent need remains for the development of uniform, non-leaking, and additive-free luminescent particles for bio-imaging.

Within our laboratories, we have recently developed an emergent class of highly promising nano-materials we will collectively refer to as GUMBOS (Group of Uniform Materials Based on Organic Salts). A range of stable GUMBOS can be formed in the nano-regime from ionic liquids (ILs) that melt above room temperature. In general, the low melting points of ILs stem from the asymmetry of the component ions and the resultant poor crystal packing,[25] a feature open to design. Of course, nanoGUMBOS developed from ILs enjoy many of the unique properties associated with this novel class of material, including negligible vapor pressure, variable solubility, non-flammability, high thermal stability, ionic conductivity, and recyclability.[26] In the current application, however, GUMBOS formed from ionic materials that do not comply with the traditional working definition of an IL and melt above 100 °C are also useful building blocks in GUMBOS formation. The most attractive feature of nanoGUMBOS is the ability to gather within the same nano-object several complementary or orthogonal properties, leading to the prospect of developing multifunctional GUMBOS. This designer characteristic borrows from lessons learned in IL technology, namely, that careful selection and pairing of a functional cation with a dissimilarly functional anion leads to a tailored material displaying bimodal properties.

In this study, we report on a new class of fluorescent nanoparticle based on the concept of GUMBOS. These nanoparticles display uniform, stable NIR luminescence suitable for fluorescence imaging applications. The unique spectral properties of these NIR fluorescent nanoGUMBOS and their performance in cellular imaging studies are summarized in this work. To the best of our knowledge, this is the first report of IL-based NIR fluorescent nanoparticles. Our results suggest that nanoGUMBOS might offer unique possibilities for *in vivo* NIR

fluorescence imaging without the need for dye carriers, providing potential as contrast agents in other medical imaging modes as well.

4.2. Materials and Methods

4.2.1. Materials

1,1′,3,3,3′,3′-hexamethylindotricarbocyanine (HMT) iodide (97%), bis (2-ethylhexyl) sulfosuccinate (AOT) sodium salt (≥99%), potassium 4-(trifluoromethyl) phenyltrifluoroborate (96%) and potassium 3,5 bis (trifluoromethyl) phenyltrifluoroborate, Sodium tetrakis[3,5-bis(1,1,1,3,3,3-hexafluoro-2-methoxy-2-propyl)phenyl]borate, sodium tetrafluoroborate, sodium tetraphenylborate and ethanol (spectroscopic grade) were purchased from Sigma Aldrich and used as received. Triply deionized water (18.2 MΩ cm) from an Elga model PURELAB ultra^{TM} water filtration system was used for all preparations of IL NIR dye nanoparticles. Vero cells were obtained from the School of Veterinary Medicine (Louisiana State University, Baton Rouge, LA). Carbon coated copper grids (CF400-Cu, Electron Microscopy Sciences, Hatfield, PA) were used for TEM imaging.

4.2.2. Synthesis and Characterization of NIR GUMBOS

The NIR GUMBOS (mostly ILs) were prepared using anion exchange procedures similar to those reported in the literature.[25-27] The synthesis of 1,1′,3,3,3′,3′-hexamethylindotricarbocyanine bis (2-ethylhexyl) sulfosuccinate ([HMT] [AOT]) is described as a representative procedure. An amount of 30 mg (0.056 mmol) of 1,1′,3,3,3′,3′-hexamethylindotricarbocyanine (HMT) iodide and 24.86 mg (0.056 mmol) of sodium bis (2-ethylhexyl) sulfosuccinate (AOT) salt were dissolved in a mixture of methylene chloride and water (2:1 v/v) and allowed to stir for 12hrs at room temperature (Scheme 4.1). The methylene chloride bottom layer was washed several times with water and the product was obtained from the organic lower layer and dried by removal of solvent *in vacuo*. Further freeze drying to remove traces of water afforded 43.02 mg (93% yield)

of [HMT] [AOT]. All GUMBOS obtained were characterized by ^{1}H NMR (Bruker 250 MHz spectrometer) and elemental microanalysis (Atlantic Microlab, Norcross, GA, USA). In addition, ^{19}F NMR was used to confirm anion exchange for fluorine containing GUMBOS. Melting points of the GUMBOS was determined using a MEL-TEMP® capillary melting point apparatus.
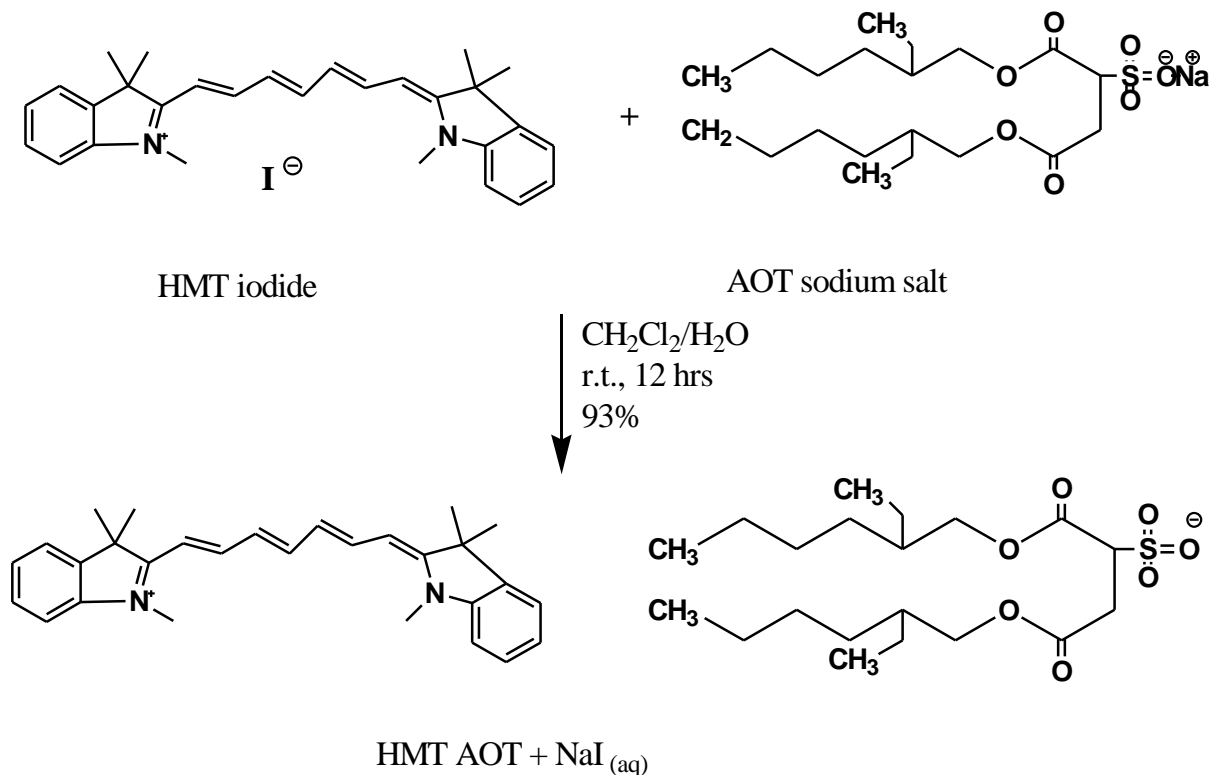
Scheme 4.1. Synthesis of [HMT] [AOT] by anion exchange reaction

4.2.3. Synthesis of NIR NanoGUMBOS

The nanoGUMBOS were prepared from GUMBOS using a modified simple, additive-free reprecipitation method similar to that used for organic nanoparticles.[24,28-31] The solvents used for preparing the nanoGUMBOS were filtered using 0.2 µm nylon membrane filters. In a typical preparation, 100 µL of a 1 mM solution of GUMBOS precursor dissolved in ethanol was rapidly injected into 5 mL of triply-deionized water in an ultrasonic bath, followed by further sonication for 2 min. Post-preparation, the particle suspension was aged for 1 h in the dark.

4.2.4. Characterization of Size and Morphology of NIR NanoGUMBOS

The average particle size and size distribution of the prepared nanoGUMBOS were obtained by use of transmission electron microscopy (TEM) and dynamic light scattering (DLS). TEM micrographs were obtained using an LVEM5 transmission electron microscope (Delong America, Montreal, Canada). The NIR nanoGUMBOS dispersion (1 µL) was dropcasted onto a carbon coated copper grid and allowed to dry in air at room temperature before TEM imaging.

4.2.5. X-Ray Diffraction Analysis of NIR NanoGUMBOS

X-ray diffraction measurements of dried nanoGUMBOS were obtained on a Nonius Kappa CCD diffractometer by long exposures with Mo Kα radiation and rotation of samples about the vertical axis.

4.2.6. Absorption and Fluorescence Studies of NIR GUMBOS and NanoGUMBOS

Absorbance measurements were performed on a Shimadzu UV- 3101PC UV-Vis-near-IR scanning spectrometer (Shimadzu, Columbia, MD). Fluorescence emission was collected using a Spex Fluorolog-3 spectrofluorimeter (model FL3-22TAU3); Jobin Yvon, Edison, NJ). A 1 cm^2 quartz cuvette (Starna Cells) was used to collect the fluorescence and absorbance against an identical cell filled with water as the blank.

4.2.7. Cellular Uptake Studies of Nano-GUMBOS by Vero Cells

HMT AOT nanoGUMBOS were used as model nanoGUMBOS for Vero cellular labeling in this study. The choice was based on its spectral properties (absorption and fluorescence) in the NIR diagnostic window. In addition, literature studies suggest that both the constituent ions in HMT AOT are expected to have non-toxic properties. Specifically, HMT cation has been used in biological optical imaging. A structurally related cyanine dye and HMT have also been used as a probe for radionuclide and fluorescence complementary studies. In addition, the AOT anion has been used as an emollient ("skin softener") in the preparation of IL-active pharmaceutical

ingredients with cations such as lidocaine (pain reliever), ranitidine (antihistamine) and didecyldimethylammonium (antibacterial). Vero cells (isolated from kidney epithelial cell lining extracted from an African green monkey, *Cercopithecus aethiops*) were used as a model cell line for this study using HMT AOT nanoGUMBOS. The cells were maintained in Dulbecco's Modified Eagle's Medium (DMEM) before studies. The Vero cells were then loaded into an eight well glass plate (2.5×10^5 cells/well) and incubated with HMT AOT nanoparticles (8 µg/mL) for 24 hrs. The cells are then washed twice with phosphate buffered saline (PBS) and immediately visualized using a Zeiss epifluorescence microscope equipped with a Zeiss digital camera for image acquisition. Negative controls were also prepared by loading the Vero cells into the wells which did not contain dye.

4.3. Results and Discussion

4.3.1. Synthesis, Characterization and Optical Properties of NIR GUMBOS and NanoGUMBOS

The GUMBOS presented in this dissertation were produced from a cationic NIR core unit following a modification of anion exchange procedures reported elsewhere.[27-29] We selected for this study, the cationic NIR-emitting cyanine dye 1,1′,3,3,3′,3′-hexamethylindotricarbocyanine (HMT) iodide. An example of an anion exchange reaction between HMT iodide and sodium bis (2-ethylhexyl) sulfosuccinate (AOT) is shown in Scheme 4.1. The various anions used in the formulation of our GUMBOS were selected for their varying hydrophobicities, geometries, and masses. All GUMBOS obtained were characterized by nuclear magnetic resonance (NMR) and elemental microanalysis and yielded results consistent with expectations.

As expected, the resulting NIR-emitting GUMBOS displayed variable physical properties (melting point, solubility) dependent upon variations in the anion (Table 4.1). This illustrates the tunability of our GUMBOS, allowing the design of a variety of physicochemical properties targeting select applications. In general, we found that the melting point decreased
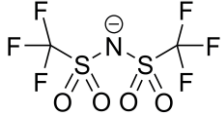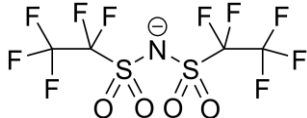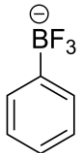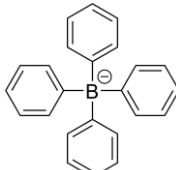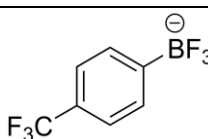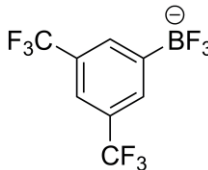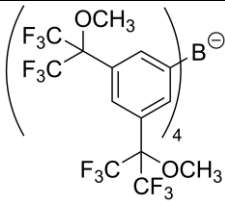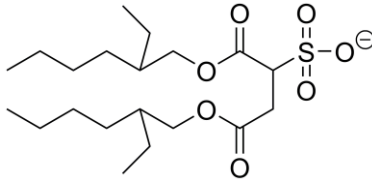
with an increase in the size of the anion. For instance, HMT (Scheme 4.2) with a relatively smaller 4-(trifluoromethyl) phenyltrifluoroborate anion had a melting point of 98°C whereas the melting point decreased to 58°C when a larger AOT anion was used (Table 4.1). This observation is consistent with that of Larsen and coworkers who investigated the factors that affect melting point for imidazolium ILs.[30] The authors concluded that the reduced crystal packing efficiency resulting from large anion incorporation played a profound role in depressing the melting point. Additionally, alkylation of the anion further frustrated the ion packing, causing a further drop in the melting point.[30] It is worth noting that databanks and semi-empirical models to predict melting points of ILs have been published.[31] References such as these serve as valuable resources when considering the design and synthesis of future GUMBOS.

The solubility of ILs in water has been shown to be highly dependent on the choice of the anion.[32] As expected, the miscibility of the various GUMBOS with water was also highly variable and dependent on the anion used in GUMBOS formation. The water-immiscible GUMBOS are suggestive of poor hydrogen bonding interactions, as exemplified by [HMT] [AOT]. However, some GUMBOS based on relatively hydrophilic iodide and boron-containing anions such as tetrafluoroborate showed enhanced aqueous solubility, possibly a consequence of the additional hydrogen bonding afforded by the degree of fluorination. In addition, the electron-withdrawing properties of fluorine may induce dipole moments, resulting in dipole–induced dipole interactions with the surrounding water molecules.[33] This postulate is supported by the
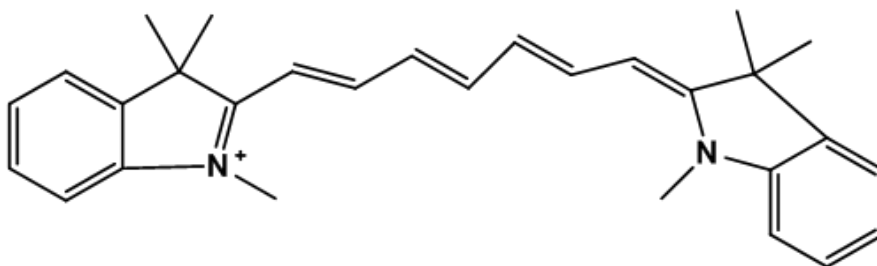
Scheme 4.2. Structure of HMT NIR dye cation

104

Table 4.1. Melting points and aqueous solubilities of [HMT$^+$]-derived GUMBOS with various anions.

NIR GUMBOS	Anion structure	mp (°C)	solubility in water
HMT NTf$_2$		220	×
HMTBETI		202	×
HMT BF$_4$		175	√
HMT TFPB		125	√
HMT TPB		96	×
HMT 4-CF$_3$BF$_3$ Phe		98	√
HMT 3,5-CF$_3$PheB		95	×
HMT (OCH$_3$)$_4$PheB		70	×
HMT AOT		58	×

aqueous solubility trend observed when comparing the mono- and di- trifluoromethyl substituted GUMBOS formed from 4-(trifluoromethyl) phenyltrifluoroborate and 3,5 bis (trifluoromethyl) phenyltrifluoroborate, respectively. In the latter case, the water immiscibility of HMT containing the 3,5 bis (trifluoromethyl) phenyltrifluoroborate anion may be attributed to a reduced net dipole moment arising from symmetric trifluoromethyl substitution.

In each case, solutions of GUMBOS based on the [HMT$^+$] cation were excellent absorbers of NIR irradiation. An example of this observation is shown in Figure 4.1A for a 1.0 µM ethanolic solution of [HMT][AOT] GUMBOS, where peak absorption occurs at 743 nm. As a result of the parent HMT cation, the GUMBOS fluoresce strongly in the NIR region, peaking near 765 nm; with the fluorescence excitation and emission spectra following the mirror-image rule (Figure 4.1B) as expected from the Franck-Condon principle. As an example, the structure of the NIR emitting [HMT$^+$] cation with bis (2-ethylhexyl) sulfosuccinate [AOT$^-$] anion is shown at the top of Figure 4.1. Note that the focus in this chapter is on the spectral properties and cellular labeling using HMT AOT as model NIR nanoGUMBOS. Detailed investigation of the spectral properties of all the GUMBOS and nanoGUMBOS will be discussed in the next chapter.

In the initial report on the preparation of nanoGUMBOS, we set forth a precedent for employing frozen ILs to manufacture size-controlled nanoparticles.[34] In our earlier study, we developed a "melt-emulsion-quench" approach for the controllable formation of particles with average diameters spanning the 45 to 3000 nm range. In the current work, the preparation of nanoGUMBOS was achieved using a modified reprecipitation method,[35-39] which is simpler to implement and more rapid. In a typical preparation, 100 µL of a 1 mM solution of GUMBOS precursor dissolved in ethanol was rapidly injected into 5 mL of triply-deionized water in an ultrasonic bath, followed by further sonication for 2 min. The ethanolic pre-GUMBOS solution
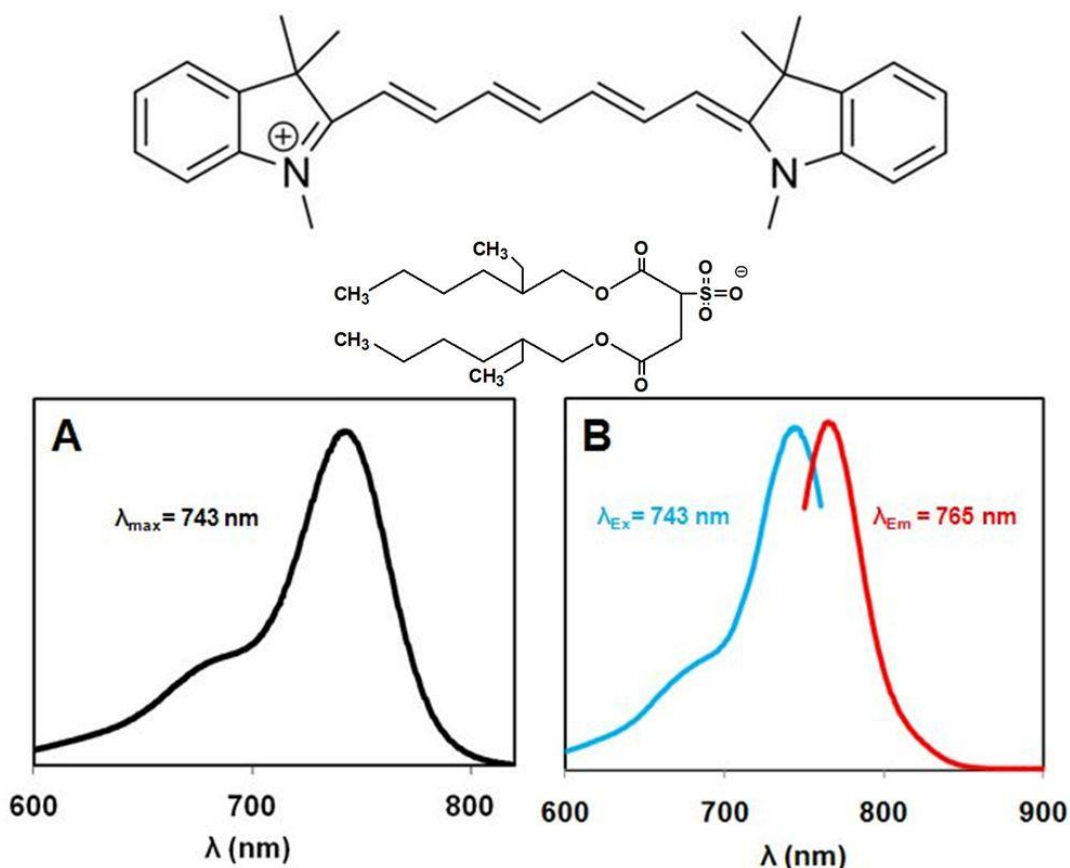
Figure 4.1. (A) Absorbance profile and (B) fluorescence excitation and emission spectra for 1.0 μM [HMT][AOT] in ethanol; $\lambda_{ex} = 743$ nm, $\lambda_{em} = 765$ nm.

and water were both filtered prior to preparation of the nanoparticles using 0.2 μm nylon membrane filters. Post-preparation, the particle suspension was aged for 1 h in the dark. The average particle size and size distribution of the prepared nanoGUMBOS were obtained by use of transmission electron microscopy (TEM) and dynamic light scattering (DLS). We note that most of the water miscible solvents such as acetonitrile, tetrahydrofuran, dimethyl sulfoxide, N-methyl pyrrolidinone, and acetone may be used in reprecipitation to obtain nanoGUMBOS dispersed in water. The reprecipitation synthetic method yields primarily spherical or slightly ovate nanoparticles as confirmed by TEM. A representative TEM micrograph of nanoGUMBOS with an average particle diameter of 79±18 nm is shown in Figure 4.2A. The polydispersity index obtained for these samples by use of DLS was generally quite good, usually under 0.100.

107
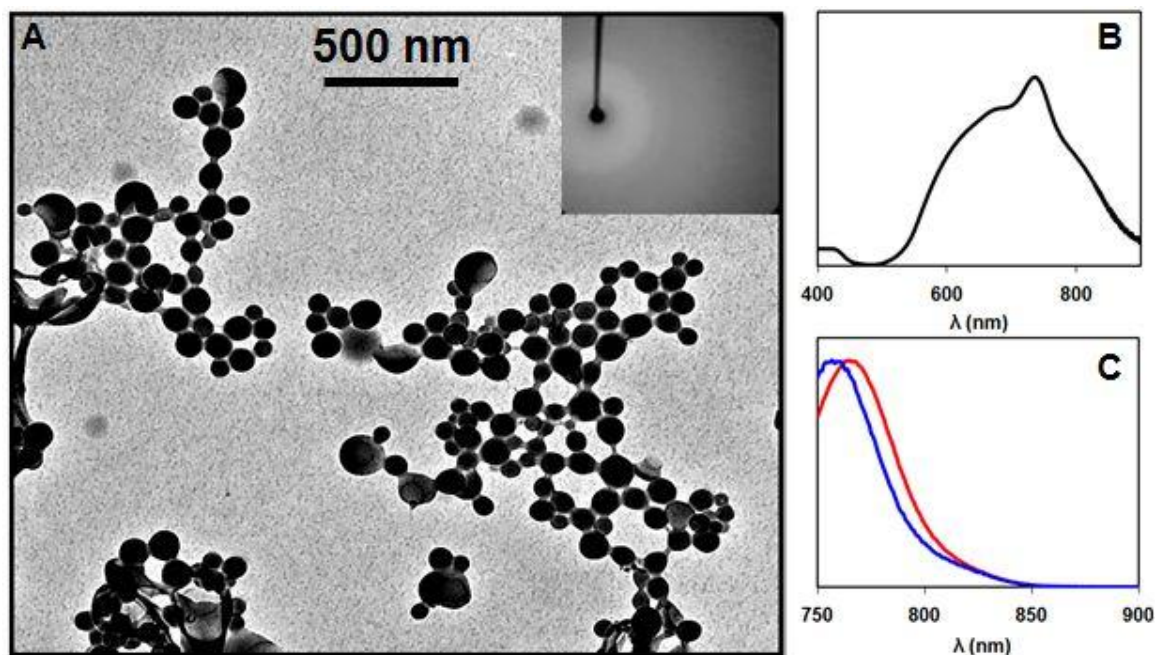
Figure 4.2. (A) TEM micrograph of [HMT][AOT] fluorescent NIR nanoGUMBOS with an average diameter near 79 ± 18 nm; the inset shows a selected area electron diffraction pattern (SAED) for the [HMT][AOT] GUMBOS. (B) Absorbance spectrum of the [HMT][AOT] nanoparticles illustrated in panel A, and (C) comparison between the fluorescence emission spectrum of the freely dissolved [HMT][AOT] IL (1.0 µM in ethanol; red profile) and [HMT][AOT] nanoGUMBOS (blue profile) for matched absorptivity at the excitation wavelength (λ_{ex} = 743 nm).

The prepared NIR-emitting nanoGUMBOS displayed optical properties which were strikingly different from that of the initial ethanolic dye solution. The absorbance spectra for our nanoGUMBOS were generally broad and bimodal, extending to significantly lower wavelengths. For example, the absorbance of the [HMT][AOT] suspension was very broad, spanning from well below 600 nm to well over 800 nm (Figure 4.2B). When measured at an equivalent absorbance value, the emission intensity for the nanoparticle suspension was slightly lower and hypsochromically shifted by roughly 8 nm as compared to the parent compound dissolved in an EtOH solution (Figure 4.2C). This observation is highly characteristic of dye aggregation,[35, 40] in this case reflecting intermolecular interactions between [HMT$^+$] units. Decreased fluorescence intensity has also been observed for highly crystalline systems as a result of enhanced internal

conversion processes.[35, 40] However, we can essentially rule out this possibility as powder X-ray diffraction measurements (data not shown) of the dried nanoGUMBOS reveal that the particles are in fact predominantly amorphous (see also the SAED pattern inset in Figure 4.2A).

If the [HMT$^+$]-derived nanoGUMBOS are dried and then redissolved in ethanol, they retain the spectral characteristics of the parent solution (Figure 4.3). This observation supports our contention that the remarkable variations in both absorbance and fluorescence properties wholly arise from the aggregation state of the [HMT$^+$] within the nanoGUMBOS material. This also demonstrates that the intrinsic spectroscopic properties and chemical identity of the GUMBOS precursor ('monomer' ion units)
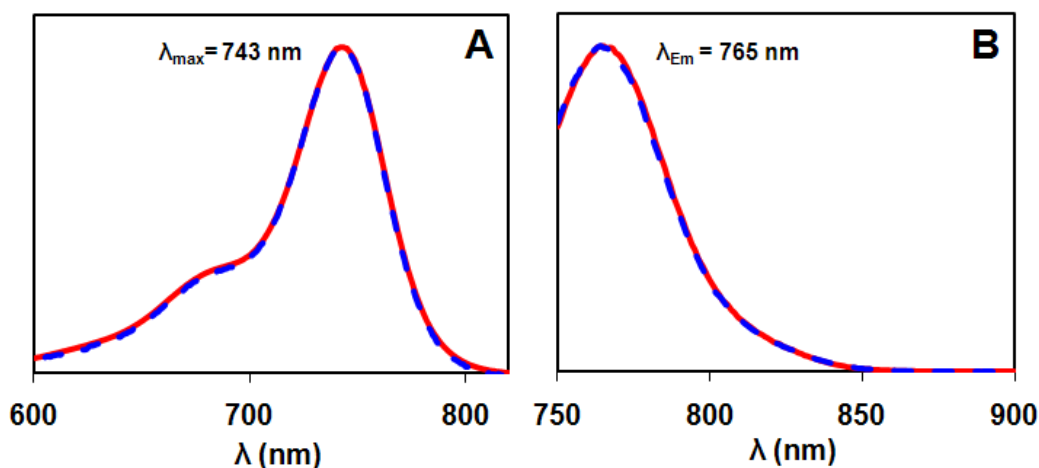
Figure 4.3. Normalized (A) absorbance and (B) fluorescence emission spectra of [HMT][AOT] (1.0 µM solution in EtOH; solid curve), and GUMBOS from Figure 4.2A redissolved in EtOH (dashed curve).

remain unaltered during nanoparticle formation. This observation is important when considering the potential of GUMBOS for use as drug delivery and therapeutic vehicles.

4.3.2. Cellular Uptake of NanoGUMBOS

In order to demonstrate the potential of nanoGUMBOS as contrast agents for biomedical imaging applications, we examined cellular uptake and fluorescence images of these particles

using monkey kidney fibroblast (Vero) cells. Vero cells have previously been used for screening *E. coli* toxin and can serve as host cells for viruses as well as eukaryotic parasites. In the present study, Vero cells were used as model cells to investigate the cellular uptake of our nanoGUMBOS. Using an epifluorescence microscope, we captured fluorescence images revealing that [HMT][AOT] nanoGUMBOS can be internalized and subsequently visualized within viable Vero cells after 24 h of incubation (Figure 4.4). These studies suggest the exciting potential of using nanoGUMBOS in cellular imaging. The apparent homogeneous fluorescence suggests that the nanoGUMBOS distribute nonspecifically inside the cells and are primarily located within the cytoplasm. The uptake of the nanoparticles is presumably due to the well
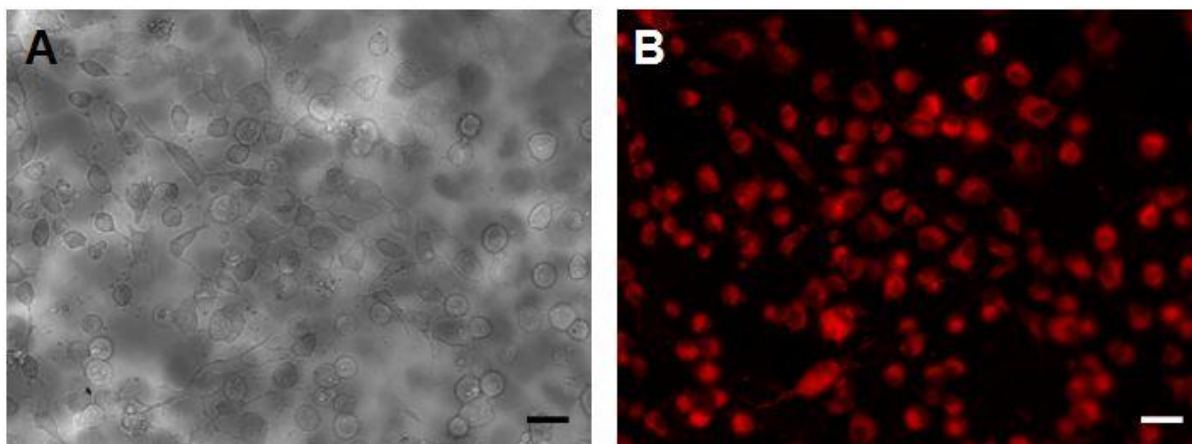
Figure 4.4. Cellular uptake studies using a monkey kidney fibroblast (Vero) cell line. (A) A phase contrast micrograph and (B) the corresponding fluorescence image of Vero cells incubated for 24 h with 8.0 µg mL^{-1} [HMT][AOT] nanoGUMBOS. The fluorescence was collected using a propidium iodide (PI) filter set: λ_{ex} = 540 nm; λ_{em} = 617 nm long pass. Scale bars in (A) and (B) are 10 µm.

known adsorptive endocytosis process previously demonstrated for mesoporous silica nanoparticles;[41] however, the exact cell-penetrating mechanism and localization of the nanoparticles is currently under investigation.

4.4. Conclusions

In summary, we have synthesized and investigated preliminary spectral and cellular uptake properties of a novel series of NIR fluorescent nanoscale ionic materials we term nanoGUMBOS. By appropriate selection of a cationic NIR dye, these fluorescent nanoparticles were designed to exhibit absorbance and luminescent properties in the tissue-accessible NIR region of the electromagnetic spectrum. In this study, nanoGUMBOS 79±18 nm in diameter were fabricated by use of a simple, rapid, repeatable, and additive-free reprecipitation method requiring neither special nor costly laboratory apparatus. Beyond the ease of preparation, this work presents an entirely new direction for preparing contrast agent nanoparticles directly from tailored ionic materials. Our approach alleviates current problems associated with dye leakage and other challenges encountered in dye encapsulation, as well as obviating intensive purification steps required when surfactants are used to prepare dye nanoparticles. It is also noteworthy that the spectral properties of our GUMBOS deviate markedly from the freely dissolved dye present in solution. Thus, the possibility for tuning the optical properties of GUMBOS by variation in the parent ions offers a unique and exciting advantage for these nanomaterials. It was also demonstrated that these NIR fluorescent nanoparticles could be efficiently taken up *in vitro* by Vero cells, suggesting intriguing potential for non-invasive biomedical imaging. Even more exciting is the prospect of tailoring nanoGUMBOS for delivery into designated cellular structures. In any case, examination of the data presented for these cellular studies highlights a new potential for biomedical imaging using NIR fluorescent nanoGUMBOS.

It should be possible to extend the findings from this investigation to fashion GUMBOS combining diverse functionalities (e.g., redox, superparamagnetic, luminescent, thermochromic, ligating) in order to arrive at truly multifunctional hybrid materials. One could easily envision

future polyfunctional nanoGUMBOS with applications including targeted diagnosis and therapy, photothermal cancer therapy, scintillators, radiosensitizers, biological separations, solar cells, and materials with defense applications (e.g., microwave-absorbers, security barcodes). The incorporation of high atomic number elements such as iodine or gold may enable their use as contrast agents for X-ray computed tomography (CT) scans. Likewise, GUMBOS carrying gadolinium chelates may open up potential for clinical diagnosis by use of magnetic resonance imaging (MRI).

4.5. References

(1)   Barone, P. W.; Parker, R. S.; Strano, M. S. *Anal. Chem.* **2005**, *77*, 7556-7562.

(2)   Shealy, D. B.; Lohrmann, R.; Ruth, J. R.; Narayanan, N.; Sutter, S. L.; Casay, G. A.; Evans, L., III; Patonay, G. *Appl. Spectrosc.* **1995**, *49*, 1815-1820.

(3)   Qian, G.; Zhong, Z.; Luo, M.; Yu, D.; Zhang, Z.; Ma, D.; Wang, Z. Y. *J. Phys. Chem. C.* **2009**, *113*, 1589-1595.

(4)   Yousaf, M.; Lazzouni, M. *Dyes Pigments.* **1995**, *27*, 297-303.

(5)   Zhang, P.; Steelant, W.; Kumar, M.; Scholfield, M. *J. Am. Chem. Soc.* **2007**, *129*, 4526-+.

(6)   Umezawa, K.; Citterio, D.; Suzuki, K. *Chem. Lett.* **2007**, *36*, 1424-1425.

(7)   Fabian, J.; Nakazumi, H.; Matsuoka, M. *Chem. Rev.* **1992**, *92*, 1197-1226.

(8)   Law, K. Y. *Chem. Rev.* **1993**, *93*, 449-486.

(9)   Jobsis, F. F. *Science* **1977**, *198*, 1264-1267.

(10)   Kim, S.; Lim, Y. T.; Soltesz, E. G.; De Grand, A. M.; Lee, J.; Nakayama, A.; Parker, J. A.; Mihaljevic, T.; Laurence, R. G.; Dor, D. M.; Cohn, L. H.; Bawendi, M. G.; Frangioni, J. V. *Nat. Biotechnol.* **2004**, *22*, 93-97.

(11)   Bashkatov, A. N.; Genina, E. A.; Kochubey, V. I.; Tuchin, V. V. *J. Phys. D: Appl. Phys.* **2005**, *38*, 2543-2555.

(12)   Loo, C.; Lowery, A.; Halas, N.; West, J.; Drezek, R. *Nano Lett.* **2005**, *5*, 709-711.

(13)   Bruchez, M., Jr.; Moronne, M.; Gin, P.; Weiss, S.; Alivisatos, A. P. *Science.* **1998**, *281*, 2013-2016.

(14)   Welsher, K.; Liu, Z.; Daranciang, D.; Dai, H. *Nano Lett.* **2008**, *8*, 586-590.

(15)   Moore, E. G.; Szigethy, G.; Xu, J.; Palsson, L.-O.; Beeby, A.; Raymond, K. N. *Angew. Chem., Int. Ed.* **2008**, *47*, 9500-9503.

(16)   Shi, X.; Royant, A.; Lin, M. Z.; Agilera, T. A.; Lev-Ram, V.; Steinbach, P. A.; Tsien, R. Y. *Science.* **2009**, *324*, 804-807.

(17)   Kim, K.; Lee, M.; Park, H.; Kim, J.-H.; Kim, S.; Chung, H.; Choi, K.; Kim, I.-S.; Seong, B. L.; Kwon, I. C. *J. Am. Chem. Soc.* **2006**, *128*, 3490-3491.

(18)   Bringley, J. F.; Penner, T. L.; Wang, R.; Harder, J. F.; Harrison, W. J.; Buonemani, L. *J. Colloid Interface Sci.* **2008**, *320*, 132-139.

(19)   Yang, Y.; Lowry, M.; Xu, X.; Escobedo, J. O.; Sibrian-Vazquez, M.; Wong, L.; Schowalter, C. M.; Jensen, T. J.; Fronczek, F. R.; Warner, I. M.; Strongin, R. M. *Proc. Natl. Acad. Sci.* **2008**, *105*, 8829-8834.

(20)   Derfus, A. M.; Chan, W. C. W.; Bhatia, S. N. *Nano Lett.* **2004**, *4*, 11-18.

(21)   Saxena, V.; Sadoqi, M.; Shao, J. *J. Photochem. Photobiol., B* **2004**, *74*, 29-38.

(22)   Burns, A.; Sengupta, P.; Zedayko, T.; Baird, B.; Wiesner, U. *Small.* **2006**, *2*, 723-726.

(23)   Yu, J.; Yaseen, M. A.; Anvari, B.; Wong, M. S. *Chem. Mater.* **2007**, *19*, 1277-1284.

(24)   Baba, K.; Pudavar, H. E.; Roy, I.; Ohulchanskyy, T. Y.; Chen, Y.; Pandey, R. K.; Prasad, P. N. *Mol. Pharmaceutics.* **2007**, *4*, 289-297.

(25)   Del Popolo, M. G.; Voth, G. A. *J. Phys. Chem. B* **2004**, *108*, 1744-1752.

(26)   Welton, T. *Chem. Rev.* **1999**, *99*, 2071-2083.

(27)   Del Sesto, R. E.; McCleskey, T. M.; Burrell, A. K.; Baker, G. A.; Thompson, J. D.; Scott, B. L.; Wilkes, J. S.; Williams, P. *Chemical Communications* **2008**, 447-449.

(28)   Bwambok David, K.; Marwani Hadi, M.; Fernand Vivian, E.; Fakayode Sayo, O.; Lowry, M.; Negulescu, I.; Strongin Robert, M.; Warner Isiah, M. *Chirality.* **2008**, *20*, 151-158.

(29)   Earle, M. J.; Gordon, C. M.; Plechkova, N. V.; Seddon, K. R.; Welton, T. *Anal. Chem.* **2007**, *79*, 758-764.

(30)   Larsen, A. S.; Holbrey, J. D.; Tham, F. S.; Reed, C. A. *J. Am. Chem. Soc.* **2000**, *122*, 7264-7272.

(31)   Huo, Y.; Xia, S.; Zhang, Y.; Ma, P. *Ind. Eng. Chem. Res.* **2009**, *48*, 2212-2217.

(32)   Freire, M. G.; Carvalho, P. J.; Gardas, R. L.; Santos, L. M. N. B. F.; Marrucho, I. M.;
         Coutinho, J. A. P. *J. Chem. Eng. Data.* **2008**, *53*, 2378-2382.

(33)   van den Broeke, J.; Stam, M.; Lutz, M.; Kooijman, H.; Spek, A. L.; Deelman, B.-J.; van
         Koten, G. *Eur. J. Inorg. Chem.* **2003**, 2798-2811.

(34)   Tesfai, A.; El-Zahab, B.; Bwambok, D. K.; Baker, G. A.; Fakayode, S. O.; Lowry, M.;
         Warner, I. M. *Nano Lett.* **2008**, *8*, 897-901.

(35)   An, B.-K.; Kwon, S.-K.; Jung, S.-D.; Park, S. Y. *J. Am. Chem. Soc.* **2002**, *124*, 14410-
         14415.

(36)   Peng, A.-D.; Xiao, D.-B.; Ma, Y.; Yang, W.-S.; Yao, J.-N. *Adv. Mater.* **2005**, *17*, 2070-
         2073.

(37)   Gesquiere, A. J.; Uwada, T.; Asahi, T.; Masuhara, H.; Barbara, P. F. *Nano Lett.* **2005**, *5*,
         1321-1325.

(38)   Xiao, D.; Xi, L.; Yang, W.; Fu, H.; Shuai, Z.; Fang, Y.; Yao, J. *J. Am. Chem. Soc.* **2003**,
         125, 6740-6745.

(39)   Wang, F.; Han, M.-Y.; Mya, K. Y.; Wang, Y.; Lai, Y.-H. *J. Am. Chem. Soc.* **2005**, *127*,
         10350-10355.

(40)   Gruszecki, W. I. *J. Biol. Phys.* **1991**, *18*, 99-109.

(41)   Slowing, I.; Trewyn, B. G.; Lin, V. S. Y. *J. Am. Chem. Soc.* **2006**, *128*, 14792-14793.

CHAPTER 5

SPECTRAL PROPERTIES OF TUNABLE AGGREGATES FROM NIR FLUORESCENT NANOGUMBOS

5.1. Introduction

In the process of exploring NIR nanoGUMBOS for biomedical imaging in the previous chapter, some striking observations were made in regard to the absorbance and fluorescence spectral properties of these NIR nanoGUMBOS. Conspicuous among these intriguing spectral properties is the broad absorption spectrum of the NIR nanoGUMBOS compared to the dilute GUMBOS solution. Such spectral differences have been associated with and may be due to formation of molecular self assemblies within the dye nanoparticles.[1] This observation prompted the investigation undertaken in this chapter to characterize the type of aggregates that may be formed by the NIR fluorescent nanoGUMBOS as a function of varying the anion. To reiterate, GUMBOS are largely frozen ILs and some have melting points in excess of 100°C. It is therefore expected that the GUMBOS and the corresponding nanoGUMBOS will enjoy the unique properties of ILs such as negligible vapor pressure, high thermal stability and tunability.[2] In addition, the GUMBOS and nanoGUMBOS will exhibit their intrinsic properties suitable for various applications.

As far as is known, there are two types of molecular dye aggregates namely, J and H-aggregates. The J-aggregates (also known as Scheibe aggregates) were discovered independently in 1936 by Jelly[3] and Scheibe.[4] In this pioneering work, a high concentration of a pseudoisocyanine dye investigated exhibited a narrow red shifted absorption band compared to the monomer. In addition, the fluorescence emission had narrow band and small Stokes shift. Initially Scheibe postulated that this was due to reversible polymerization of chromophores.[4] This observation is now ascribed to strong coupling between transition dipole moments of the molecules resulting in excitonic states upon optical excitation.[5, 6]

Conceptually, the molecules are arranged in a "brickwork" manner (head-to-tail arrangement) in J-aggregates whereas in H-aggregates, the molecules exhibit "card-pack" arrangement (face-to-face stacking).[7] In general, the type of aggregate formed determines the type of transitions from the excitonic interactions between electronically coupled chromophores. Since their inception, considerable attention has been paid to molecular dye aggregates due to their potential applications in various fields such as light harvesting[8-10], photovoltaics[8, 11, 12] and light emitting diodes.[13, 14]   In addition, the possibility of both H and J aggregates exhibiting superradiance, a phenomena resulting from cooperative emission has sparked tremendous interest in studies of molecular self assemblies.[15, 16]

The aggregation phenomena has been well explained by the exciton theory illustrated by the energy level diagram (Figure 1.14).[17, 18] In general, the type of aggregate formed determines the type of transitions from the excitonic interactions between electronically coupled chromophores. Large hypsochromic shift in absorption typical for dye H-aggregates is attributed to transition dipole interactions between two or more chromophores (H-aggregates) arranged parallel to each other with a small dislocation. The excited state is split into two components, due to the interaction of two transition dipoles. In this type of molecular assemblies, transition from ground state to higher energy state is allowed and hence the hypsochromic shift in absorbance and large Stokes shift in emission.[17] In addition, fast internal conversion process from higher energy state to a non-emitting intermediate state leads to quenched emission in H-aggregates. In contrast, the allowed higher energy state in J-aggregates has a lower energy relative to the monomer leading to bathochromic shift in absorbance. In addition, there is no internal conversion to an intermediate non-emitting state and hence J-aggregates are highly fluorescent with a small Stokes shift.[17]

Several factors affect the type of aggregates formed including dye structure, dye concentration, solvent polarity, pH, ionic strength, and temperature.[19, 20] It is worth noting that the properties of dye aggregates may also be influenced by interaction with biomolecules.[7] For instance, such an interaction may enhance the low fluorescence quantum yield of H-aggregates while quenching the more fluorescent J-aggregates. The fluorescence enhancement phenomenon has been utilized by Gabor and coworkers for non-covalent labeling of the biomolecules. The ability to control the type of molecular aggregation for desired applications is one of the major challenges in the field of supramolecular chemistry. Supramolecular assemblies result from various non-covalent interactions such as electrostatic, hydrogen bonding, solvophobic and π-π stacking interactions. Several strategies have been employed to afford control of the type of aggregation. For instance, intramolecular heavy atom modification has been performed to prevent aggregation of a series of NIR tricarbocyanine dye commonly used as biological probes.[21] The formation and spectral properties of dye aggregates have been controlled by use of various additives such as salts[22-24], surfactants[22], reverse micelles[25], polymers[26], and proteins.[27]

Due to the aforementioned challenge of controlling the dye aggregation, organic fluorescent nanomaterials have recently attracted considerable interest because of the possibility of functionalization that may afford control of the resultant aggregates. Organic fluorescent nanomaterials have also found applications such as in OLEDs.[28, 29] However, research on fluorescent organic nanoparticles is still in its infancy compared to their fluorescent inorganic counterparts that have been widely used in applications such as fluorescent biological labels[30], photovoltaic cells[31], light-emitting diodes[32, 33], and optical sensors.[33]

A number of reports on fluorescent organic nanoparticles mostly prepared using reprecipitation method have recently appeared.[22-26] For example, Yao and coworkers have designed pyrazoline nanoparticles and determined their size dependent spectral properties.[34]

They observed a bathochromic shift in absorption transition and hypsochromic shift in emission of the nanoparticles with increasing size and attributed it to the restraint of vibronic relaxation and configurational reorganization.[34] The organic molecules which are highly fluorescent in dilute solutions, mostly show significant quenching of fluorescence in the solid state due to increased intermolecular interactions.[28] In addition to intermolecular interactions, such fluorescent switching in organic nanomaterials may also be due to conformation change or intramolecular planarization. Several studies in the last few years reported the preparation of fluorescent dye nanoparticles and explained its fluorescent properties as an effect of J-aggregation[35] or sometimes absence of aggregation within the particle.[36] As aforementioned, significant amount of work has been done in an attempt to control the aggregation behavior in dye assemblies in solutions, solid films, or nanoparticle templates. However, to our knowledge, there is no report on the control of aggregation within the dye nanoparticle itself. This study seeks to unveil a novel, simple method of controlling the aggregation within the NIR nanoGUMBOS by varying the anion. Considering that the H and J aggregates have interesting applications unique to their spectral properties, controlling the type of aggregation within the dye nanoparticle is highly desirable. The possibility of achieving such unprecedented controlled aggregation with the same chromophore may provide tremendous potential of a single dye being used in various applications; the exact reason for undertaking this study. The goal of this study is to explore this possibility by determining the changes in spectral properties and the aggregation behavior of fluorescent NIR GUMBOS and nanoGUMBOS as a function of varying the anion.

5.2. Materials and Methods

5.2.1. Materials

1,1′,3,3,3′,3′-hexamethylindotricarbocyanine (HMT) iodide (97%), bis (2-ethylhexyl) sulfosuccinate (AOT) sodium salt (≥99%), lithium bis(trifluoromethane) sulfonimide, potassium

3,5 bis (trifluoromethyl) phenyltrifluoroborate, Sodium tetrakis[3,5-bis(1,1,1,3,3,3-hexafluoro-2-methoxy-2-propyl)phenyl]borate, and ethanol (spectroscopic grade) were purchased from Sigma Aldrich and used as received. Lithium bis(pentafluoroethane) sulfonimide (LiBETI) was gladly donated by Gary Baker (Oakridge, TN). Triply deionized water (18.2 MΩ cm) from an Elga model PURELAB ultra^{TM} water filtration system was used for all preparations of NIR nanoGUMBOS. Carbon coated copper grids (CF400-Cu, Electron Microscopy Sciences, Hatfield, PA) were used for TEM imaging.

5.2.2. Synthesis and Characterization of NIR GUMBOS and NanoGUMBOS

The NIR GUMBOS (mostly ILs) were prepared using anion exchange procedures similar to those reported in the literature and as described in the previous chapter. The nanoGUMBOS were prepared from GUMBOS using a modified simple, additive-free reprecipitation method similar to that used for organic nanoparticles and explained in chapter 4 of this dissertation. Briefly, 100 µL of a 1 mM solution of GUMBOS precursor dissolved in ethanol was rapidly injected into 5 mL of triply-deionized water in an ultrasonic bath, followed by further sonication for 2 min. Post-preparation, the particle suspension was aged for 1 h in the dark.

5.2.3. Characterization of NIR NanoGUMBOS

The average particle size and size distribution of the prepared nanoGUMBOS were obtained by use of transmission electron microscopy (TEM) and dynamic light scattering (DLS). TEM micrographs were obtained using an LVEM5 transmission electron microscope (Delong America, Montreal, Canada). The NIR nanoGUMBOS dispersion (1 µL) was dropcasted onto a carbon coated copper grid and allowed to dry in air at room temperature before TEM imaging. X-ray diffraction measurements of dried nanoGUMBOS were obtained on a Nonius Kappa CCD diffractometer by long exposures with Mo Kα radiation and rotation of samples about the vertical axis.

**5.2.4. Absorption and Fluorescence Studies of NIR GUMBOS and NanoGUMBOS**

Absorbance measurements were performed on a Shimadzu UV- 3101PC UV-Vis-near-IR scanning spectrometer (Shimadzu, Columbia, MD). Fluorescence studies were performed using a Spex Fluorolog-3 spectrofluorimeter (model FL3-22TAU3); Jobin Yvon, Edison, NJ). A 0.4 cm quartz cuvette (Starna Cells) was used to collect the fluorescence and absorbance against an identical cell filled with water as the blank. The absorption and emission spectra were deconvoluted using a Spec32 software based on principal component analysis and fits with chisquare values as low as the order of 10^{-5} were accepted. The absorption spectra were deconvoluted using a Gaussian fit and the emission spectra using a Lorentzian fit. Both normalized and unnormalized spectra were deconvoluted using this software and it was observed that the ratio of all the three components in each spectrum remained the same in both the cases. The contribution from each component was calculated considering it to be proportional to the area under the corresponding component of the deconvoluted spectra.

5.3. Results and Discussions

5.3.1. Synthesis and Characterization of HMT NIR GUMBOS and NanoGUMBOS

As explained earlier in the previous chapter, the resulting NIR-emitting GUMBOS displayed variable physical properties (melting point, solubility) dependent upon variations in the anion. This illustrates the tunability of our GUMBOS, allowing the design of a variety of physicochemical properties targeting select applications.

The water insoluble GUMBOS were used to fabricate nanoGUMBOS dispersed in water, and a detailed investigation of their spectral properties as a function of varying the anion is investigated in this chapter of the dissertation. Once again, the structure of HMT cation used (Scheme 5.1) and the anions used (Table 5.1) are as shown.
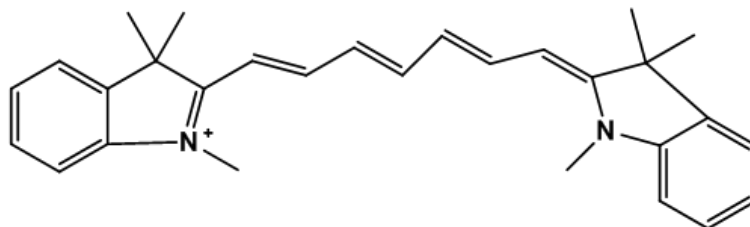
Scheme 5.1. Structure of HMT NIR dye cation

Table 5.1. Chemical structures of the aqueous insoluble [HMT$^+$]-derived GUMBOS with various anions used.

NIR GUMBOS	Anion structure	solubility in water
HMT NTf$_2$		×
HMTBETI		×
HMT 3,5-CF$_3$PheB		×
HMT (OCH$_3$)$_4$PheB		×
HMT AOT		×

5.3.2. TEM Characterization of NanoGUMBOS

TEM was performed as reported in the previous chapter. To reiterate, TEM characterization showed that the nanoGUMBOS are mainly spherical as further confirmed by

electron diffraction patterns. This suggests the amorphous nature of the nanoGUMBOS. Such amorphous character of nanoparticles has been reported to minimize quenching from internal conversion processes commonly observed in crystalline systems. This information is of significance to the study in this chapter because it prompted the investigation of the underlying factors that maybe influencing the spectral properties of nanoGUMBOS such as aggregation; which is the subject of this study.

5.3.3. UV-visible Absorption Properties of HMT NanoGUMBOS

The UV-visible absorption spectra of dilute ethanolic solutions of all the HMT GUMBOS with various anions are virtually overlapping (Fig 5.1). In addition, the maximum absorption is at the same wavelength (743 nm) as the ethanolic solution of [HMT][I] precursor. This indicates, HMT cation retain its intrinsic NIR optical properties after anion exchange to form HMT GUMBOS. In contrast, upon fabrication of nanoGUMBOS via reprecipitation in water, strikingly different absorption spectra were observed. In general, broad absorption spectrum was observed for all nanoGUMBOS but the spectral shape was unique for each nanoGUMBOS (Fig 5.2). The broadening of the absorption spectra extended to both longer and shorter wavelength regions compared to the monomeric dilute HMT GUMBOS solution. Specifically for [HMT][AOT], [HMT][NTF$_2$] and [HMT][3,5-(CF$_3$)$_2$PhBF$_3$ nanoGUMBOS, the spectra seems to develop absorption shoulders in both the red and blue region with respect to the absorbance of the monomer. The broadness of the absorption band is considered to be either due to superposition of the absorption bands of preoriented molecules around 735 nm and the formed aggregates or due to the oscillation or rotation of the aggregates beyond the resolution of the spectrometer.

A better insight into the intriguing absorption spectra of the nanoGUMBOS was gained by deconvolution of the spectra using software based on principal component analysis.
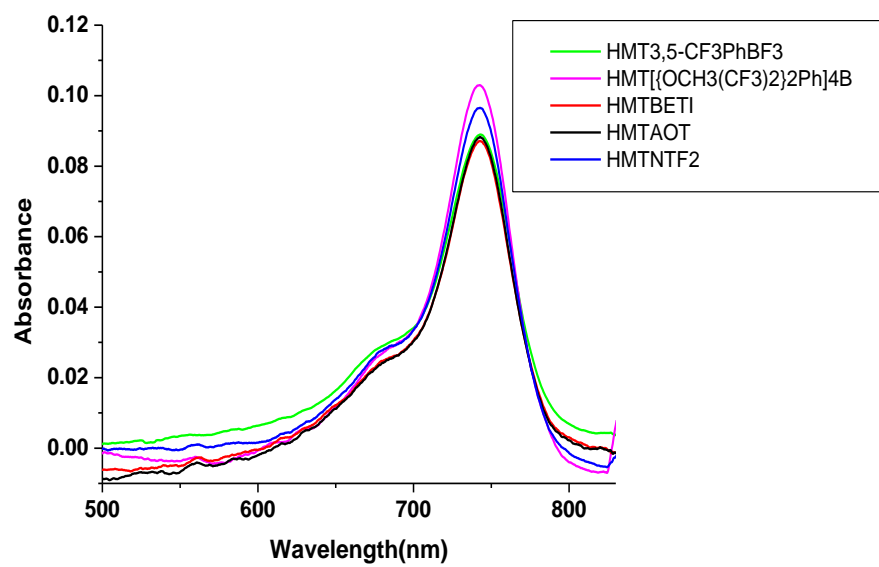
Figure 5.1. Absorption spectra of dilute ethanolic solutions (1 µM) of HMT GUMBOS
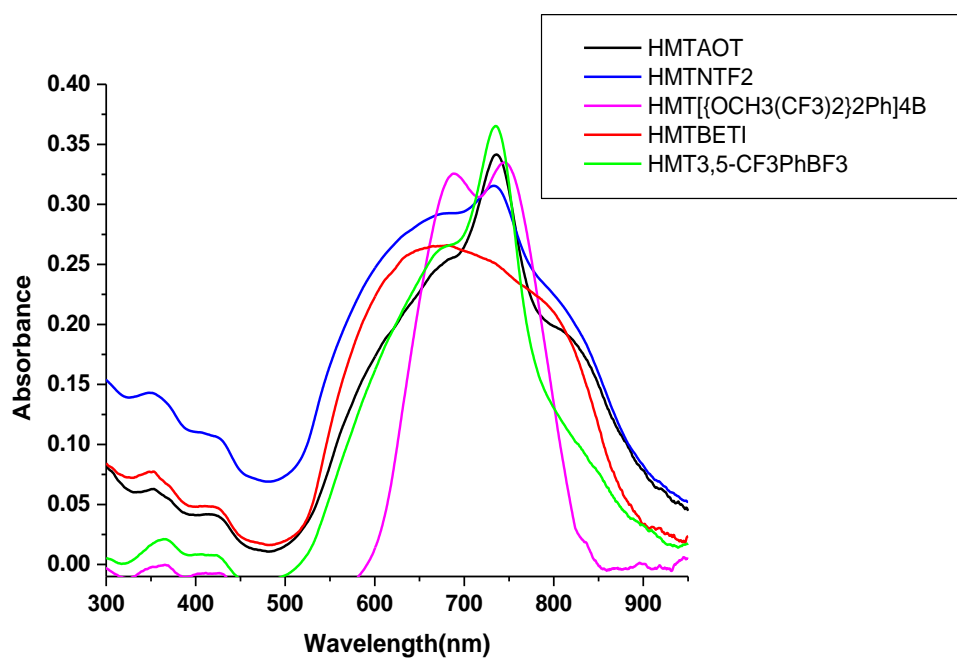

Figure 5.2. Absorption spectra of HMT nanoGUMBOS

Interestingly, the resolved absorption spectra reveal that each absorption spectrum is composed of three bands which maybe assigned to three different types of absorbing species (Fig. 5.3). The component absorbing near 735 nm is assigned to those aggregates in the nanoGUMBOS whose transition dipoles are randomly oriented and are expected to absorb in the monomer region (recall that the dilute ethanolic solutions of HMT GUMBOS absorbance peaks near this wavelength). The bathochromically shifted component absorbing near 753-783 nm is assigned to the J-type of aggregates in which the transition dipoles are arranged in a head-to–tail manner. On the other hand, the hypsochromically shifted absorbance in the range 580-672 nm maybe assigned to the H-type of aggregates in which the transition dipoles tends to align parallel to each other.

It can be deduced from the deconvoluted absorption spectra (Figure 5.3), that H-type, J-type and randomly oriented aggregates were formed in relatively different proportions. This may explain the differences in broad shapes of the absorption bands for different nanoGUMBOS as a function of varying the anion. It is observed that in [HMT][AOT], [HMT][NTF$_2$] and [HMT][3,5-CF$_3$PhBF$_3$] nanoGUMBOS, the J-component predominates over the H-component (Figure 5.3). In contrast, the H-components are predominant in HMTBETI and [HMT][(OCH$_3$(CF$_3$)$_2$)$_2$Ph$_4$B] nanoGUMBOS (Figure 5.3). It is also observed that among the three dyes with predominant J-aggregates the contribution of the randomly oriented species is maximum for [HMT][3,5-(CF$_3$)$_2$PhBF$_3$] followed by [HMT][AOT] and [HMT][NTF$_2$]. These J/H ratios and contributions from the randomly oriented species play a profound role in influencing the fluorescence emission properties of the nanoGUMBOS.

5.3.4. Fluorescence Emission Properties of HMT NanoGUMBOS

Steady state fluorescence results were complementary to absorption studies (both resolved and non-resolved spectra). All HMT GUMBOS ethanolic dilute solutions displayed
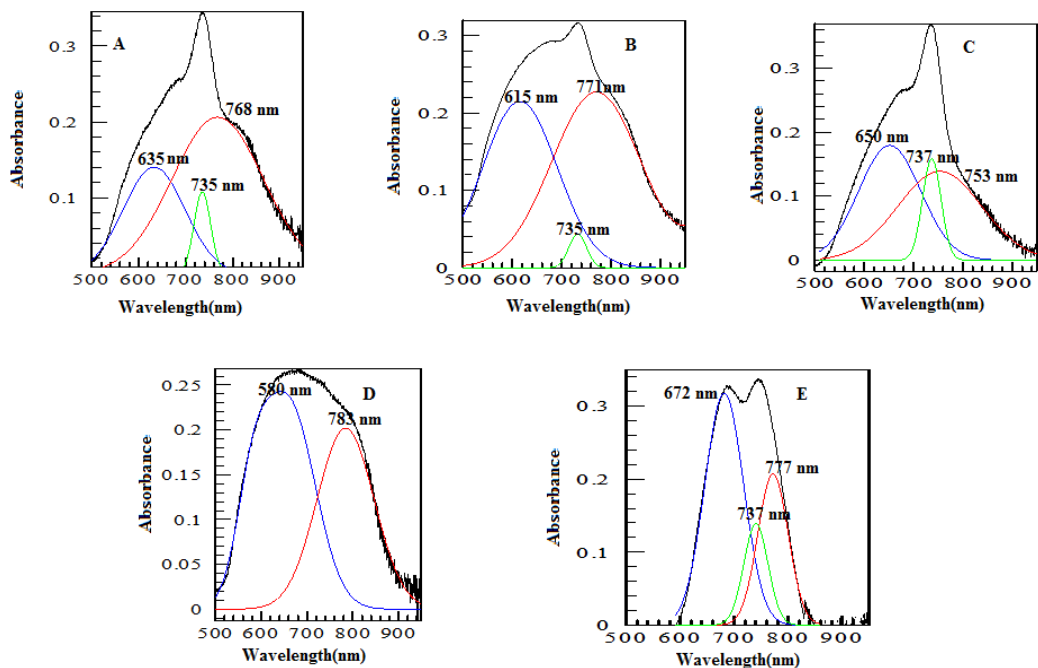
Figure 5.3. Resolved absorption spectra of HMT (A) AOT (B) NTf$_2$ (C) 3, 5-CF$_3$ (D) BETI (E) OCH$_3$ nanoGUMBOS

comparable fluorescence intensities with emission maxima at 765 nm (Figure 5.4A). Surprisingly, the nanoGUMBOS dispersed in water had variable emission properties based on the anion used in the GUMBOS. Specifically, the [HMT][AOT] and [HMT][3,5-CF$_3$PhBF$_3$] nanoGUMBOS were found to be the most fluorescent (Figure 5.4B). This was followed by [HMT][NTF$_2$] nanoGUMBOS with modest fluorescence emission intensity (Figure 5.4B). However, the [HMT][BETI] nanoGUMBOS were weakly fluorescent and [HMT][(OCH$_3$(CF$_3$)$_2$)$_2$Ph$_4$]B nanoGUMBOS being virtually non-fluorescent (Figure 5.4B). Approximately 10 nm blue shift in the emission maxima of the nanoGUMBOS compared to that of ethanolic solution is probably due to the negative solvatochromic effect.

Considering the three species of the resolved absorption spectra, the major contribution to fluorescence emission comes from the randomly oriented component and the J-component. Thus though the HMT NTF$_2$ nanoGUMBOS has higher J/H ratio compared to HMT 3,5-CF$_3$PhBF$_3$

(Figure 5.5), the latter has relatively better fluorescence yield due to the highest contribution from the randomly oriented component (Figure 5.6). It is therefore not surprising that HMT AOT
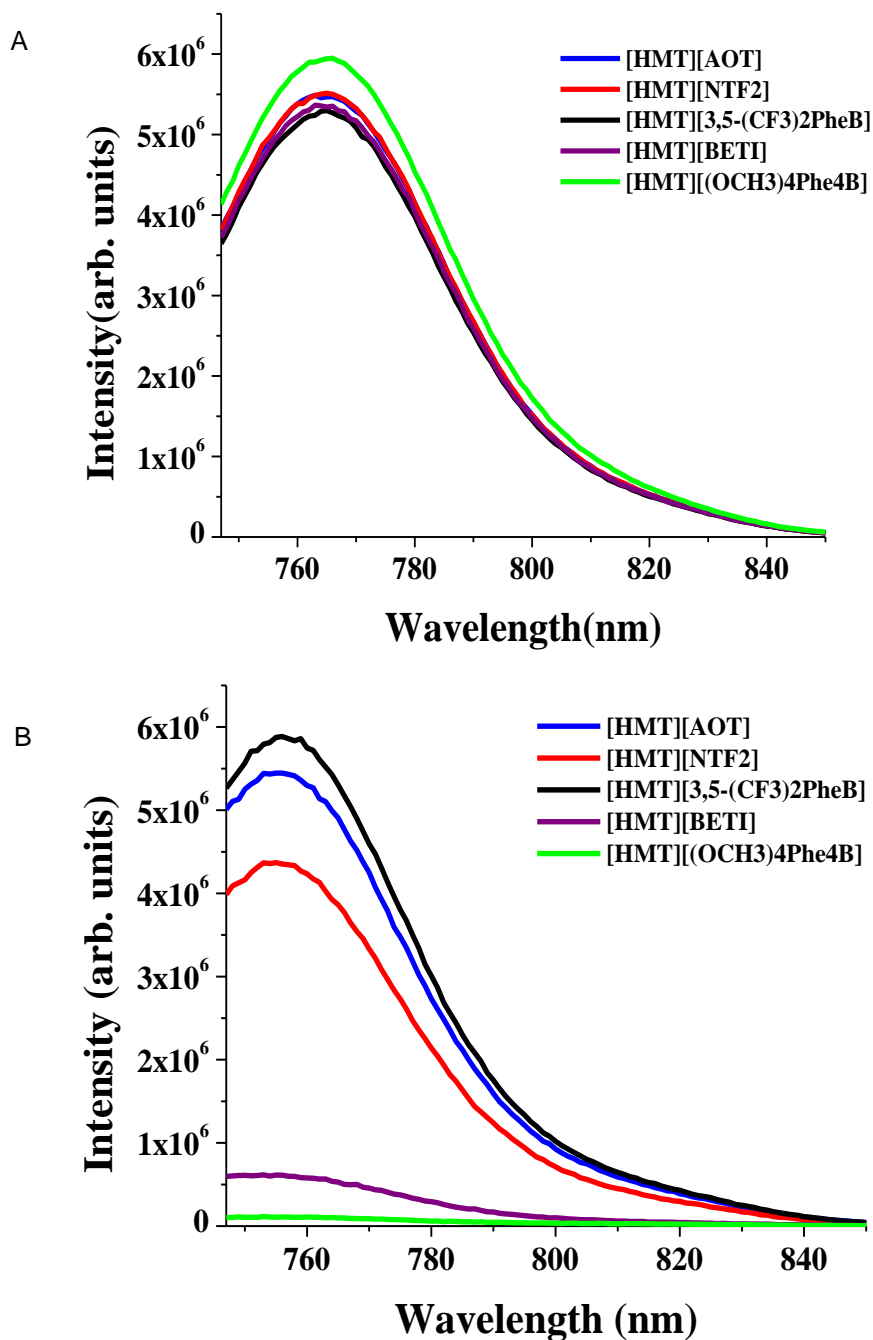
Figure 5.4. Fluorescence emission properties of HMT (A) GUMBOS (1 µM ethanolic solution) and (B) nanoGUMBOS

nanoGUMBOS with the highest J/H ratio and significant contribution of randomly oriented species (Figure 5.5 and 5.6) is the most fluorescent in the series. The weak fluorescence behavior of HMT BETI may be due to the lower J/H ratio (<1) and higher contribution from H-type of aggregates. Whereas the lowest J/H (<1) ratio and the highest contribution from H-component of the HMT $[OCH_3(CF_3)_{22}Ph]_4B$ nanoGUMBOS (Figure 5.5) may account for the extremely quenched fluorescence emission.

The emission spectra of the nanoGUMBOS were also deconvoluted and three different emitting species were observed for HMT AOT and HMT NTf$_2$ as representative nanoGUMBOS (Fig 5.7). The emission near 750 nm is assigned to the randomly oriented component. The two emission peaks near 760 and 780 nm are probably due to the fluorescence of two different types of J-aggregates that maybe formed within the nanoGUMBOS.
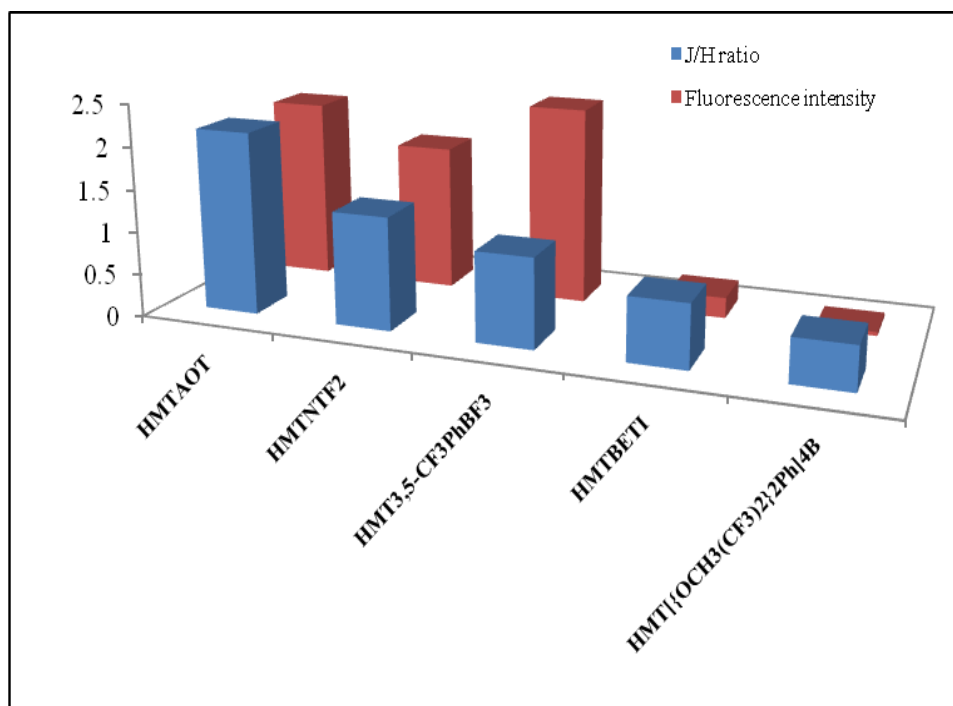
Figure 5.5. Normalized J/H ratio of the various HMT nanoGUMBOS
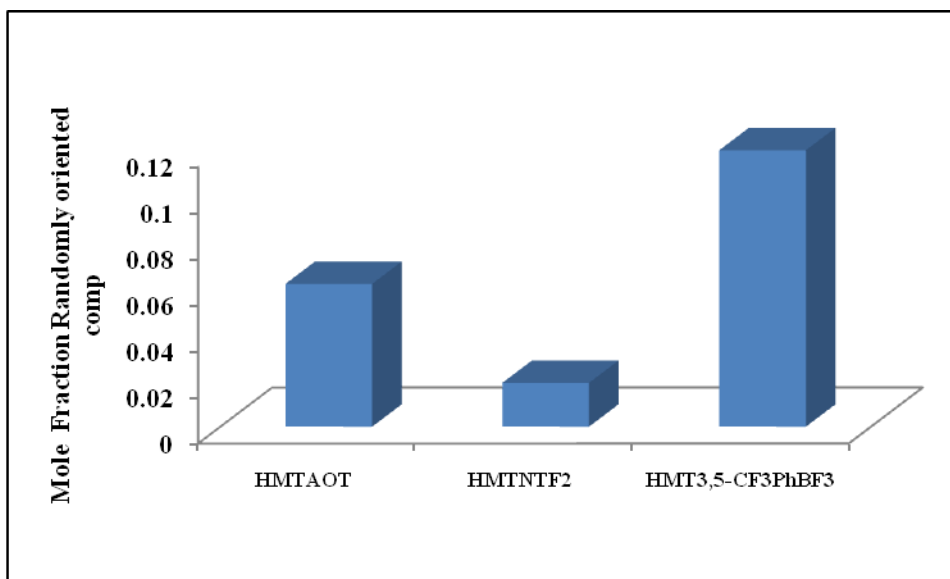
Figure 5.6. Mole fraction of the randomnly oriented components of HMT nanoGUMBOS

Fig. 5.7. Representative resolved emission spectra of nanoGUMBOS (A) HMTAOT (B) HMT NTf$_2$

It is interesting to note that [HMT][AOT] and [HMT][3,5-(CF$_3$)PhBF$_3$] nanoGUMBOS

have comparable fluorescence to that of the corresponding dilute ethanolic GUMBOS solutions.

128

The fluorescence of [HMT][NTF$_2$] nanoparticles are slightly less than the corresponding ethanolic solutions while that of [HMT][BETI] and [HMT][(OCH$_3$(CF$_3$)$_2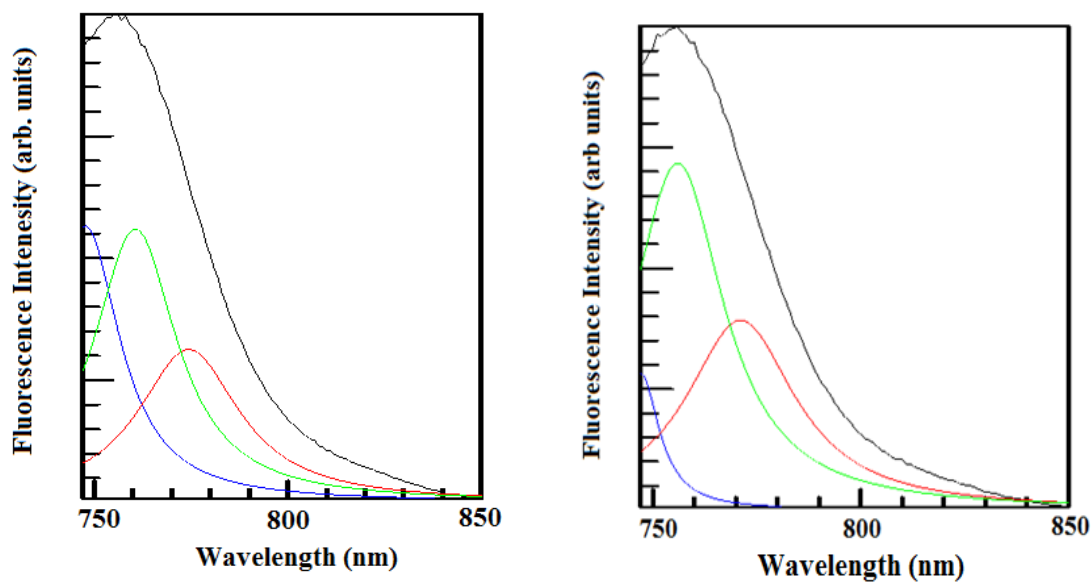$)$_2$Ph)$_4$B] are highly quenched compared to the corresponding ethanolic solution. This variation in fluorescence yield of the nanoGUMBOS maybe explained by the type of preferred relative orientation of the individual dye molecules in the nanoparticle. Consistent with this explanation, the more J-aggregating HMT nanoGUMBOS have greater fluorescence yield and the vice versa is true for the predominantly H-aggregating nanoGUMBOS having the least fluorescence yield (Figures 5.4 and 5.5).

It can be inferred from these spectral properties that within the nanoGUMBOS of HMTAOT, [HMT][NTF$_2$] and [HMT][3,5-CF$_3$PhBF$_3$], head-to-tail type of arrangements are thermodynamically more favored compared to stacking imparting highly fluorescent properties to the nanoGUMBOS. In contrast, molecular stacking maybe more favored in [HMT][BETI] and [HMT][(OCH$_3$(CF$_3$)$_2$)$_2$Ph$_4$B], making these nanoGUMBOS weakly fluorescent to virtually non-fluorescent. It has been reported that cyanine dyes with longer polymethine chain are more H-aggregating in solution. Despite having a long polymethine chain, the spectral properties of HMT cationic cyanine dye used in this study suggest that J-aggregation likely occurs depending on the anion used.

In general, solubility of ILs in water has been shown to be dependent on the anion.[37] Hydrophobic anions such as BETI and NTF$_2$ enhance the formation of hydrophobic GUMBOS.[38] Generally, BETI has longer alkyl chain and more hydrophobic than NTF$_2^-$ anion.[38] We note that the presence of fluorines have been reported to induce some hydrophilic properties.[39] This suggests that hydrophobicity may not be influenced solely by the length of the alkyl chain. Therefore, in addition to structural factors which might determine the type of aggregation within the nanoGUMBOS, the extent of hydrophobicities of the anions can be roughly correlated to the

preferred orientation of the transition dipoles within the nanoparticles. The experimental results from this study suggest that a higher degree of hydrophobicity of an anion within a given family might induce a preferred stacking of the transition dipoles forming more H-type of aggregates.

5.3.5. Fluorescence Anisotropy Studies of HMT GUMBOS and NanoGUMBOS

In fluorescence anisotropy the rotational diffusion of a molecule is related to its size and shape. It is a useful technique to measure the binding interaction between two molecules since bound molecules rotate slowly resulting in higher anisotropy.[40, 41] Fluorescence anisotropy is calculated using the formula: r = (Ivv-GIvh)/(Ivv+2GIvh); where G is the grating factor that has been included to correct the wavelength response for polarization response of the emission optic and the detector. I_{vv} and I_{vh} are the fluorescence intensity measured parallel and perpendicular to the vertically polarized excitation, respectively.[40, 41]

Fluorescence emission anisotropy studies were performed for both dilute HMT GUMBOS ethanolic solutions as well as the nanoGUMBOS exciting at 737 nm. These measurements reveal that the dilute ethanolic solutions of all the HMT GUMBOS have significantly low anisotropies lying between 0.01-0.02 (Table 5.2). The anion has no significant effect on the anisotropy in dilute solutions. All the HMT nanoGUMBOS possess higher anisotropies than their corresponding dilute GUMBOS solutions (Table 5.2) and exhibit fluorescence emission anisotropy spectra with different features for the different anions.

The [HMT][AOT] and [HMT][NTF$_2$] which were found to be more J-aggregating possess a low anisotropy value over the entire emission wavelength with an intense band near 775nm (Figure 5.8) which is approximately the absorption wavelength of the J-aggregates for these nanoparticles as observed in the deconvoluted spectra. Thus it can be stated that the main emitting species in these two cases are the J-aggregates having resonance fluorescence properties. While for [HMT][3,5-(CF$_3$)$_2$PhBF$_3$] the fluorescence anisotropy spectra exhibits a

minima near 750 nm (Figure 5.8) revealing the fact that in this case the main emitting species is the randomly oriented component which emits near the monomer region along with its J-aggregate which absorbs and emits near 754 nm as seen in the resolved spectra. As mentioned earlier, J-aggregates are characterized by resonance fluorescence. But the value of anisotropy of the particle is much greater than that of the corresponding monomer in dilute solutions suggesting that the emitting species is within the particle and not in solution. This fact also supports our deconvoluted data which shows maximum randomly oriented component for this GUMBOS anion pair in which the J-aggregate absorbs near 754 nm. Fluorescence anisotropy values of HMT BETI nanoparticles are much higher over the entire emission range with two intense bands near 770 nm and 810 nm respectively (Figure 5.8) suggesting the presence of two significantly different types of aggregates.

The fact that the fluorescence anisotropy of the dye aggregates in the nanoGUMBOS is higher than the corresponding dilute dye solutions suggests that the rotational diffusion of the dye within the nanoGUMBOS are much slower. Furthermore, negligible amount of energy is lost through energy migration within the dye aggregates in the nanoGUMBOS. Another observation that the NIR nanoGUMBOS with higher J/H ratio has lower values of emission anisotropy might suggest that the rotational diffusion of the dye within the J-type of aggregates is faster compared to that in randomly oriented or H-type of aggregates.

It is well established that anisotropy depends on the direction of transition moments.[40, 41] In case of dye aggregates the transition dipoles are oriented in a definite manner and hence the response to parallel and perpendicularly polarized light is quite distinct in the emission spectra.[40, 41] In this study, it was observed that a significant difference exists between the intensities of perpendicular and parallel polarized emission for those HMT dye anion pairs in which the transition dipoles are mostly oriented in head to tail manner i.e. forming J-type of aggregates. In

addition, difference between the two emission intensities decreases with the decreasing J-component. For example, [HMT][AOT] and [HMT][NTF$_2$] has maximum difference between I$_{vv}$ and I$_{vh}$ suggesting that these nanoGUMBOS contain maximum amount of J-aggregates (Figure 5.8). From the resolved absorption and emission spectra of [HMT] [3,5-(CF3)$_2$PhBF$_3$], the J-component is comparatively lower. Consequently, the difference between I$_{vv}$ and I$_{vh}$ decreases which is further diminished in predominantly H-aggregating HMT BETI nanoGUMBOS.
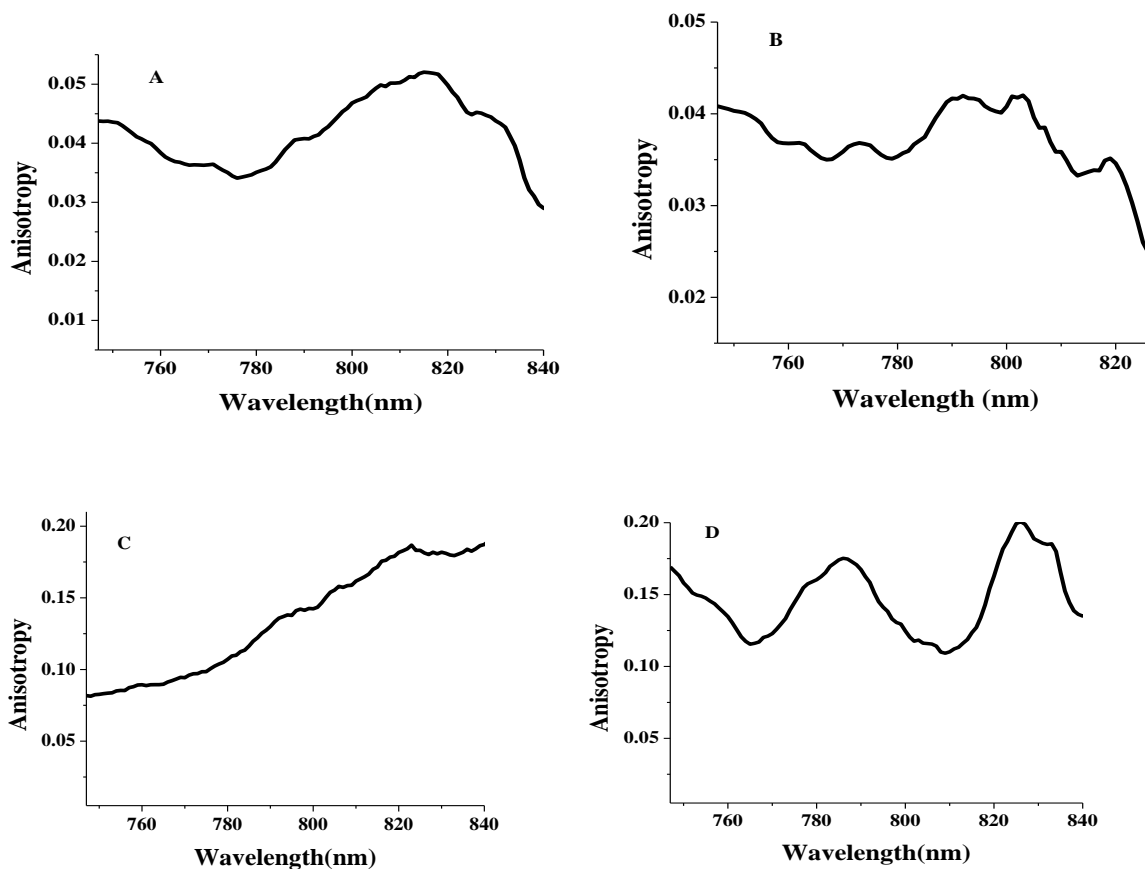

Figure 5.8. Fluorescence emission anisotropy of (A) HMT AOT and (B) HMT NTF$_2$ nanoGUMBOS (C) HMT 3, 5 (CF$_3$)$_2$ PheB (D) HMT BETI

Table 5.2. Steady state anisotropy values of various HMT GUMBOS 1 µM ethanolic solution and nanoGUMBOS aqueous suspension at 750 and 775 nm.

Abbreviation	Anisotropy			
	HMT GUMBOS 1 µM ethanolic solution		HMT nanoGUMBOS aqueous suspension	
	750 nm	775 nm	750 nm	775 nm
HMT AOT	0.0215	0.02196	0.0435	0.0344
HMT35(CF$_3$)PheB	0.01858	0.01904	0.08265	0.09846
HMT NTf2	0.01922	0.01723	0.04052	0.0365
HMT BETI	0.01103	0.01257	0.15809	0.14442

5.4. Conclusions

In summary, we have successfully presented a novel idea of controlling the type of aggregation within the NIR nanoGUMBOS by retaining the same dye skeleton and simply varying the anion. Though the various dye anion pairs have similar spectral properties in solution phase, the nanoGUMBOS display intriguingly different properties as a function of varying the anion. This tunable spectral behavior in the nanoGUMBOS is mainly attributed to the difference in the arrangement of individual transition dipoles within the particles. The findings from this study suggest that more hydrophobic anions may preferably induce H-aggregation in the nanoGUMBOS. In contrast, J-aggregation may be preferred with less hydrophobic anions. It is also possible that this observation may be dependent on the structure of the dye being investigated.

5.5. References

(1)   Daehne, L. *J. Am. Chem. Soc.* **1995**, *117*, 12855-12860.

(2)   Welton, T. *Chem. Rev.* **1999**, *99*, 2071-2083.

(3)   Jelley, E. E. *Nature* **1936**, *138*, 1009-1010.

(4)   Scheibe, G. *Angew. Chem.* **1936**, *49*, 563.

(5)   Kirsten, S.; Daehne, S. *Int. J. Photoenergy* **2006**, 3/1-3/21.

(6)   Knoester, J. *Int. J. Photoenergy* **2006**, 4/1-4/10.

(7)   Kim, J. S.; Kodagahally, R.; Strekowski, L.; Patonay, G. *Talanta* **2005**, *67*, 947-954.

(8)   Mann, J. R.; Gannon, M. K.; Fitzgibbons, T. C.; Detty, M. R.; Watson, D. F. *J. Phys. Chem. C* **2008**, *112*, 13057-13061.

(9)   Miller, R. A.; Presley, A. D.; Francis, M. B. *J. Am. Chem. Soc.* **2007**, *129*, 3104-3109.

(10)   McDermott, G.; Prince, S. M.; Freer, A. A.; Hawthornthwaite-Lawless, A. M.; Papiz, M. Z.; Cogdell, R. J.; Isaacs, N. W. *Nature* **1995**, *374*, 517-521.

(11)   Hoeben Freek, J. M.; Jonkheijm, P.; Meijer, E. W.; Schenning Albertus, P. H. J. *Chem Rev* **2005**, *105*, 1491-1546.

(12)   Sirimanne, P. M. *Renewable Energy* **2008**, *33*, 1424-1428.

(13)   Mal'tsev, E. I.; Lypenko, D. A.; Brusentseva, M. A.; Perelygina, O. M.; Vannikov, A. V. *High Energy Chem.* **2008**, *42*, 566-568.

(14)   Tischler, J. R.; Bradley, M. S.; Zhang, Q.; Atay, T.; Nurmikko, A.; Bulovic, V. *Org. Electron.* **2007**, *8*, 94-113.

(15)   Meinardi, F.; Cerminara, M.; Sassella, A.; Bonifacio, R.; Tubino, R. *Phys. Rev. Lett.* **2003**, *91*, 247401/247401-247401/247404.

(16)   De Boer, S.; Wiersma, D. A. *Chem. Phys. Lett.* **1990**, *165*, 45-53.

(17)   Peyratout, C.; Donath, E.; Daehne, L. *J. Photochem. Photobiol., A* **2001**, *142*, 51-57.

(18)   McRae, E. G.; Kasha, M. *J. Chem. Phys.* **1958**, *28*, 721-722.

(19)   Chen, Z.; Lohr, A.; Saha-Moeller, C. R.; Wuerthner, F. *Chem. Soc. Rev.* **2009**, *38*, 564-584.

(20)   Herz, A. H. *Adv. Colloid Interface Sci.* **1977**, *8*, 237-298.

(21)   Flanagan, J. H., Jr.; Owens, C. V.; Romero, S. E.; Waddell, E.; Kahn, S. H.; Hammer, R. P.; Soper, S. A. *Anal Chem* **1998**, *70*, 2676-2684.

(22)   Sorokin, A. V. *J. Appl. Spectrosc.* **2009**, *76*, 234-239.

(23)   von Berlepsch, H.; Boettcher, C. *J. Phys. Chem. B* **2002**, *106*, 3146-3150.

(24)   Kitahama, Y.; Yago, T.; Furube, A.; Katoh, R. *Chem. Phys. Lett.* **2008**, *457*, 427-433.

(25)   Nikolenko, L. M.; Ivanchihina, A. V.; Brichkin, S. B.; Razumov, V. F. *J. Colloid Interface Sci.* **2009**, *332*, 366-372.

(26)   Demir, M. M.; Ozen, B.; Ozcelik, S. *J. Phys. Chem. B* **2009**, *113*, 11568-11573.

(27)   Granzhan, A.; Ihmels, H.; Viola, G. *J Am Chem Soc* **2007**, *129*, 1254-1267.

(28)   Friend, R. H.; Gymer, R. W.; Holmes, A. B.; Burroughes, J. H.; Marks, R. N.; Taliani, C.; Bradley, D. D. C.; Dos Santos, D. A.; Bredas, J. L.; Logdlund, M.; Salaneck, W. R. *Nature* **1999**, *397*, 121-128.

(29)   Tang, C. W.; VanSlyke, S. A. *Appl. Phys. Lett.* **1987**, *51*, 913-915.

(30)   Bruchez, M., Jr.; Moronne, M.; Gin, P.; Weiss, S.; Alivisatos, A. P. *Science* **1998**, *281*, 2013-2016.

(31)   Hagfeldt, A.; Graetzel, M. *Chem. Rev.* **1995**, *95*, 49-68.

(32)   Ryu, S. Y.; Hwang, B. H.; Park, K. W.; Hwang, H. S.; Sung, J. W.; Baik, H. K.; Lee, C. H.; Song, S. Y.; Lee, J. Y. *Nanotechnology* **2009**, *20*, 065204/065201-065204/065205.

(33)   Shipway, A. N.; Katz, E.; Willner, I. *ChemPhysChem* **2000**, *1*, 18-52.

(34)   Xiao, D.; Xi, L.; Yang, W.; Fu, H.; Shuai, Z.; Fang, Y.; Yao, J. *J. Am. Chem. Soc.* **2003**, *125*, 6740-6745.

(35)   An, B.-K.; Kwon, S.-K.; Jung, S.-D.; Park, S. Y. *J. Am. Chem. Soc.* **2002**, *124*, 14410-14415.

(36)   Yao, H.; Yamashita, M.; Kimura, K. *Langmuir* **2009**, *25*, 1131-1137.

(37)   Freire, M. G.; Carvalho, P. J.; Gardas, R. L.; Santos, L. M. N. B. F.; Marrucho, I. M.; Coutinho, J. A. P. *J. Chem. Eng. Data* **2008**, *53*, 2378-2382.

(38)   Papaiconomou, N.; Salminen, J.; Lee, J.-M.; Prausnitz, J. M. *J. Chem. Eng. Data* **2007**, *52*, 833-840.

(39)   van den Broeke, J.; Stam, M.; Lutz, M.; Kooijman, H.; Spek, A. L.; Deelman, B.-J.; van Koten, G. *Eur. J. Inorg. Chem.* **2003**, 2798-2811.

(40)   Lakowicz, J. R. *Principles of Fluorescence Spectroscopy*, 2nd ed.; Plenum Press: New York, 1999.

(41)   Lakowicz, J. R. *Principles of Fluorescence Spectroscopy*, 1983.

CHAPTER 6

CONCLUSIONS AND FUTURE DIRECTIONS

In addition to designing CILs for enantiomeric recognition, the work presented in this dissertation is part of the effort to develop new nanomaterials from a new class of compounds termed Group of Uniform Materials Based on Organic Salts (GUMBOS). The first part involves the use of CILs that are liquid at room temperature (RTILs) for enantiomeric recognition of various chiral analytes using fluorescence spectroscopy. The second part of this dissertation mainly explores novel NIR fluorescent nanoGUMBOS as contrast agents for biomedical imaging and investigates the tunability of the spectral properties of the nanoGUMBOS as a function of varying the anion.

The first chapter provides a synopsis of the topics related to the work presented in this dissertation such as ILs, CILs, chirality, NIR GUMBOS and nanoGUMBOS. The synthesis, characterization and applications of CILs and nanoGUMBOS is described. In chapter 2, the synthesis of a series of CILs in both enantiomeric forms form alanine *tert*-butyl ester chloride is described. The alanine *tert*-butyl ester bis (trifluoromethane) sulfonylimide was obtained as liquid at room temperature with high thermal stability. Both enantiomeric forms of alanine *tert*-butyl ester bis (trifluoromethane) sulfonylimide could be used as solvent and chiral selector for enantiomeric recognition of various fluorescent analytes, alleviating the need for use of environmentally damaging solvents to dissolve the analyte.

In Chapter 3, the work in chapter 2 is extended to include enantiomeric recognition of analytes with reduced fluorescence by developing CILs from intrinsically fluorescent amino acids. The synthesis, characterization and investigation of the enantiomeric recognition properties of a fluorescent CIL, L-phenylalanine ethyl ester bis (trifluoromethane) sulfonimide (L-PheC$_2$NTf$_2$) is reported for the first time. Such a CIL is advantageous over previously

reported non-fluorescent CILs, whose applications were limited to the use of less sensitive modes of detection such as absorption, or to the use of fluorescence in discrimination of a small subset of intrinsically fluorescent analytes.

The results of an effort towards development of new nanomaterials in our research group is presented in chapter 4 with the evaluation of novel NIR nanoGUMBOS derived form a cationic NIR dye for biomedical imaging applications. It was also demonstrated that these NIR fluorescent nanoGUMBOS could be efficiently taken up *in vitro* by Vero cells, suggesting an interesting potential for non-invasive biomedical imaging applications. The nanoGUMBOS were fabricated by use of a simple, rapid and additive-free reprecipitation method. Considering the ease of preparation, this work presents an entirely new direction for preparing contrast agent nanoGUMBOS directly from tailored ionic materials. The approach described alleviates current problems associated with dye leakage and other challenges encountered in dye encapsulation, as well as obviating intensive purification steps required when surfactants are used to prepare dye nanoparticles. We note that the spectral properties of our GUMBOS were strikingly different from the freely dissolved dye present in solution. Thus, the possibility for tuning the optical properties of GUMBOS by variation in the parent ions offers a unique and exciting advantage for these nanomaterials. Since the NIR fluorescent nanoGUMBOS could be efficiently taken up *in vitro* by Vero cells, the prospect of tailoring nanoGUMBOS for delivery into designated cellular structures is an exciting new research possibility. In addition, this work could easily be extended to include GUMBOS with more than one property. For instance, incorporating a magnetic anion with the NIR nanoGUMBOS provides fluorescent and magnetic bimodal imaging modes.

Chapter 5 seeks answers to the intriguing observations made on the spectral properties of the NIR nanoGUMBOS upon variation of the anion. These NIR nanoGUMBOS described in chapter 4 displayed broad absorption spectra and the fluorescence emission of the

nanoGUMBOS was blue shifted compared to the dilute solution of the monomeric dye. These observations have been previously attributed to molecular aggregation and efforts to explain and control this phenomenon are detailed in the dissertation. The findings from this study suggest that both H and J aggregation occur at relatively different proportions depending on the anion. As far as is known, the most interesting part of our study is the unprecedented possibility of controlling the type of aggregation within the NIR nanoGUMBOS by retaining the same dye cationic skeleton and simply varying the counterion. In future, the possibility of preparing NIR nanoGUMBOS system containing both H and J aggregates exhibiting superradiance (a phenomena resulting from cooperative emission) will be of tremendous interest. In addition to varying the anion, the design of cation/ anion combination or conditions that can exclusively achieve the desired aggregate (H or J) for specific applications will be a useful study. Further, it is interesting that J aggregates derived from non-chiral molecules have been noted to be CD active due to the helical arrangement of J aggregates. This is another possible investigation on the NIR nanoGUMBOS to distinguish the various aggregates since the H aggregates and monomers do not exhibit this chiral activity.

APPENDIX
LETTER OF PERMISSION

From: David Bwambok <dbwamb1@tigers.lsu.edu>
To: permissionsUS@wiley.com
Subject: Permission to reproduce published work in dissertation

Dear Sir/Madam,

I am currently writing my doctoral dissertation and I hereby request permission to reproduce text, data and figures in my dissertation from the publication listed below:

David K. Bwambok, Hadi M. Marwani, Vivian E. Fernand, Sayo O. Fakayode, Mark Lowry, Ioan Negulescu, Robert M. Strongin, and Isiah M. Warner. "Synthesis and Characterization of Novel Chiral Ionic Liquids and Investigation of their Enantiomeric Recognition Properties" *Chirality*, 2008, 20, 151-158.

Thank you for your consideration on my request.

Sincerely,
David K. Bwambok,
Ph.D. Candidate
232 Choppin Hall,
LSU, Chemistry Department,
Baton Rouge, LA 70803
Fax: 225-578-3971
Telephone: 225-578-3919

From Campbell, Brenton - Hoboken <brenton.campbell@wiley.com>
To: <dbwamb1@tigers.lsu.edu>

Date Fri, Oct 9, 2009 at 1:53 PM
Subject: your permission request
mailed-bywiley.com

Dear David Bwambok,

I am happy to grant permission to republish the content you requested.

Best wishes,
Brent

Mr. Brenton R. Campbell - Global Rights Assistant - John WIley & Sons, Inc.
111 River St., MS 4-02 - Hoboken, NJ 07030-5774
brcampbell@wiley.com - ph: 201-748-5825 - fax: 201-748-6008

A01_First_Name: David
A02_Last_Name: Bwambok
A03_Company_Name: Louisiana State University
A04_Address: 232 Choppin Hall
A05_City: Baton Rouge
A06_State: LA
A07_Zip: 70803
A08_Country: USA
A09_Contact_Phone_Number: 2255783919
A10_Fax: 225 578 7231
A11_Emails: dbwamb1@tigers.lsu.edu
A12_Reference:
A13_Book_Title: Chirality
A40_Book_or_Journal: Journal
A14_Book_Author:
A15_Book_ISBN:
A16_Journal_Month: December
A17_Journal_Year: 2008
A18_Journal_Volume: 20
A19_Journal_Issue_Number: 2
A20_Copy_Pages: 151-158
A21_Maximum_Copies: 1
A22_Your_Publisher: Louisiana State Univerisity
A23_Your_Title: TASK SPECIFIC IONIC LIQUIDS FOR ENANTIOMERIC RECOGNITION AND NANOMATERIALS FOR BIOMEDICAL IMAGING
A24_Publication_Date: 12/12/09
A25_Format: Intranet
A41_Ebook_Reader_Type:
A26_If_WWW_URL:
A27_If_WWW_From_Adopted_Book:
A28_If_WWW_Password_Access:
A45_WWW_Users:
A29_If_WWW_Material_Posted_From:
A30_If_WWW_Material_Posted_To:
A42_If_Intranet_URL: www.lsu.edu
A32_If_Intranet_From_Adopted_Book:
A33_If_Intranet_Password_Access: Yes
A48_Intranet_Users: 26000
A34_If_Intranet_Material_Posted_From: 12/12/2009
A35_If_Intranet_Material_Posted_To: 12/12/2012
A50_If_Software_Print_Type:
A60_If_Other_Type:
A37_Comments_For_Request:

PERMISSION GRANTED
BY: _____
Global Rights Dept., John Wiley & Sons, Inc.

NOTE: No rights are granted to use content that appears in the work with credit to another source

thesis

VITA

David Kipkogei Arap Bwambok was born in Nandi District, Kenya, to Mr. William Kibwambok Arap Sawe and the late Mrs. Flomena Jesang Sawe. He was raised up in Chepkober village where he attended Chepsioch Primary School. Upon completion of primary education, he was admitted to Kemeloi High School where he successfully completed his High School Education in 1992. While in High School, he joined the Science Club and became fascinated by some projects that manifested chemistry in an interesting way. One such project is the use of a natural product for fishing. The metabolite was found to make fish float after heavy rains and interestingly the fish did not die since after a while they would swim again. It sounded like a myth but it captured David's attention and sparked an interest on discovering more about the marvels of chemistry. David was also active in sports and always liked to play soccer and volleyball. Mr. Bwambok joined Moi University in 1994 for undergraduate studies and earned a First Class Honors Degree in Bachelor of Education Science with a major in chemistry in 1998. While at Moi University, he was a member of the Chemical Association of Moi University. In 2002, he got an assistantship to pursue graduate studies at State University of New York at Binghamton and graduated in 2005 with a Master of Science Degree in chemistry. He then proceeded to pursue doctoral studies at Louisiana State University in August 2005 and has worked under the diligent guidance of Professor Isiah M. Warner. Mr. Bwambok has since been productive in research and his efforts were recognized with outstanding research scholar award in May 2008. He also won the outstanding graduate seminar award in May 2009. He is a member of the American Chemical Society and National Organization of Black Chemists and Chemical Engineers. David Kipkogei Bwambok is currently a candidate for the Doctor of Philosophy in analytical chemistry at Louisiana State University, to be awarded in December 2009. His

scholarly publications and professional conference presentations during his graduate career include:

Publications

• **Bwambok, David K**.; Marwani, Hadi M.; Fernand, Vivian E.; Fakayode, Sayo O.; Lowry, Mark; Negulescu, Ioan; Strongin, Robert, M.; Warner, Isiah M. "Synthesis and characterization of novel chiral ionic liquids and investigation of their enantiomeric recognition properties" *Chirality*, 2008, *20*, 151-158.

• A. Tesfai, B. El-Zahab, **Bwambok David K**., G. A. Baker, S. O. Fakayode, M. Lowry, and I. M. Warner. "Controllable Formation of Ionic Liquid Micro- and Nanoparticles via a Melt–Emulsion–Quench Approach" *Nano letters*, 2008, *8*, 897-901.

• **Bwambok, David K**.; El-Zahab Bilal; Challa, Santhosh; Li, Min; Gary A. Baker; Chandler, Lin; Warner, Isiah M. "Near infrared fluorescent nanoGUMBOS for biomedical imaging" *ACS Nano,* 2009, *Accepted.*

• **Bwambok, David K**.; Challa, Santhosh; Lowry, Mark; Warner, Isiah M. "Chiral discrimination using a fluorescent amino acid based chiral ionic liquid" To be submitted to: *Analytical Chemistry.*

• Min Li, Sergio L De Rooy, **Bwambok David K**., Bilal El-Zahab, John F. Ditusa, and Isiah M. Warner "Chiral Magnetic Fluids Based on Amino Acid-Derived Room Temperature Ionic Liquids" *Chemical Communications,* 2009*,* In *Press.*

• Li, Min; Gardella, Jerry; **Bwambok, David K**.; El-Zahab, Bilal; de Rooy, Sergio; Cole, Marsha; Lowry, Mark; Warner, Isiah M "Combinatorial Approach to Enantiomeric Discrimination: Synthesis and ^{19}F NMR Screening of a Chiral Ionic Liquid-Modified Silane Library" *Journal of Combinatorial Chemistry*, 2009, *11*(6), 1105-1114.

• Susmita Das, **David K. Bwambok**, Bilal El-Zahab, Santhosh Challa, Min Li, Joshua Monk, Francisco Hung, Isiah M. Warner "Tuning the Spectral Properties of Near IR Fluorescent NanoGUMBOS" In preparation for prospective submission to: *Journal of American Chemical Society*.

• Fernand, V. E.; Losso, J. N.; Traux, R.E.; Villar, E.E.; **Bwambok, D.K**.; Fakayode, S.O.; Lowry, M.; Warner, I. M. "Rhein as Inhibitor of Hypoxia-Induced Tumor Angiogenesis in Non-Invasive Breast Cancer Cells" *Breast Cancer Research and Treatment* 2009, *Submitted.*

• Sergio L. de Rooy, Min Li, **David K. Bwambok**, Bilal El-Zahab, Santhosh Challa, and Isiah M. Warner "Ephedrinium-Based Protic Chiral Ionic Liquids for Enantiomeric Recognition" To be submitted to: *Chirality.*

• Fakayode, Sayo O.; Sumpter, JaPeL K.; Magee, Paula; Mohammed, Abdul K.; Pollard, David A.; **Bwambok, David K**.; Ganea, Gabriela M.; Warner, Isiah M. "Investigation of chiral

recognition and binding mechanism of chiral guest-host complexes using FTIR, UV-visible and fluorescence spectroscopy." *Applied Spectroscopy* 2009, *Submitted.*

• **David K. Bwambok**, Min Li, Gary A. Baker and Isiah M. Warner "Chiral ionic liquid derived from Mosher's acid" In *preparation.*

• **David K. Bwambok**, Min Li, Bilal El-Zahab and Isiah M. Warner "NIR fluorescent nanoGUMBOS derived fom indocyanine green" In *preparation.*

Patent

• Warner, Isiah M.; El-Zahab, Bilal; Tesfai, Aaron; **Bwambok, David**; Baker, Gary A.; Fakayode, Sayo O.; Lowry, Mark; Tolocka, Michael P.; De Rooy, Sergio. Production methods and applications of frozen ionic liquid microparticles and nanoparticles. PCT Int. Appl. (2009).

Book Chapter

• Min Li; **David K. Bwambok**; Sayo O. Fakayode and Isiah M. Warner. "Chiral Ionic Liquids in Chromatographic Separation and Spectroscopic Discrimination." In: "Chiral Recognition in Separation Methods: Mechanisms and Applications." Berthod Alain (Editor) 2009, *Submitted.*

Professional Presentations

• **David K. Bwambok**, Bilal El-Zahab, Santhosh K. Challa, Mark Lowry, Min Li, Lin Chandler, and Isiah M. Warner. "Novel near infrared fluorescent ionic liquids for biomedical imaging." 238th ACS National Meeting, Washington, DC, USA, August 2009.

• **David K. Bwambok,** Santhosh K.Challa, Mark Lowry, and Isiah Warner. "A fluorescent amino acid-based chiral ionic liquid for enantiomeric discrimination." 21st International Conference on Chirality, Breckenridge, CO, USA, July 2009.

• **Bwambok David K.**, Bilal El-Zahab, Mark Lowry, Gabor Patonay, Gary A. Baker, and Isiah Warner. "Novel near infrared dyes and nanoparticles derived from ionic liquids." NOBCChE, St. Louis, MO, USA, April 2009.

• **Bwambok David K.**; Santhosh K. Challa; Mark Lowry; Warner, Isiah M. "Chiral discrimination using a fluorescent amino acid based chiral ionic liquid." PITTCON, Chicago, IL, USA, March 2009.

• Challa, Santhosh; Lowry, Mark; **Bwambok, David K**.; Warner, Isiah M. "Improved enantiomeric recognition based on multidimensional fluorescence of intrinsically fluorescent amino acid-based chiral selectors." 238th ACS National Meeting, Washington, DC, USA, August 2009.

• Fakayode, Sayo O.; Sumpter, JaPeL K.; Magee, Paula; Mohammed, Abdul K.; Pollard, David A.; **Bwambok, David K**.; Ganea, Gabriela M.; Warner, Isiah M. "Investigation of chiral recognition and binding mechanism of chiral guest-host complexes using FTIR, UV-visible and fluorescence spectroscopy." 238th ACS National Meeting, Washington, DC, USA, August 2009

• Sergio L. de Rooy, Min Li, **David K. Bwambok**, Bilal El-Zahab, Santhosh Challa, and Isiah M. Warner "Ephedrinium-Based Protic Chiral Ionic Liquids for Enantiomeric Recognition" 21st International Conference on Chirality, Breckenridge, CO, USA, July 2009.

• **Bwambok David K.,** Marwani, Hadi M.; Fernand, Vivian E.; Fakayode, Sayo O.; Lowry, Mark; El-Zahab, Bilal; Baker, Gary A.; Negulescu, Ioan I.; Strongin, Robert M.; Warner, Isiah M. "Spectroscopic investigations of enantiomeric recognition using chiral ionic liquids derived from amino acid esters." 235th ACS National Meeting, New Orleans, LA, USA, April, 2008.

• **Bwambok David K**., Hadi Marwani, Vivian Fernand, Sayo Fakayode, Mark Lowry, Ioan Negulescu, Robert Strongin and Isiah Warner. "Synthesis and Characterization of Novel Chiral Ionic Liquids (CILs) and Investigation of their Enantiomeric Recognition Properties." PITTCON, New Orleans, LA, USA, March 2008.

• **Bwambok David K**., Hadi Marwani, Vivian Fernand, Sayo Fakayode, Mark Lowry, Bilal El-Zahab, Gary Baker, Ioan Negulescu, Robert Strongin and Isiah Warner. "Enantiomeric Recognition Using Chiral Ionic Liquids Derived from Amino Acid Esters by Spectroscopy." NOBCChE, Philadelphia, PA, USA, March 2008.

• **Bwambok David K.,** Hadi Marwani, Vivian Fernand, Sayo Fakayode, Mark Lowry, Bilal El-Zahab, Gary Baker, Ioan Negulescu, Robert Strongin and Isiah Warner. "Investigation of Enantiomeric Recognition Using Chiral Ionic Liquids Derived from Amino Acid Esters by Spectroscopy." MRS Symposium Series, San Francisco, CA, USA, March 2008.

• Fernand, V.E**.**; Losso, J.N.; **Bwambok, D. K**.; Fakayode, S.O.; Warner, I. M. "Effect of Rhein on MDA-MB-435s Breast Cancer Cells under Hypoxic Conditions." American Chemical Society (ACS), New Orleans, LA, USA, April 2008.